UNCLASSIFIED

AD NUMBER

AD873313

NEW LIMITATION CHANGE

TO

Approved for public release, distribution unlimited

FROM

Distribution: Controlled: all requests to Director, Defense Atomic Support Agency, Washington, D. C. 20305.

AUTHORITY

DTRA ltr, 3 Nov 99

THIS PAGE IS UNCLASSIFIED

AD873313

DASA 2519-1

Final Report — Part A

May 1970

PROJECT 617 RADAR READINESS ACHIEVEMENT PROGRAM
Part A — Data Processing and Analysis

By: M. J. BARON O. de la BEAUJARDIERE B. CRAIG

Prepared for:

DIRECTOR
DEFENSE ATOMIC SUPPORT AGENCY
WASHINGTON, D.C. 20305

CONTRACT DASA01-67-C-0019

STANFORD RESEARCH INSTITUTE
MENLO PARK, CALIFORNIA

SRI

This document may be further distributed by any holder only with specific prior approval of Director, Defense Atomic Support Agency, Washington, D.C. 20305.

STANFORD RESEARCH INSTITUTE
Menlo Park, California 94025 · U S A

DASA 2519-1

Final Report — Part A

May 1970

PROJECT 617 RADAR READINESS ACHIEVEMENT PROGRAM
Part A — Data Processing and Analysis

By: M. J. BARON O. de la BEAUJARDIERE B. CRAIG

Prepared for:

DIRECTOR
DEFENSE ATOMIC SUPPORT AGENCY
WASHINGTON, D.C. 20305

CONTRACT DASA01-67-C-0019

This work sponsored by the Defense Atomic Support Agency under NWER/Subtask HA 048.

SRI Project 6291

Approved by:

DAVID A. JOHNSON, *Director*
Radio Physics Laboratory

RAY L. LEADABRAND, *Executive Director*
Electronics and Radio Sciences Division

Copy No. 32

PRECEDING PAGE BLANK-NOT FILMED

ABSTRACT

This report describes in detail the use of the Project 617 radar for making incoherent scatter measurements of the ionosphere. The data processing and analysis methods are fully explained, including all the assumptions, interpolations, and extrapolations. Two new major computer programs were implemented. Portions of the radar hardware that are especially important to the incoherent scatter measurements and portions that have been developed, modified, or improved during the past year are also described. The development and implementation of a digital autocorrelator, in combination with new computer software, has resulted in an order-of-magnitude improvement in data processing time, as well as a significant improvement in measurement accuracy.

PRECEDING PAGE BLANK-NOT FILMED

CONTENTS

CONTENTS (Concluded)

PRECEDING PAGE BLANK-NOT FILMED

ILLUSTRATIONS

ILLUSTRATIONS (Concluded)

TABLES

I INTRODUCTION

The incoherent scatter technique has made possible the measurement of ionospheric electron densities and electron and ion temperatures with a single, ground-based radar system. These ionospheric parameters are important to the Defense Atomic Support Agency (DASA) nuclear weapons test program. During the past five years, Stanford Research Institute has--for DASA--designed, constructed and operated an incoherent scatter radar to develop the techniques for operating in a nuclear environment, to improve the radar system, and to conduct ionospheric researches on the natural ionosphere.

During the past twelve months, the objectives of this project have been to implement a program of equipmental and operational improvements to the Mighty Sky Project 617 radar in order to achieve a high degree of test readiness. Specifically, the project efforts during the last half of 1969 and the first quarter of 1970 have been directed towards:

(1) Implementing computer programs and procedures to speed up and automate data processing and data analysis

(2) Implementing a digital autocorrelator to enable spectral analysis to be performed in (nearly) real time

(3) Conducting ionospheric studies using the incoherent scatter technique for the purpose of better understanding ionospheric phenomena

(4) Planning the move of the radar to the auroral zone

(5) Maintaining a current awareness in the progress of the incoherent scatter technique so that maximum usefulness of this technique for DASA's purposes will be realized.

This report, Final Report--Part A, describes the results of the work performed to satisfy Objectives 1 and 2. It is also intended for use as a reference document that describes in detail the hardware, software, and procedures used in processing and analyzing the incoherent scatter data. Since many changes in hardware and software have been made during the past five years, and since the radar will be relocated to Alaska and used by personnel less familiar with its operation, it was felt that a report collecting in one volume all the pertinent information concerning the receiver system, calibration system, analog-to-digital conversion (ADC) system, digital subsystem, and computer processing system would be extremely useful.

The work performed under Objective 3 of this project is described in a separate report, Final Report--Part B. That report includes the results of three 48-hour data runs (June, July, and August 1969) taken before the installation of the digital autocorrelator and at least three 48-hour data runs (February, March, and April 1970) taken after the installation of the autocorrelator. In addition, data were taken and analyzed for two partial solar eclipses--one on 11 September 1969 in which the sun was about 70 percent obscured, and one on 7 March 1970, in which the sun was less than 30 percent obscured.

The work performed under Objective 4 of this project has been completed; it resulted in a proposal entitled "DASA Project 617 Radar Relocation," which was submitted to DASA in early March 1970. Included in that proposal is a description of the work done under Objective 4.

Objective 5--maintaining a current awareness of the progress of the incoherent scatter technique--is applicable to all the other objectives of this project. The achievement of this objective is evidenced by the improvements and results described in both Part A and Part B of this Final Report.

The plasma physics theory governing incoherent scattering of radio waves from the ionosphere is well described in the literature[1,2,3*] and will not be repeated here. However, the equations, assumptions, interpolations, and extrapolations used in the data processing and analysis are described in Section II, Measurement Technique. That section gives the mathematical procedures used in the processing of the incoherent scatter data so as to yield electron densities and electron and ion temperatures.

Section III of this report describes the radar system hardware, including:

(1) Receiving and calibration equipment

(2) Analog-to-digital conversion equipment

(3) Digital autocorrelator

(4) Computer interfacing equipment.

The software developed for and used by the Project 617 radar is described in Section IV. Included are the on-line data collection program and the off-line data processing and analysis program, both of which were implemented during the past nine months.

Section V summarizes the improvements incorporated into the system during the past year and points out further improvements that could be made in the future.

---

* References are listed at the end of this report.

PRECEDING PAGE BLANK-NOT FILMED

II MEASUREMENT TECHNIQUE

Incoherent scatter is basically a technique for measuring ionospheric electron densities and electron and ion temperatures by using a ground-based radar facility. Several alternative measurement methods are possible.[4] This report discusses in detail only the monostatic pulsed radar technique implemented for the DASA Project 617 L-band radar. Measurements of received power as a function of range and of the frequency spectrum of the received signal as a function of range are used to determine the ionospheric parameters.

A. Power Profile

Equation (1) is the formulation of the radar equation applicable to the incoherent scatter measurements:[5]

$$N = \left(\frac{i28\sqrt{2}\,\pi^2}{c\sigma_m}\right)\left(\frac{1}{G_o^2\theta_{\frac{1}{2}}^2\lambda^2\eta}\right)\left(\frac{1}{P_T\tau}\right)\left(\frac{R^2P_r}{1}\right)\left[\frac{(1+\alpha^2+T_r)(1+\alpha^2)}{2}\right] \quad , \quad (1)$$

where*

N = electron density at range R (el/m^3)

c = velocity of light (m/s)

σ_m = 0.5×10^{-28} m^2 = backscatter cross section of single electron, assuming $\alpha^2 = 0$, $T_r = 1$

---

* All terms are listed and defined in the Glossary, which precedes the References.

G_o = antenna gain along main axis = 47.15 dB

$\theta_{\frac{1}{2}}$ = antenna half beamwidth (radians) = 0.3 π/180

λ = radar wavelength (meters)

η = product of transmit and receive system losses = -1.9 dB

P_T = transmitted power (watts)

τ = transmitted pulse length (seconds)

P_R = received power at range R (watts)

T_r = electron-to-ion temperature ratio at range R

$\alpha^2 = (kD)^2 = 14.22 \times 10^6 T_e/N$ at $\lambda = 0.23$ m.

The numerical constants (first bracket) and unchanging radar parameters (second bracket) can be evaluated and combined to give:

$$N = \left(0.475 \times 10^{20}\right)\left(\frac{1}{P_T \tau}\right)\left(R^2 P_r\right)\left[\frac{(1 + \alpha^2 + T_r)(1 + \alpha^2)}{2}\right] \quad (2)$$

In this form, the equation is separated into a numerical constant (first bracket), variables that may be changed but are fixed for any particular data run (second bracket), variables that are directly measured (third bracket), and variables that must be inferred from other--frequency spectrum--measurements (fourth bracket). An additional complication is introduced by the fact that α^2 is itself a function of N. Thus, to determine the electron density, one must first know, or at least estimate, the electron density. The solution of this problem is discussed later. As a first step in the data analysis procedure, the density is computed by assuming $\alpha^2 = 0$ and $T_r = 1$, giving what we call the raw electron density,

$$N' = \left(\frac{C_s}{P_T \tau}\right)\left(R^2 P_r\right) \quad , \tag{3}$$

where

$C_s = 0.475 \times 10^{20}$ = system constant.

To determine the electron density from Eq. (2) or (3) above, a careful measurement of the magnitude of the received power is required. Also, since the received signal is at best only a few times larger than the noise level, and at most ranges less than the noise level, an accurate subtraction of the receiver noise level from the receiver output containing both incoherent scatter signal and noise must be made. Furthermore, the receiving system gain changes as a function of temperature and is periodically adjusted by the operator. The received noise power also changes due to (1) reception of signals from interfering radars, (2) rotation of the celestial sphere through the antenna beam, and (3) variations in the gain of the receiving system parametric amplifiers.

To account for gain and noise power changes, the received noise level is continuously monitored and recorded. The noise level and the signal-plus-noise level are calibrated by periodically injecting a noise pulse of accurately known amplitude into the receiver chain in front of the first parametric amplifier. This pulse is called the "calibrate pulse." Figure 1 shows how the detected received output as a function of time would look on an idealized A-scope display if a square-law detector were employed. The ordinate is average received power, and the abscissa is time within one interpulse period. The following equation is used to determine the received power, P_r, at range R:

$$\bar{P}_r = \left(\frac{\bar{P}_j - \bar{P}_n}{\bar{P}_c - \bar{P}_n}\right) P_k \quad , \tag{4}$$

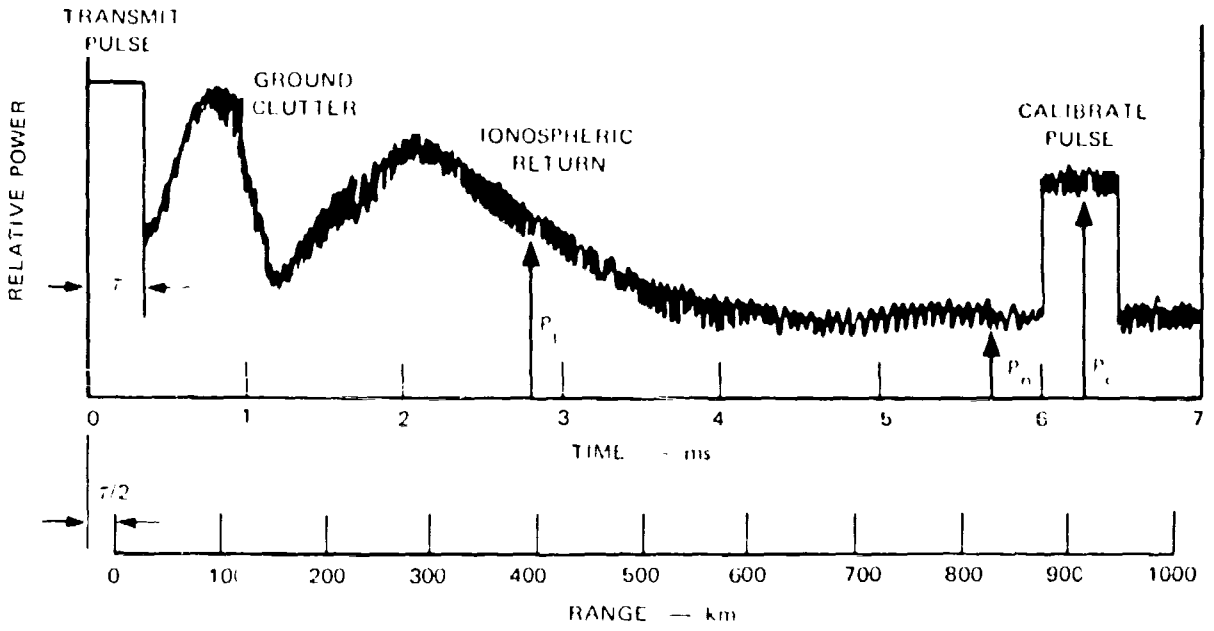

FIGURE 1 RECEIVED POWER AS A FUNCTION OF TIME (RANGE)

where

$\bar{P}_j$ = the received power measured at the j^{th} range

$\bar{P}_n$ = the received power measured at a range where no signal is present

$\bar{P}_c$ = the received power measured at ranges where the calibrate pulse is present

P_k = the injected calibrate noise pulse power = KT_kB_D

B_D = the receiver noise bandwidth of the detected channel.

Bars over the quantities are used to indicate time averages. Since the incoherent scatter signal is noiselike, all measurements must be done statistically, i.e., quantities must be measured and time averaged in order to determine their magnitudes. Typically, a noise pulse temperature (T_k) of 70°K is used for our measurements.

The received powers (P_j, P_n, P_c) are measured digitally by sampling with an analog-to-digital converter (ADC) the linearly detected received signal voltage. Squaring of the voltages to obtain power and averaging of the power is done digitally in real time in a general purpose digital computer.

At this point, a comment on the measurement of radar range, R, is in order. For a hard radar target, and at a radar frequency well above the plasma frequency of the ionosphere, where the group velocity is very close to the velocity of light, the range can be measured by simply measuring the time delay between the leading edge of the transmitted pulse and the leading edge of the target. For this situation,

$$R = \frac{ct}{2} \quad , \tag{5}$$

where t is time delay, and the factor of 2 accounts for the two-way propagation path. For a "soft" (distributed) target such as the ionosphere or an ionized cloud, the returned energy represents the convolution of the transmitted pulse with the target. A simple calculation for this case shows that the range to the center of a distributed target symmetric in range is given by the time delay from the center of the transmitted pulse to the center of the target. Thus Eq. (5) must be modified for incoherent scatter measurements to be

$$R = \frac{c}{2}\left(t - \frac{\tau}{2}\right) \quad , \tag{6}$$

where τ is the transmitted pulse length.

We can now summarize the power profile measurements as follows. The received signal is linearly detected and sampled by an ADC at uniform intervals (30 or 60 μs for our system) during the interpulse period. The sampled voltages are fed into a computer where they are squared to give the P_j's; j is the index indicating the radar range at which the sample was taken. For each j, the P_j's from many consecutive interpulse periods are averaged to give $\bar{P}_j$'s. Then $\bar{P}_c$ and $\bar{P}_n$ are calculated by averaging the $\bar{P}_j$'s over the range intervals where the calibrate pulse is injected and over the intervals where no incoherent scatter signal exists, respectively. Next, the P_r's for each j are computed, according to Eq. (4). From the P_r's and R's calculated as indicated by Eq. (6), the raw density N' is calculated by using Eq. (3). Then, when the temperatures, T_e and T_i, have been determined (discussed in the next section), the true density can be calculated by

$$N = N'(1 + T_r + \alpha^2)(1 + \alpha^2)/2 \quad . \qquad (7)$$

The terms in parentheses indicate how the scattering cross section changes with changes in α^2 and T_r.

This method assumes that one has very accurate knowledge of the radar system parameters that go into the system constant, C_s, and that these parameters do not change or are continuously measurable during the course of a data run and from day to day and month to month. In practice, we have found it is easier and more accurate to obtain the shape of the density profile as discussed above but to normalize the maximum density to the density indicated by measuring f_oF2 with an ionosonde.

B. Temperature Measurements

1. Background

The spectrum of the incoherent backscatter signal is of great importance because it contains all the information on electron and ion temperatures. These temperatures are of interest in themselves, and they are also necessary for proper computation of electron density profiles [Eq. (2)].

Figure 2 shows the spectrum (that is, the returned power per unit bandwidth plotted as a function of Doppler shift) of the incoherent scatter signal for a transmitted frequency of 1290 MHz. The half spectrum is shown here, with the total spectrum being symmetric around zero Doppler shift in the absence of ionospheric drifts or currents. Also shown in this figure are the effects on the spectrum shape of various electron-to-ion temperature ratios, T_r. As T_r increases, the "wing" of the spectrum becomes more pronounced. Therefore, a practical way of estimating T_r is by measuring the ratio of power (wing)/power (center frequency).

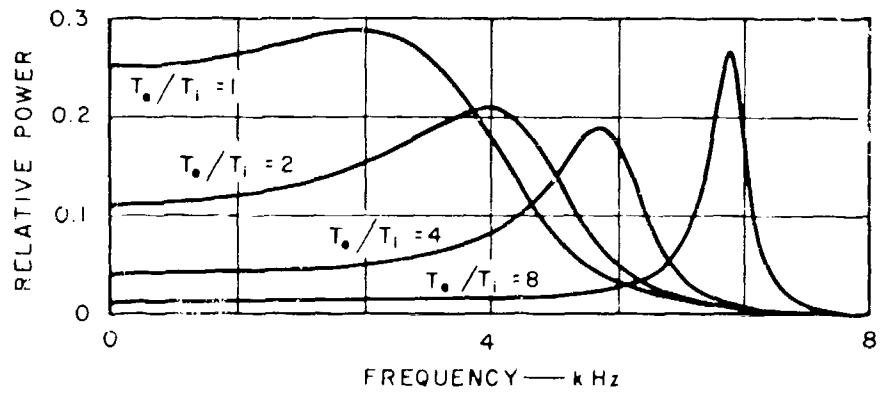

FIGURE 2 CALCULATED INCOHERENT-SCATTER IONIC SPECTRA kD = 0, O^+ IONS, T_i = 825°K, T_e/T_i VARYING

The ion temperature can also be deduced from the measured spectra. The total spectral width is approximately proportional to $[(T_e + T_i)^2]^{1/2}$. Figure 3 shows the effect on the spectrum of increasing T_i while keeping T_r fixed. Thus by measuring two parameters of the spectrum, say peak-to-valley ratio and width, one can theoretically solve for the two quantities of interest, T_e and T_i.

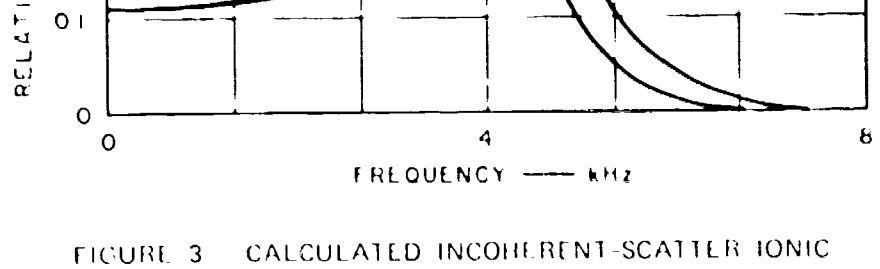

FIGURE 3 CALCULATED INCOHERENT-SCATTER IONIC SPECTRA kD = 0, 0' IONS, T_e/T_i = 20, T_i VARYING

In practice, and particularly at our 23-cm wavelength, an additional complication arises. The ratio (α) of the Debye length, $[D = 69(T_e/N)^{1/2}]$, to the operating wavelength affects the shape of the spectrum as well as the backscatter cross section, as discussed earlier. Figure 4 shows the effect on the spectrum of changing α by varying N but leaving the ion and electron temperatures unchanged. Notice that both the bandwidth and the peak-to-valley ratio of the spectrum are affected. The effect on the scattering cross section can also be seen. Since the cross section is proportional to the area under the spectrum, as α increases, the cross section can be seen to decrease.

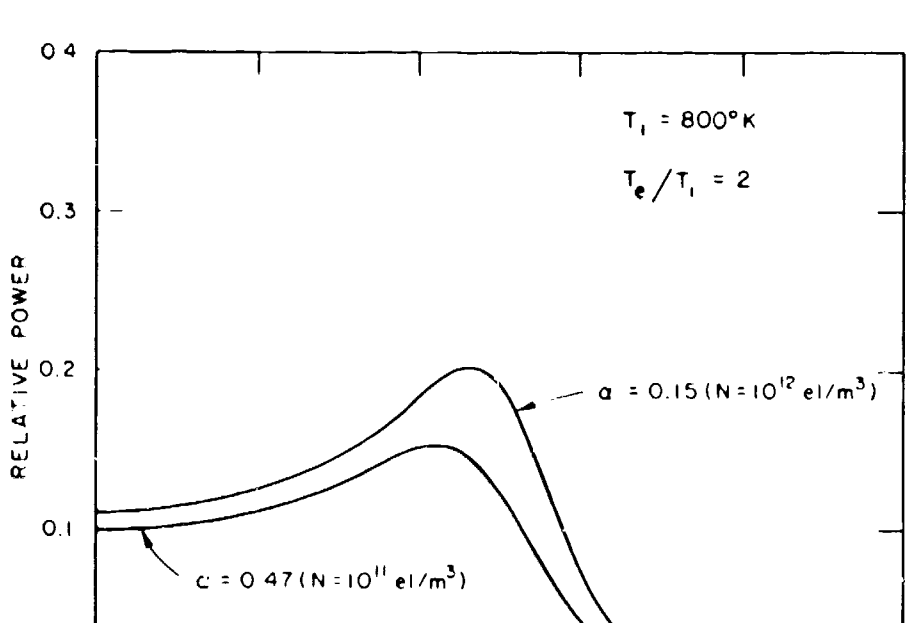

FIGURE 4 CALCULATED INCOHERENT-SCATTER IONIC SPECTRA O⁺IONS T_i = 800 K, T_e/T_i = 2, kD VARYING

At this point we can summarize by listing the three physical quantities that affect the shape of the incoherent scatter spectra: (1) electron temperature; (2) ion temperature; and (3) electron density. If one of these quantities is known, the other two can be deduced, but because of their complex interrelationships, all three cannot be experimentally deduced from spectrum measurements alone. For example, the change in the spectrum shape due to changing N in Figure 4 can be closely duplicated by changing only T_e and T_i while leaving N fixed.

2. Instrumental Effects

Proper measurement and analysis of the spectra is necessary for correct interpretation of ionospheric densities and temperatures. Two principal factors complicate the measurement: (1) the signal-to-noise ratio is low--very often less than unity; and (2) the measuring

system itself (transmitter, receiver, and digital processor) distorts the spectrum. Low signal-to-noise ratios limit the accuracy and height regime over which measurements can be made and lead to the use of relatively long integration times (minutes to tens of minutes). The effects of the measuring system on the spectrum can be calculated and then corrected for in processing the data. However, the measurement accuracy is somewhat reduced, since, as will be pointed out later, the equipmental effects are such as to make the inferred parameters T_e and T_i more sensitive to errors in spectral shape determination.

Let us now briefly discuss the effects of the measuring instrument (a pulsed radar system) on the measurement. In the discussion we make use of the fact that multiplication of two functions in the time (frequency) domain is equivalent to convolution of their Fourier transforms in the frequency (time) domain. Let us represent the power spectrum of density fluctuations in the ionospheric plasma by $S(f)$, where f is the Doppler shift frequency. This is the incoherent scatter spectrum that would result if the measuring equipment did not perturb the signal. [The equations for calculating $S(f)$ have been given in a previous report,[c] and Figures 2, 3, and 4 are some representative plots of $S(f)$ vs. f.] The quantity $S(f)$ is the spectrum that would result from the scattering by the plasma of a spectrally pure CW signal.

Since a pulsed radar is used for our measurements, which means we transmit not a single frequency but a band of frequencies, the fluctuation spectrum $S(f)$ must be convolved with the power spectrum of the transmitted pulse. The result of this convolution operation represents the spectrum of the incoherent scatter signal at the receiving antenna terminals. Representing the power spectrum of the transmitted pulse by $P(f)$, the signal, $S_1(f)$, present at the antenna terminals is

$$S_1(f) = S(f) * P(f) \quad , \tag{8}$$

where the asterisk indicates the convolution operation.

The signal $S_1(f)$ then passes through the receiver chain, including several amplifiers, mixers, and filters which have bandpass characteristics that affect the signal. Letting the frequency response curve of the receiver chain be represented by $B(f)$, the signal, $S_2(f)$, after passing through the receivers, is related to $S_1(f)$ by

$$S_2(f) = S_1(f)B(f) \quad . \tag{9}$$

Next the signal is range-gated to obtain spectra at a number of radar ranges (ionospheric heights). The range-gating process can be represented in the time domain by multiplication of the signal by the gating waveform (a square pulse). This is equivalent in the frequency domain to convolving $S_2(f)$ with the Fourier transform, $G(f)$, of the autocorrelation function of the square pulse. This operation gives

$$S_3(f) = S_2(f) * G(f) \quad , \tag{10}$$

where $S_3(f)$ is the incoherent scatter spectrum, perturbed by the measuring instrument, which is measured by the radar system.

The sequence of operations described above is indicated graphically in Figure 5. Equivalent operations in both the time (autocorrelation) domain and the frequency (power spectrum) domain are shown. Passing from one side to the other of the dashed vertical line indicates using the Fourier transform.

Figure 6 is an example of the effect on the spectrum of a finite pulse length and a receiver range gate. For this figure the receiver bandpass has been assumed to be flat. Notice that the greatest change is in the peak-to-valley ratio, which is closely related to T_e/T_i. Also

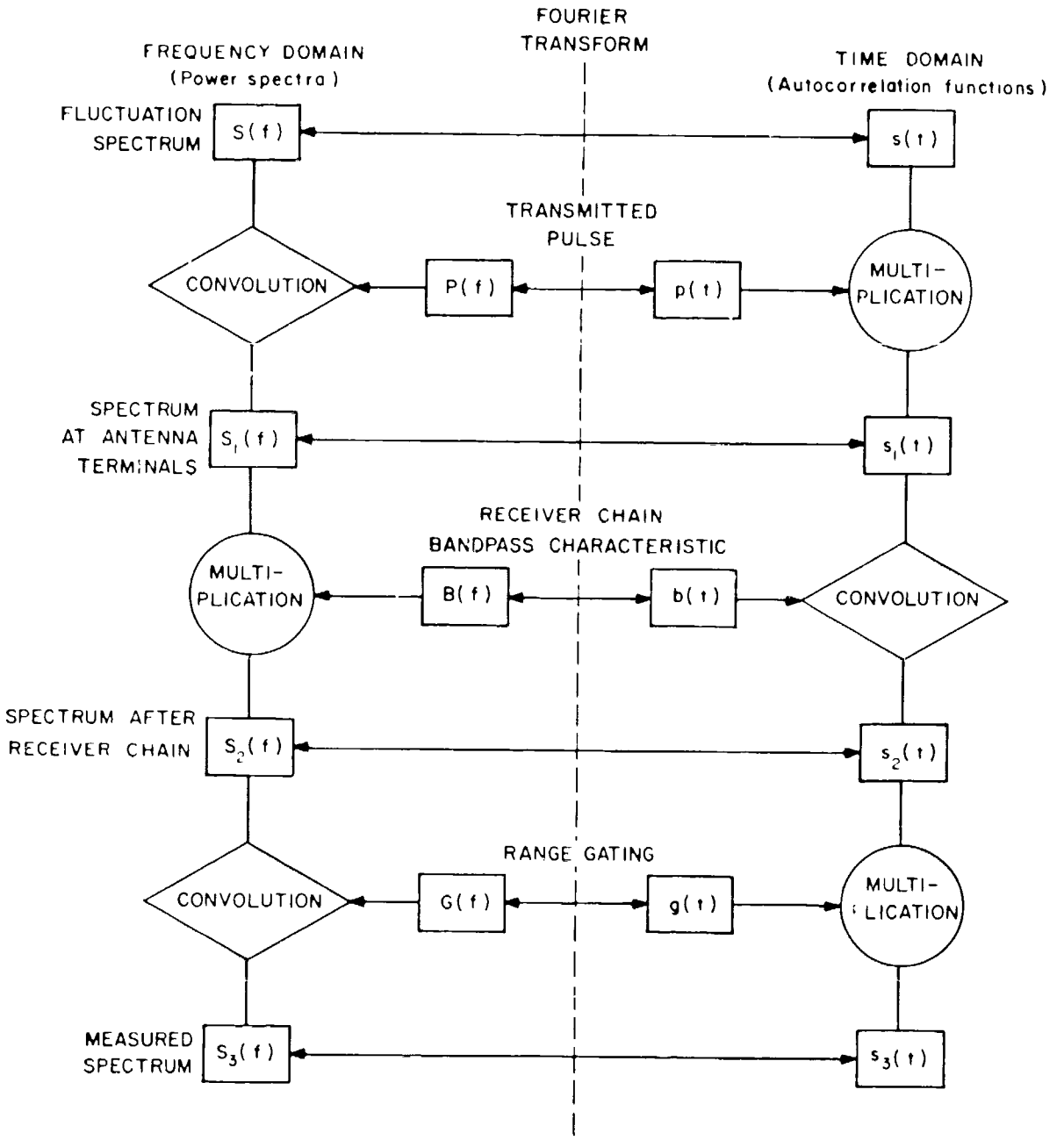

FIGURE 5 SPECTRUM-PERTURBATION BLOCK DIAGRAM

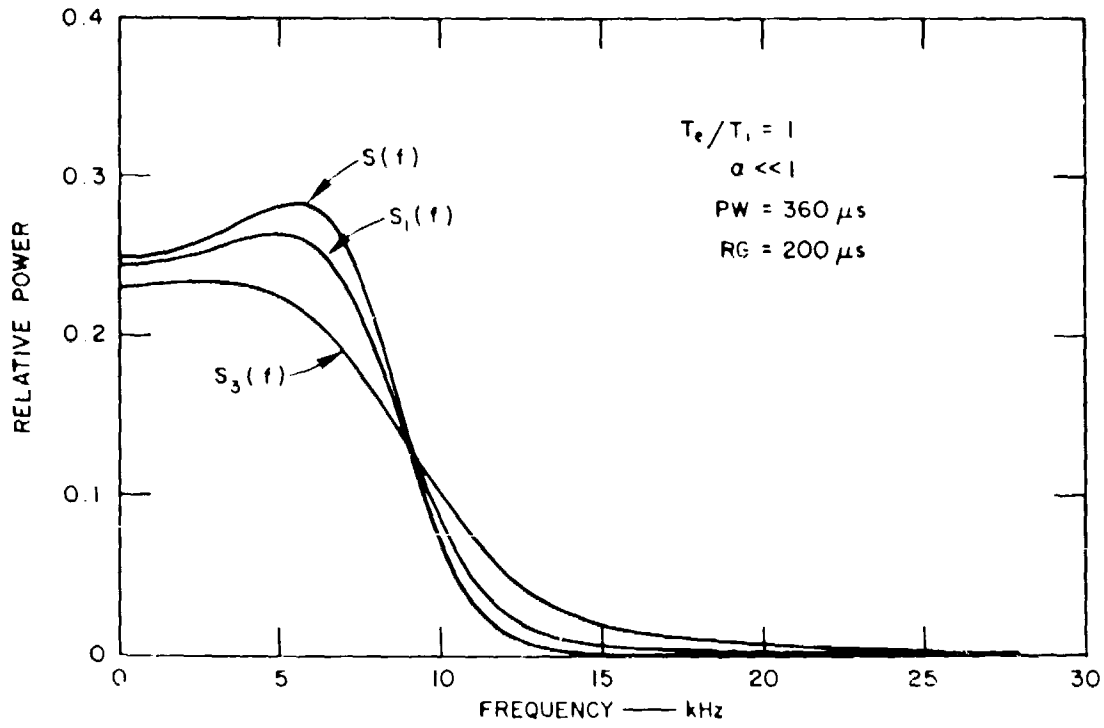

FIGURE 6 CALCULATED INCOHERENT-SCATTER SPECTRA, SHOWING EFFECT OF FINITE PULSE WIDTH AND RECEIVER RANGE GATING

changes in the peak-to-valley ratio for a given change in T_e/T_i are not as great, leading to reduced ability to detect small changes in T_e/T_i and thus somewhat reduced accuracy. If the spectral perturbations discussed in this section were not allowed for in the data processing and analysis, one would underestimate T_e/T_i and overestimate T_i.

3. Interpretation for $\alpha^2 = 0$

As mentioned earlier, the parameters T_e, T_i, and N, as well as the pulse length, τ, and the range gate width, w, all affect the shape of the measured spectra, $S_3(f)$. Throughout a data run τ and w remain fixed and can be accounted for in the computation of the theoretical spectral shapes used for comparison with measurement. Let us for the moment assume that N is very large such that $\alpha^2 \approx 0$ and see how one then

interprets the data to obtain T_e and T_i. Later we will show how smaller densities (larger α^2) are accounted for in the interpretation of the measurements.

One way of obtaining T_e and T_i from a measured spectrum would be to precompute and store in a library in a computer a vast number of theoretical spectra, for many values of T_e and T_i. The spectra so computed and stored would include the perturbations due to the pulse length and range gate. Then one could have the computer compare the measured spectrum with the library of computed spectra and, through some best-fit procedure, decide which combination of T_e and T_i best matched the data. This technique would require a considerably larger computer than we have available with our radar system.

An alternative method, the one actually used, requires much less computer time and storage. It involves scaling two easily identifiable features, the peak-to-valley ratio (PV) and the bandwidth (BW), from the measured spectra, and using what we call a spectrum scaling chart to interpret these parameters in terms of T_r and T_i. This can be done easily and quickly in our computer. Figures 7 through 10 show the spectrum scaling charts used for our system. They were prepared for the four most commonly used combinations of pulse width and range gate width: τ = 360 μs and w = 240, 300, 320, 400 μs. From any measured spectrum, the computer determines the peak-to-valley ratio (the ratio of the power at the peak of the spectrum to that at the center frequency) and the bandwidth (the frequency difference measured from zero Doppler shift to the frequency at which the spectral energy has fallen by 3 dB relative to the peak energy). With these two values as abscissa and ordinate of the scaling chart, the computer then determines, from the skewed grid, β and T_i; β is just the temperature ratio, T_e/T_i, which is inferred under the assumption $\alpha^2 = 0$.

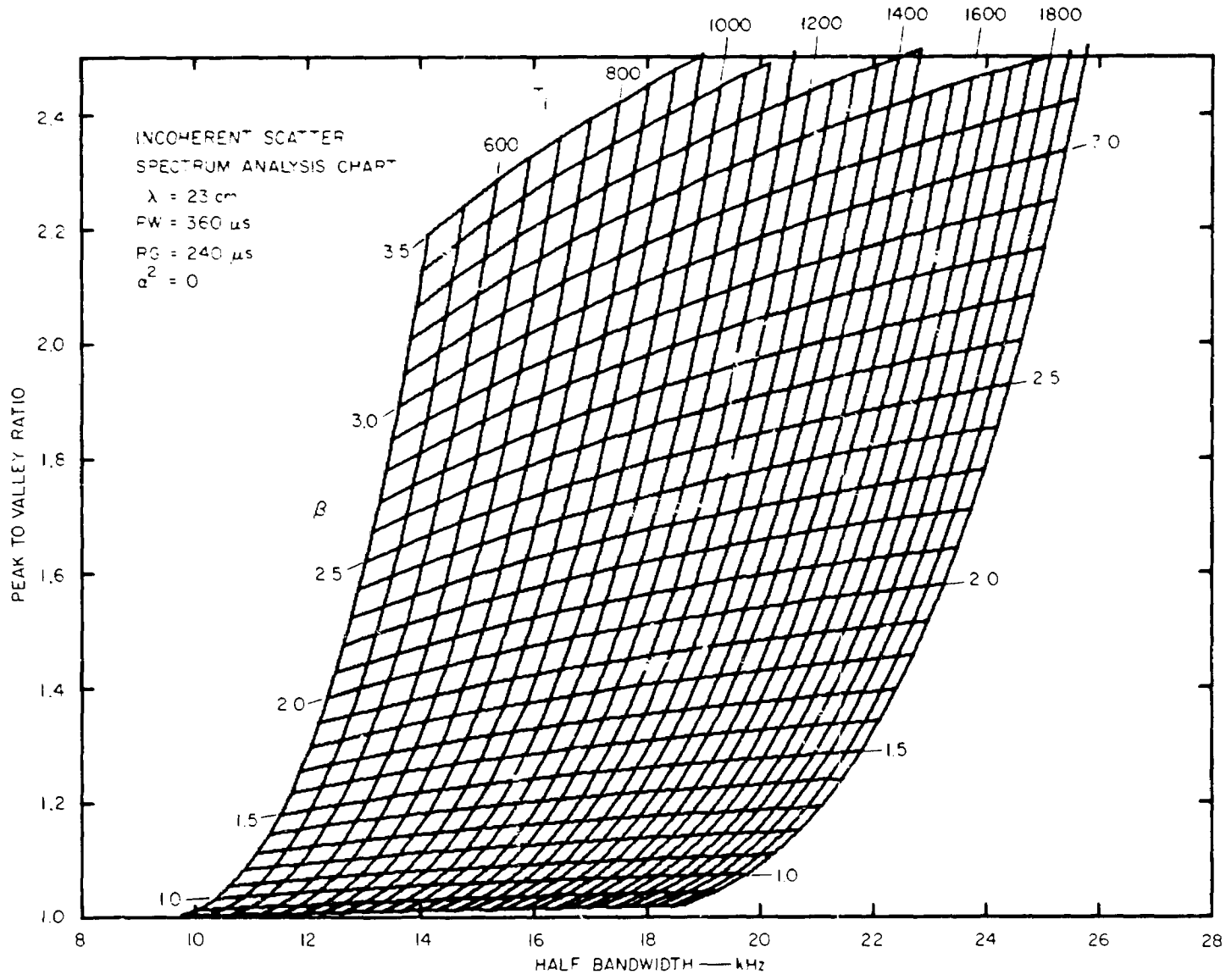

FIGURE 7 INCOHERENT SCATTER SPECTRUM ANALYSIS CHART λ = 23 cm, PW = 360 μs, RG = 240 μs, α^2 = 0

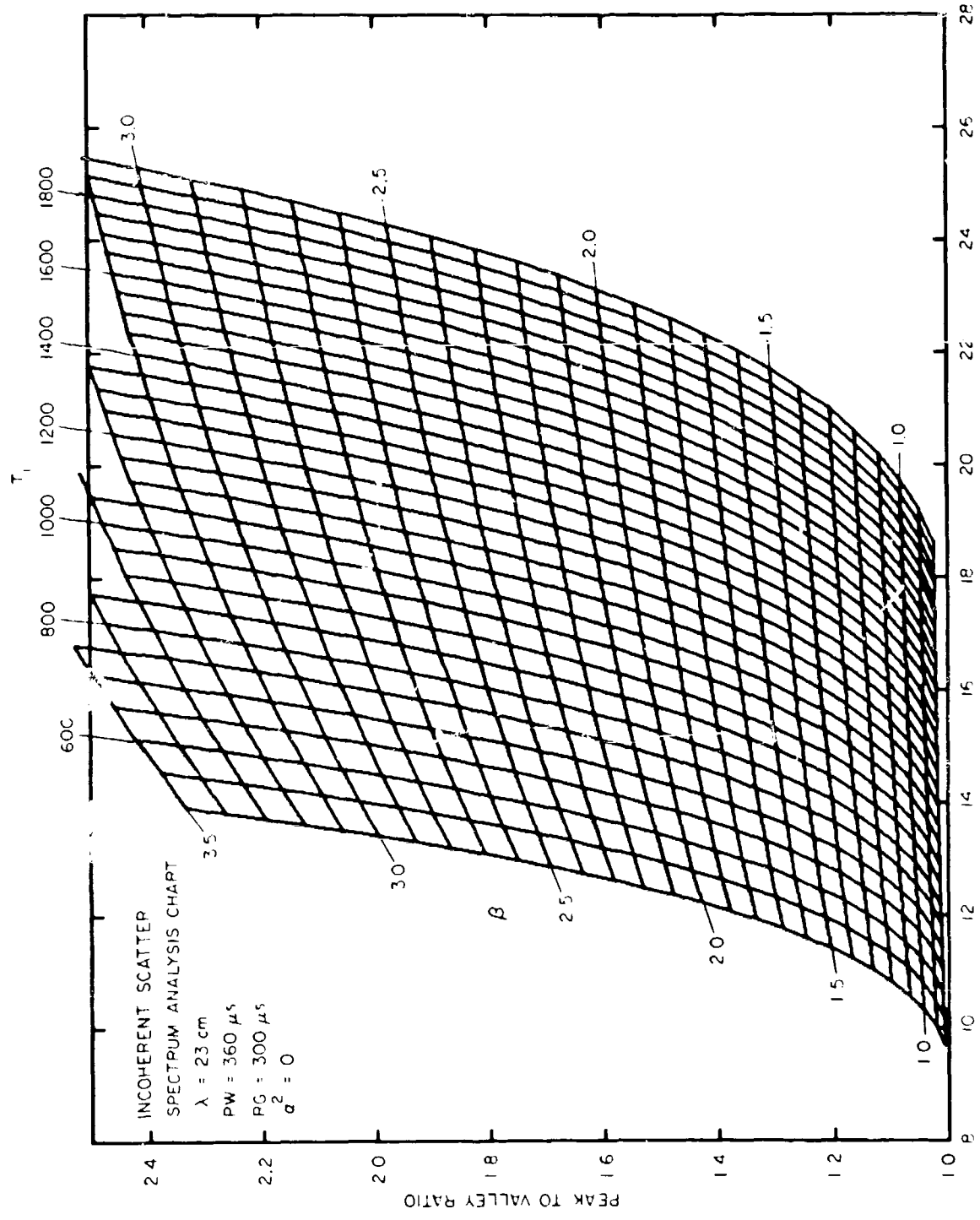

FIGURE 8 INCOHERENT SCATTER SPECTRUM ANALYSIS CHART λ = 23 cm, PW = 360 μs, RG = 300 μs, α^2 = 0

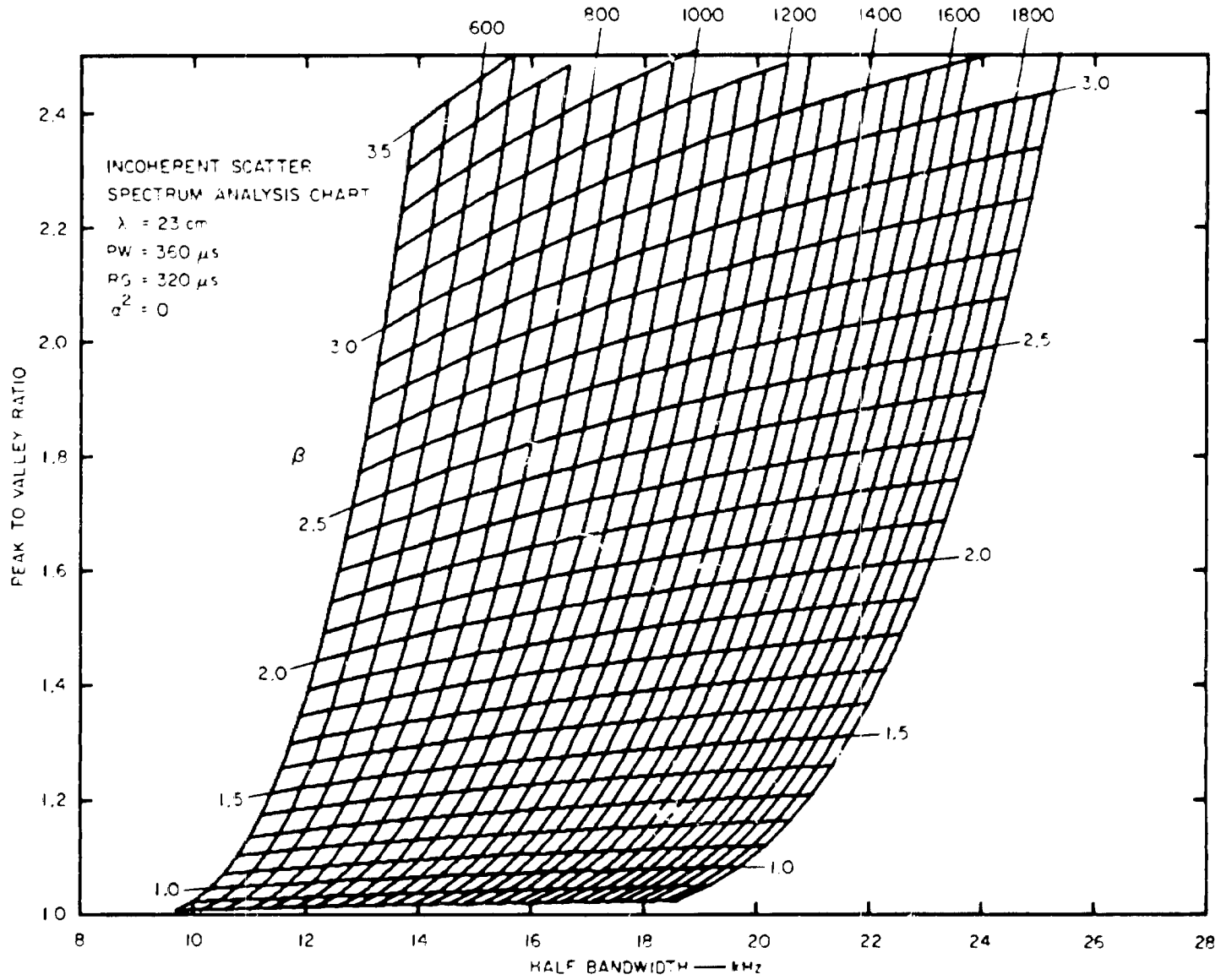

FIGURE 9 INCOHERENT SCATTER SPECTRUM ANALYSIS CHART λ = 23 cm, PW = 360 μs, RG = 320 μs, α^2 = 0

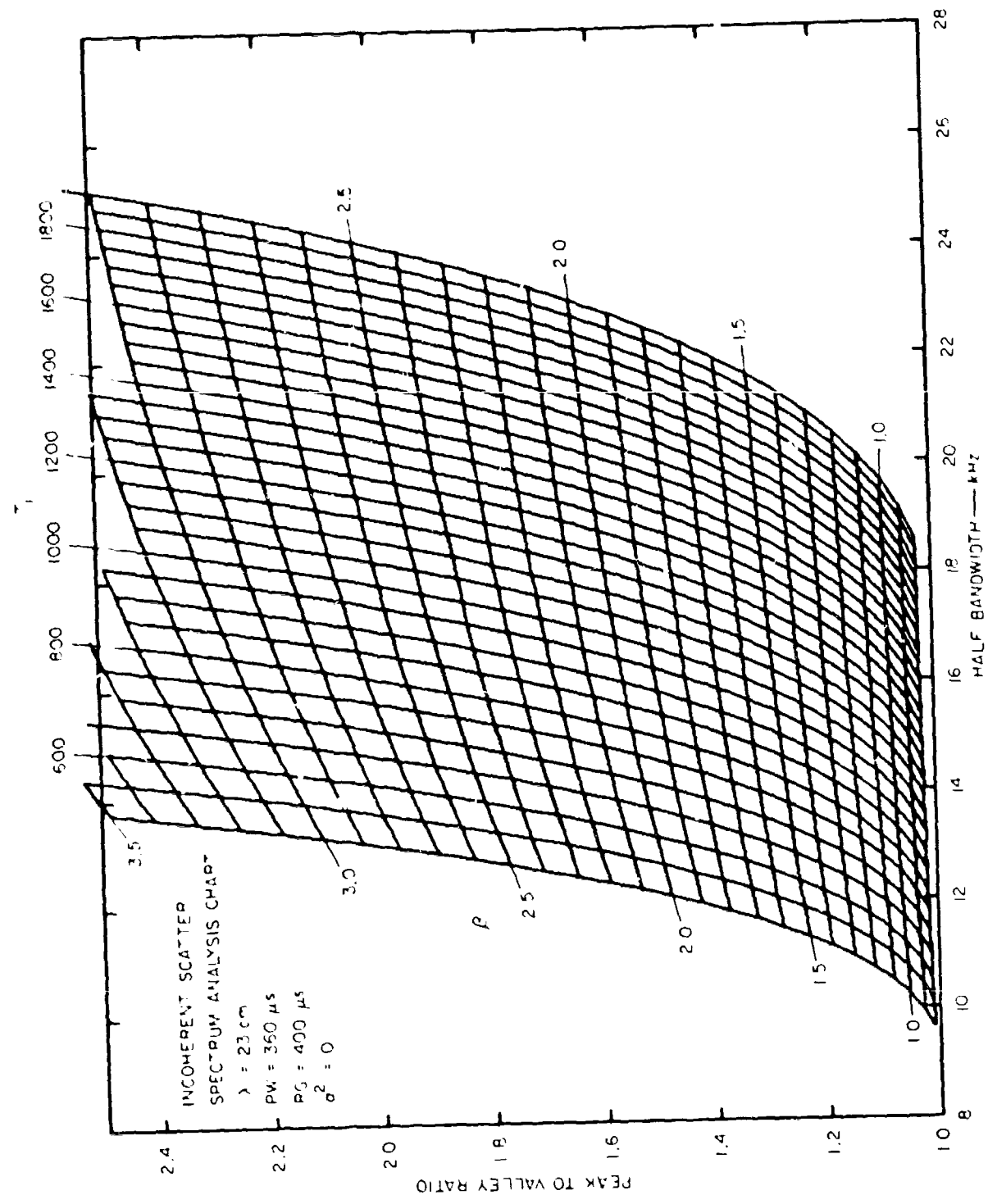

FIGURE 10 INCOHERENT SCATTER SPECTRUM ANALYSIS CHART λ = 23 cm, PW = 360 μs, RG = 400 μs, $\sigma^2 = 0$

4. Interpretation for $\alpha^2 < 1$.

Now let us relax the restriction we previously placed on N and thus on α^2. We let N assume its proper value, and thus α^2 will be non-zero. We require only $\alpha^2 \lesssim 1$. This is a reasonable requirement and will hold true throughout most of the ionosphere. As $\alpha^2 > 1$, the character of the spectra changes drastically, and the distinctive spectral features disappear.

The terms in the equation describing the incoherent scatter spectrum are so arranged that the spectral shape depends on α^2 in the same way that it depends on T_e/T_i. Moorcroft[7] showed if T_r is the true value of the electron-to-ion temperature ratio and β the fictitious ratio that would cause the same shaped spectrum if α^2 were zero, then

$$T_r = (1 + \alpha^2)\beta \qquad \alpha < 1 \quad . \tag{11}$$

This can be seen by examining the equation for the backscatter spectrum. From Final Report 2 [p. 10, Eq. (111-13)][8] we can write the denominator of the equation for the backscatter spectrum. (The numerator does not depend on T_r or α, only on T_i, and thus is not changed by changing T_r or α.) From Eq. (111-13) and assuming singly charged ions so that $|Z_2/Z_1| = 1$, the denominator, d, is

$$d = \{1 + \alpha^2 + T_r[\text{------}]\}^2 + T_r^2(\text{------}) \quad . \tag{12}$$

The terms indicated by dashes in parentheses determine the frequency dependence and are not affected by R_r or α. Substituting Eq. (11) in Eq. (12) we get

$$d = \{(1 + \alpha^2) + (1 + \alpha^2)\beta[\text{------}]\}^2 + (1 + \alpha^2)^2\beta^2(\text{------}) \tag{13}$$

and then, collecting terms,

$$d = (1 + \alpha^2)^2 \left\{ \left[1 + \beta \left[\text{------} \right] \right]^2 + \beta^2 \left(\text{------} \right) \right\} \quad . \qquad (14)$$

Thus we can see that the denominator has the same form for β and $\alpha = 0$ as it does for the real α and T_r. This will enable us, in data reduction, to use only one spectrum scaling chart (the chart for $\alpha = 0$) rather than separate scaling charts depending on the local electron density at each altitude.

The magnitude of the denominator is increased by $(1 + \alpha^2)^2$, thus reducing the total power in the spectrum by this same factor. This conclusion is verified by inspecting the equation for the scattering cross section:

$$\sigma = \frac{\sigma_e}{[1 + \alpha^2 + T_r](1 + \alpha^2)} \qquad (15)$$

where σ_e is the classical radar cross section of a single electron ($= 10^{-28} m^2$). Substituting $\beta(1 + \alpha^2)$ for T_r we get

$$\sigma = \frac{\sigma_e}{[1 + \alpha^2 + (1 + \alpha^2)\beta](1 + \alpha^2)} = \frac{\sigma_e}{(1 + \alpha^2)^2(1 + \beta)} \quad , \qquad (16)$$

which again shows the scattered power reduced by the factor $(1 + \alpha^2)^2$.

Now we can define an iterative procedure to determine T_e, T_i, and N, given T_i, β, and N', the raw density deduced from the power profile under the assumptions $T_r = 1$, $\alpha^2 = 0$. The parameters of interest are interrelated in the following ways:

(1) T_i and β are functions of PV and BW as obtained from the spectrum scaling chart for $\alpha = 0$.

(2) $$T_e = T_r * T_i = \beta(1 + \alpha^2)T_i. \quad (17)$$

(3) $$\alpha^2 = 14.22 \times 10^6 T_e/N. \quad (18)$$

(4) $$N = [N'(1 + \alpha^2)^2(1 + \beta)]/2. \quad (19)$$

The factor of 2 in Eq. (19) results from the assumption $T_r = 1$, $\alpha = 0$ used in calculating N'. The processing procedure is as follows:

Given: Measured parameters N', PV, and BW

Deduce: β, T_i from spectrum scaling chart

Initially: $\alpha^2 = 0$

Estimate: T_e from Eq. (17)

N from Eq. (19)

Calculate: α^2 from Eq. (18)

Next: Recalculate T_e, N, and α^2, and iterate around these three equations [(17), (18), and (19)] until a consistent solution is obtained.

In practice, the iteration is continued until both T_e and N change by less than 1 percent. This usually takes less than five iterations.

C. Assumptions, Interpolations, and Extrapolations

One assumption basic to the whole analysis procedure is that only one species of ion, namely O^+, is present in the ionospheric height regime over which we are probing. This is probably a good assumption over the height region where our radar is capable of making spectrum measurements (200 to 550 km), particularly at our midlatitude location at the present time near sunspot maximum. The presence of other ions, NO^+ or O_2^+ at low altitudes and He^+ or H^+ at high altitudes, would not significantly change the scattering cross section. Therefore, the power profile measurement of raw density is not affected. However, significant amounts (>10 percent) of other ions would markedly affect the incoherent scatter spectrum. The effect of multiple ionic species has been discussed by Moorcroft.[7] For any single species, the shape of the spectrum remains essentially unchanged, with the width of the spectrum being inversely proportional to the square root of the ion mass. For a mixture of ions, the spectral shape now depends on the relative abundance of the species present.

Our assumption of only O^+ ions being present may under certain conditions lead to errors in the deduced temperature at both high and low altitudes. At the high altitudes, if lighter ions were present, our T_r would be underestimated and our T_i would be overestimated. At low altitudes, if some heavier ions were present, we would again underestimate T_r and also underestimate T_i.

Another assumption used in the data processing is that no ionospheric drifts or currents are present. If drifts or currents, or both, were present, they would cause shifts or asymmetries, or both, in the measured spectra. In the processing procedure, the spectra are folded about their center frequency, and the two sides are averaged prior to the determination of peak-to valley ratio and bandwidth. This is done to increase the

signal-to-noise ratio and thus improve measurement accuracy. But this procedure masks any shifts or asymmetries that might be present. Attempts have been made to detect these drifts and currents. No currents (spectral asymmetries) have been found. Small drifts (spectral shifts) have been found. These shifts, when they are present, are of the order of 100 to 300 Hz (11.5 to 34.5 m/s). Their effects on the temperatures inferred, assuming zero drift, are very small. The measured bandwidth is not changed, but the measured peak-to-valley ratio is slightly underestimated, leading to slight underestimates of T_r and overestimates of T_i. The errors in inferred temperature introduced by drifts of 20 m/s are less than 5 percent.

Spectral measurements are performed only at eight discrete heights--generally 200, 250, 300, 350, 400, 450, 500, and 550 km--while raw density measurements are made every few kilometers between roughly 150 and 900 km. In order to calculate true densities between altitudes at which spectra (temperatures) are available, the temperatures are linearly interpolated between the measured data points. Then, by using the interpolated temperatures and the raw density, the true density can be computed by using Eq. (7).

Raw density measurements can be made to lower altitudes than temperature measurements. Since received power is measured every 4.5 km but the spectral measurement is made within a relatively long range gate (36 to 60 km), it is common for ground clutter to pollute the spectral measurement while not polluting the raw density measurement. For example, if ground clutter existed out to a range of 185 km, the spectrum range gate centered at 200 km would include some ground clutter, since it extends from 182 to 218 km. But the power profile measurement would be free of ground clutter for all ranges greater than 185 km. The lowest altitude (R_L) at which temperatures are obtained would be 250 km for

this case, and some means of extrapolating the temperatures downward to 185 km is needed in order to obtain true densities from raw densities over the range 185 to 250 km. The method employed makes use of the assumption that the ion and neutral temperatures are equal below R_L. There is good theoretical evidence[9,10] that this must be the case at least up to 250 km. The variation of neutral, and thus ion, temperature was assumed to be of the form adopted in the CIRA 1965 model atmosphere,

$$T_i = T_i(R_L) - [T_i(130)] \exp [-s(h - 130)] \quad , \qquad (20)$$

where T_i(130 km) is taken to be 550°K, and the exponent, s, is given the value 0.028.

Below R_L an assumed form for T_r as a function of altitude is also needed. The assumption, backed by evidence,[11] that $T_r = 1$ at 130 km and below is used, and T_r is linearly interpolated between its value at R_L and the value 1 at 130 km by using Eq. (21),

$$T_r = 1 + [T_r(R_L) - 1.0]\left[\frac{h - 130}{R_L - 130}\right] \qquad (21)$$

Using these extrapolated values for T_r and T_i, T_e can be computed and the true density then found through Eq. (7).

At high altitudes (h > 500 km or so) another extrapolation of temperatures is necessary, since low signal-to-noise ratios limit the upper altitudes at which spectral measurements can be made before they limit the power profile measurements. The topside extrapolation is based on the assumption that T_e is essentially isothermal above the highest altitude (R_U), at which spectra are obtained, usually about 500 km. This is to be theoretically expected in the absence of major heat sources at or

above these altitudes and because of the high thermal conductivity of the gas. An additional assumption used is that T_r varies linearly from its measured value at R_U to 1.0 at h = 800 km and that it is equal to unity above 800 km. Thus the temperature extrapolations at altitudes above which usable spectra are available are summarized by the following equations:

$$T_e(h) = T_e(R_U) \qquad h > R_U \qquad (22)$$

$$T_r(h) = T_r(R_U) + [1 - T_r(R_U)]\left[\frac{h - R_U}{800 - R_U}\right] \qquad : R_U < h < 800 \qquad (23)$$

$$T_r(h) = 1 \qquad h > 800 \qquad (24)$$

$$T_i(h) = T_e(h)/T_r(h) \quad , \qquad (25)$$

where R_U is the uppermost altitude at which temperatures are measured, and all altitudes are in kilometers. With these extrapolated temperatures, the raw density given by the power profile measurement is then corrected by using Eq. (7) to obtain true density.

PRECEDING PAGE BLANK-NOT FILMED

III HARDWARE

The DASA Project 617 radar used for the incoherent scatter measurements consists of a number of basic subsystems; the major subsystems are: (1) transmitter and waveguide, (2) antenna and feed, (3) receivers, (4) calibration equipment, (5) analog-to-digital conversion, (6) digital autocorrelator, and (7) computer. Several modifications and additions have been made to the system during the past year. This section describes the new equipments and the new configurations of existing equipments implemented during the past year. Table I reviews the radar system parameters.

A. Receiving and Calibration System

In order to match the final IF frequency of the receiver to the digital autocorrelator sampling frequency, several changes have been made in the receiv -local oscillator chain. Figure 11 is a block diagram of the receiver chain. The signal, after reception by the antenna, passes through a directional coupler, duplexer, and second directional coupler before entering the parametric amplifiers. The two directional couplers are used to insert calibration signals as required. (The calibration signals are considered further later.) Two parametric amplifiers are cascaded in series, resulting in a 110°K system noise temperature, with the pa amps operated at room temperature (not cooled). After the paramps, the power is split and travels down two mixer-amplifier chains, one for the normal on-frequency component of the incoherent scatter signal and one for the "plasma-line" component, which returns from the ionosphere frequency-shifted from the transmitted frequency by the plasma frequency. Focusing on the normal channel (right-hand side of Figure 11), we see

Table 1

DASA RADAR SYSTEM PARAMETERS

Parameter	Adjustment Range	Normal Operation
Transmit Frequency	1280-1300 MHz	1290 MHz
Transmit Power (peak)	0-5 MW	4 MW
Duty Cycle (max.)	3%	2.7%
Transmit Polarization		RHC
Receive Polarization		LHC
Antenna Diameter		88 ft
Antenna Aperture		180 m^2
Antenna Gain		47.1 dB
System Noise Temperature		110 ^{o}K
Pulse Length	10-500 μs	360 μs
Receiver Video Bandwidth	4-200 kHz	32 kHz
Receiver IF Bandwidth	$\leq$10 MHz	50 kHz

that the RF signal at 1290 MHz is mixed with 1320.425 MHz to obtain an IF frequency of 30.425 MHz, which is then preamplified. So far, all the mixing and amplifying of the signal is done in the torque tube of the antenna, as close as possible to the antenna feed. The 30.425-MHz IF is then sent from the torque tube to the equipment van, where it is again mixed, this time with a 30-MHz signal to obtain a 425-kHz IF. After amplification, the signal splits into two channels. One channel passes through an adjustable bandwidth filter and is then linearly detected. This channel, after analog-to-digital conversion, supplies the power profile data to the digital autocorrelator, which passes it on to the computer. The second 425-kHz IF channel is mixed with a 500-kHz signal to obtain a 75-kHz IF signal, which is amplified, bandpass filtered to a bandwidth of 50 kHz, and sampled by another ADC. This channel is used as input to the digital autocorrelator and carries all the spectral information.

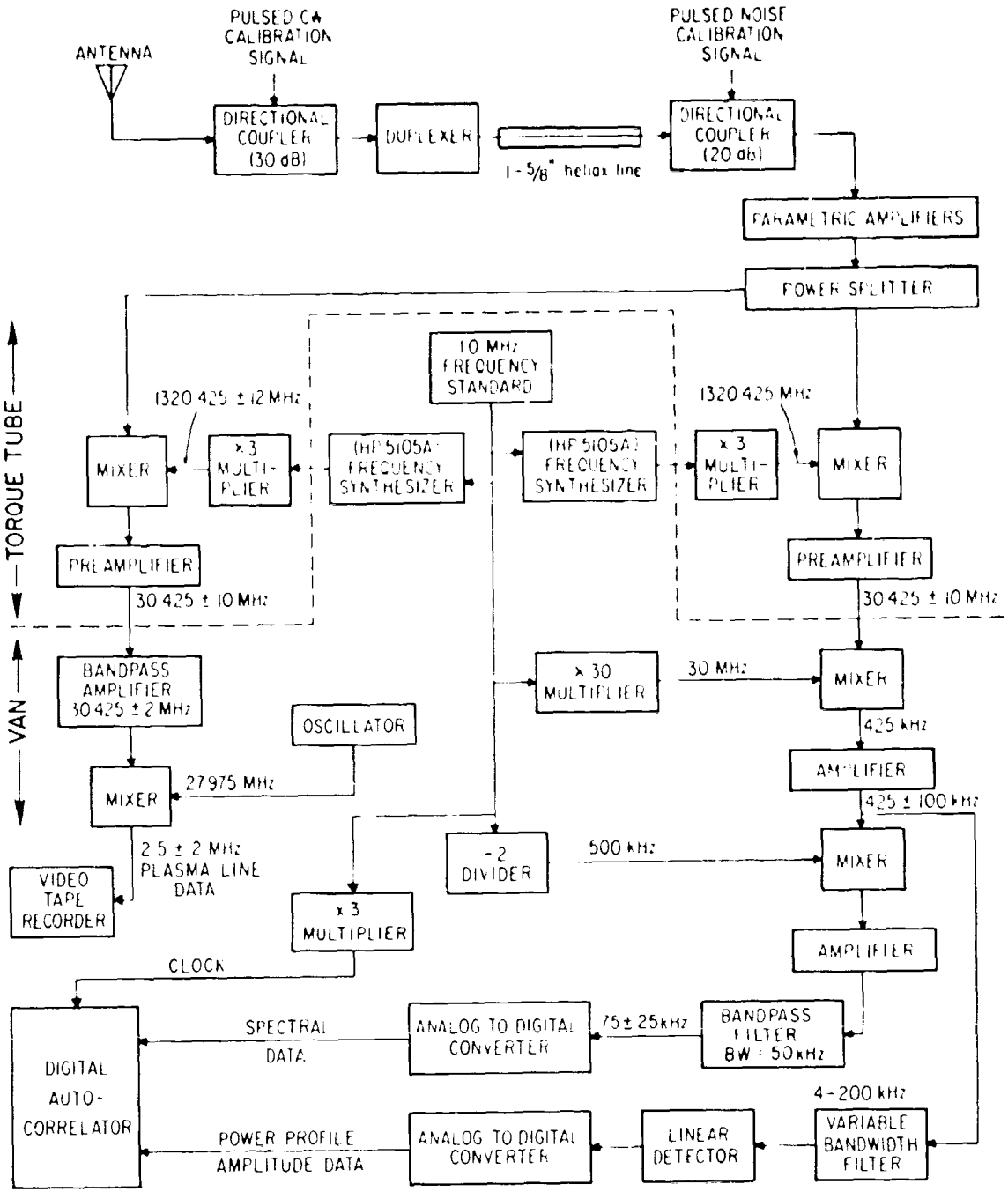

FIGURE 11 RECEIVER SYSTEM BLOCK DIAGRAM

Returning now to the plasma line chain (left-hand side of Figure 11), the power that was split off following the paramps enters a mixer. The mixing frequency is selected by the operator so as to be offset from 1320.425 MHz by the approximate plasma frequency of the F layer. The output of the mixer and the preamplifier following the mixer is thus a band of frequencies with f_p centered at 30.425 MHz, where f_p is the plasma frequency. After passing from the torque tube to the van, the signal is amplified and bandlimited to a 4-MHz bandwidth and mixed with 27.975 MHz to obtain a signal at 2.5 ± 2 MHz, which can then be video-tape recorded.

All local oscillator frequencies, except the last one in the plasma line chain, are derived from frequency synthesizers locked to a common frequency standard. The clock pulses used by the digital autocorrelator and the triggers for the ADCs are derived from the same frequency standard.

Provisions for inserting either a pulsed CW calibration signal or a pulsed noise source calibration signal are included in the receiver system. The CW calibration is provided by a signal generator located in the van, which is continuously tunable in frequency and continuously adjustable in amplitude. This signal is inserted through a 30-dB directional coupler immediately following the antenna and is used for making frequency response, gain, and loss measurements throughout the receiver system. It is not used for continuous calibration of the system during the course of a data run, since the signal generator frequency stability is not sufficient to keep it within the 50-kHz band for more than a few tens of seconds without constant retuning.

The pulsed noise source, inserted through a 20-dB directional coupler in front of the paramps, is used to continuously calibrate and monitor the receiving system performance during the course of a data run. Figure 12 is a block diagram of the pulsed noise calibration system. The system uses a broadband neon noise source (noise temperature 18,000°K),

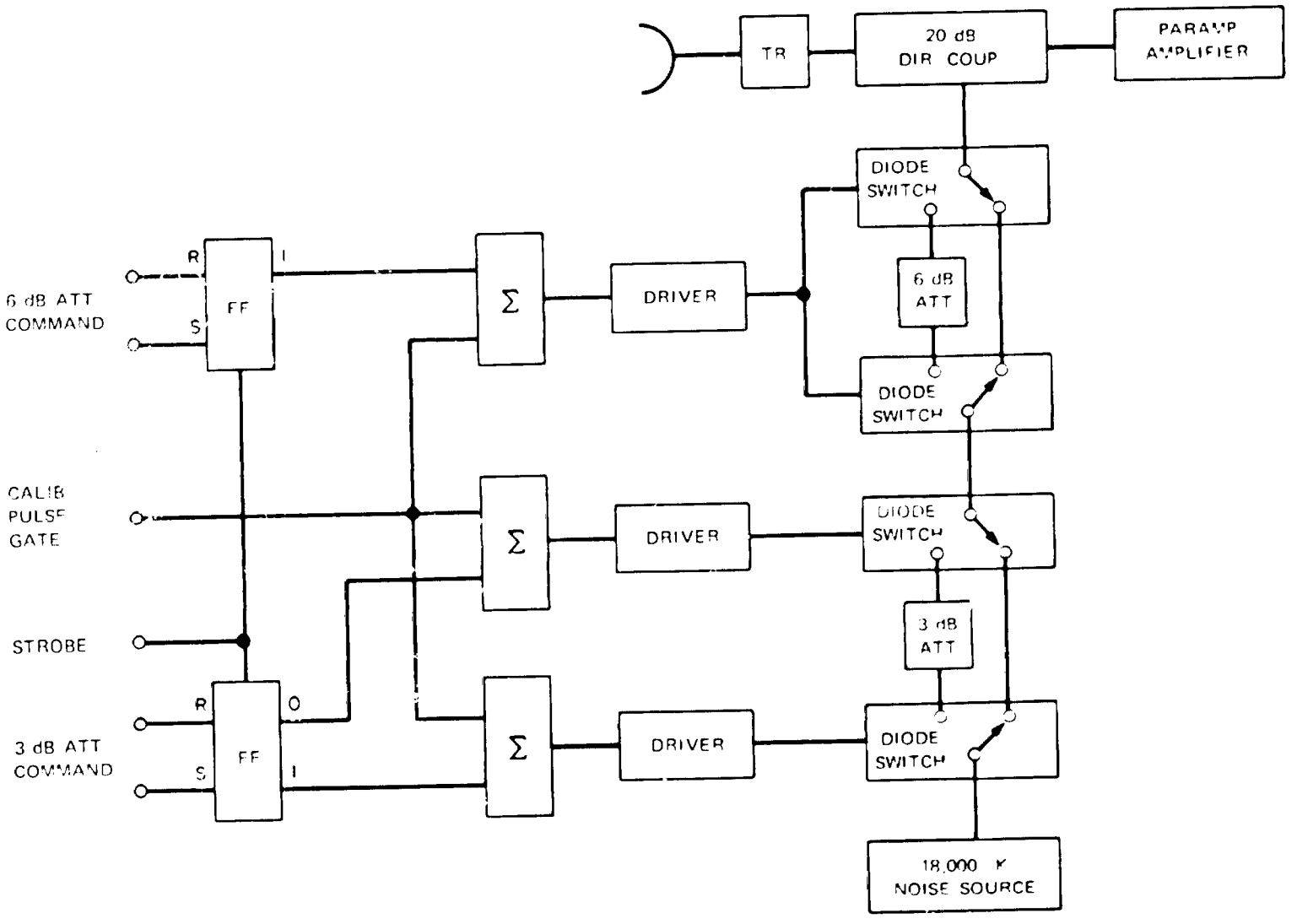

FIGURE 12 CALIBRATION SYSTEM BLOCK DIAGRAM

digitally controlled diode switches, and calibrated attenuators to enable any of four selectable amplitudes of wideband pulsed noise to be injected into the receiver chain. With this system, the four equivalent noise temperatures that can be used are 70°, 35°, 17.5°, and 8.75°K, after taking into account approximately 1 dB of loss introduced by each diode switch.

Attenuation commands and strobe are supplied by the computer. The gate supplies pulsed modulation of the injected noise once per interpulse period. The gating waveform is supplied by the radar synchronizer and generated by counting down the density channel ADC trigger pulses to ensure that it always occurs in the same position during the interpulse period. The countdown circuits are so arranged that the gating waveform always occurs during the last sixteen of the 192 samples taken by the ADC.

B. Analog-to-Digital Conversion Equipment

Two ADCs are used with the system, one to digitize the detected video signal and one to digitize the 75-kHz IF signal.

The density channel (detected video) data are digitized by an Adcom 208C unipolar ADC. This unit is capable of digitization speeds up to 100,000 samples per second and has 8-bit resolution; that is, the signal is quantized into 256 discrete values. Sample triggers for it are generated in the Adcom computer interface and occur at either 30- or 60-μs intervals, selectable by the operator. The first sample trigger occurs at an operator-selected delay past the leading edge of the transmitted pulse; 192 samples are taken during each interpulse period. Figure 13 shows the sample timing; DTE is the "delay time end," the time at which the first sample is taken. Equation (26) may be used to calculate the apparent radar range to the position of the first sample, with DN

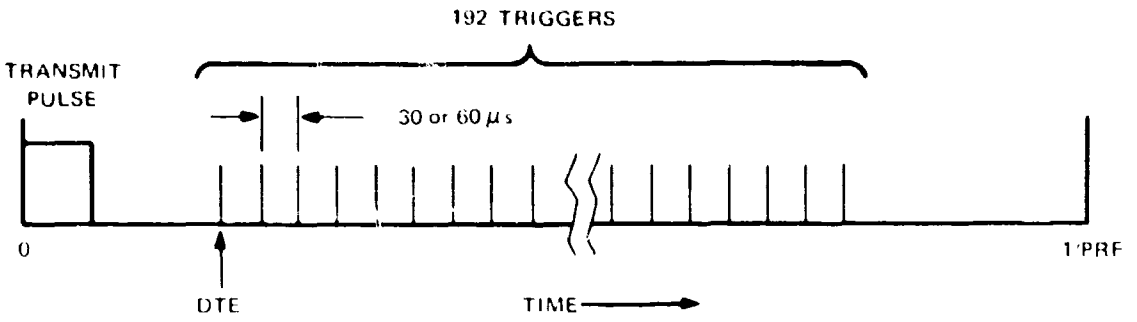

FIGURE 13 DENSITY CHANNEL SAMPLE TIMING

being the number set into the thumbwheel switches used to count down the delay:

$$\text{DTE (km)} = 3.3 + 20\,(DN - 1) \quad . \qquad (26)$$

During the last sixteen of the 192 samples, the pulsed noise calibration signal is present. The sixteen samples in front of the calibration pulse are generally used to estimate the baseline noise level, $\bar{P}_n$. Digital numbers produced by the ADC are fed into the XDS 930 computer after routing through the digital autocorrelator chassis, which controls placing the numbers in computer memory.

The 75-kHz IF signal is digitized by a Preston Scientific 8500 MS ADC. This unit is a 9-bit bipolar (2's complement) converter capable of operating at a maximum speed of 250 kHz. The most significant 8 bits of each sample are passed on to the digital autocorrelator, which uses them in its autocorrelation computation. Triggers for the Preston ADC are generated by the autocorrelator. Figure 14 shows the IF channel sample timing for a typical operating setup. Nine bursts of samples are taken, eight at ranges where the incoherent scatter signal is present and one at a range where no signal, only receiver noise, is present. Each burst consists of 24 (or 32) samples spaced by 10 μs (or 12). The delays R1, RN, and Δr are determined by one-shot multivibrators which the

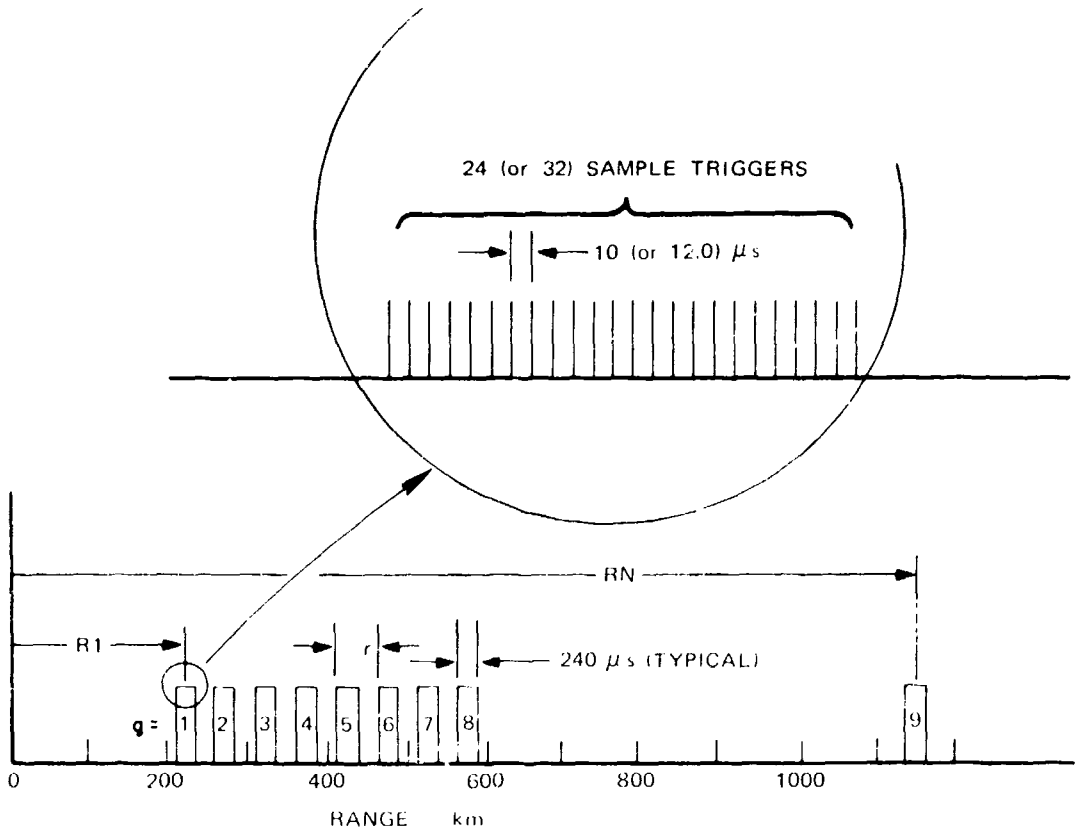

FIGURE 14 IF CHANNEL SAMPLE TIMING

operator may adjust as required. The burst of samples centered at R1 is used by the autocorrelator to produce the autocorrelation coefficients for range R1, which are then passed on to the XDS 930 computer, and similarly for the other eight sample bursts.

C. Digital Autocorrelator

1. Introduction

As part of the processing of incoherent scatter data, it is necessary to determine the autocorrelation function (or equivalently, the spectrum) of the received radar signal in order to obtain ionospheric electron and ion temperatures. To measure these temperatures as a function of altitude, the correlation function must be measured at a number of radar ranges.

Several alternatives for measuring the correlation function or spectrum are possible. A bank of analog filters and integrators could be implemented, into which the range-gated received signal could be played. This approach has several disadvantages: (1) Construction of such a filter bank is expensive; (2) achieving identical transfer characteristics for each filter in the bank is difficult; (3) achieving identical gains in each filter-integrator channel is almost impossible; and (4) compensating for nonidentical filter characteristics and unequal gains in the post-filtering processing of the data is tedious and expensive.

A single fixed-frequency analog filter could be used, and heterodyning technique could be used for successive analysis of each frequency in the received signal through the same filter. This approach has several disadvantages, stemming from the requirement of range-gating the received signal and also from the desire to minimize the measurement time by measuring many frequency components simultaneously.

Another possible technique is to sample the received signal with an ADC and then perform the autocorrelation calculation in a general purpose digital computer. The principal disadvantage of this technique is that a large amount of computer time is consumed in the calculation, making it impossible to process the data from more than a very few range gates in real time. Thus, the data from several range gates must first be recorded on digital tape and then processed later. This technique has been used with the Project 617 radar during the past two years, but three times as much computer time was required to process the data as to record them.

During the past year, a Digital Autocorrelator was designed and constructed. This device is essentially a special-purpose computer that calculates the autocorrelation functions at nine range gates in real time and passes the correlation coefficients to the on-line computer for

integration and recording. The recorded data can then be processed very quickly (faster than real time), since the bulk of the computations have already been done in real time by the Digital Autocorrelator.

A block diagram of the incoherent scatter processing system is shown in Figure 15. The 75-kHz IF signal is first bandlimited to frequencies between 50 and 100 kHz and then sampled at a 100-kHz rate. This allows a 50-kHz band of frequencies to be analyzed, and "aliasing" folds the 50-to-100-kHz band into the 0-to-50-kHz region. It is important for the presampling bandpass filter to have very sharp skirts so that spurious frequency components in the 0-to-50-KHz band and at frequencies above 100 kHz do not appear at the input to the ADC. Figure 16 shows the frequency response of the presampling filter used in our system. Sampling and analog-to-digital conversion of the IF signal is performed by the Preston Scientific ADC, as was described in the previous section. Timing in the correlator is generated by counting down a stable 3-MHz clock signal generated by a frequency synthesizer. A group of 24 or 32 samples

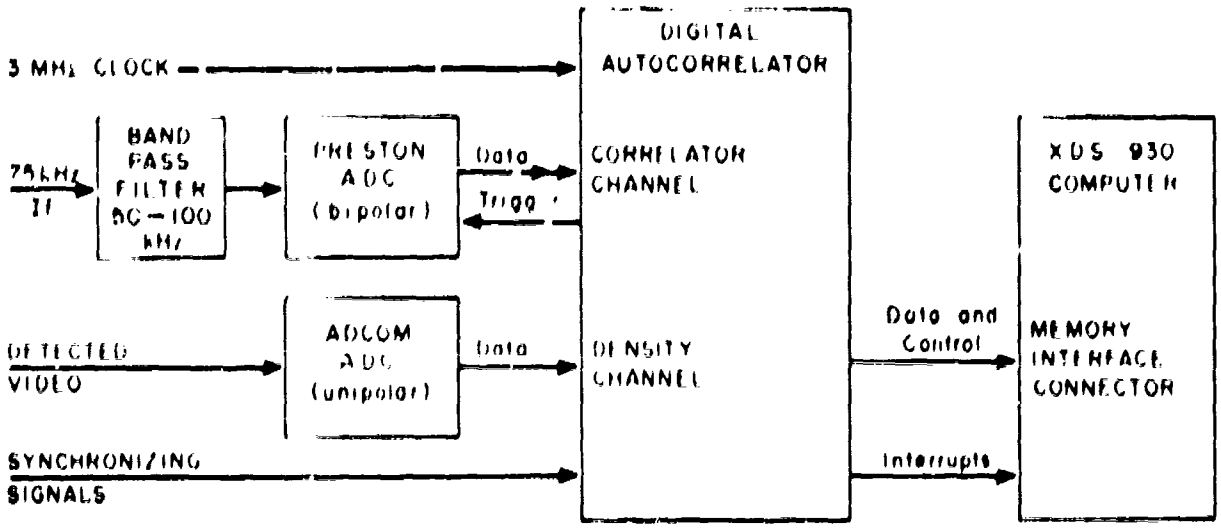

FIGURE 16 SYSTEM BLOCK DIAGRAM

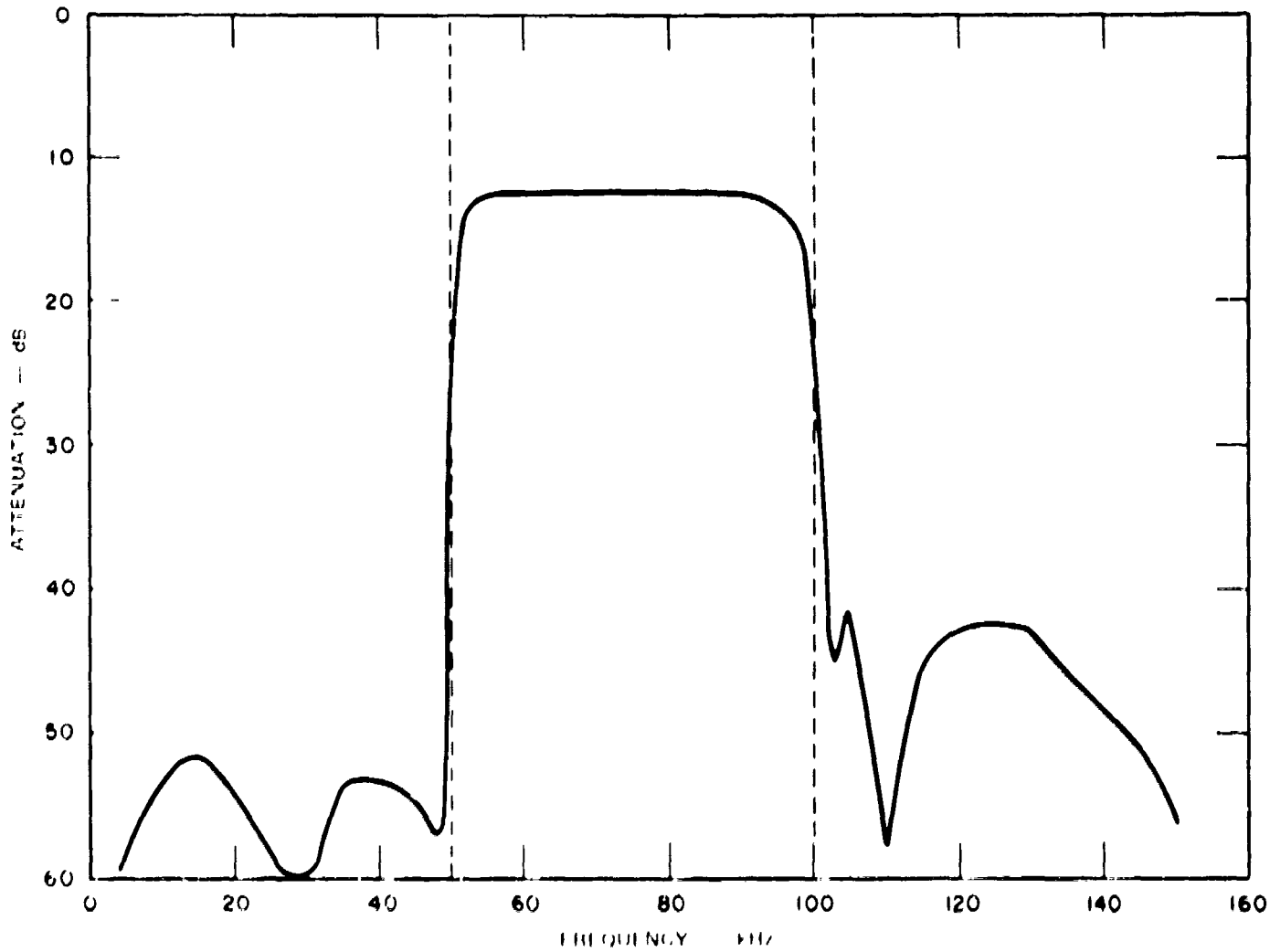

FIGURE 16 PRESAMPLING BANDPASS FILTER

(switch selectable) is taken, and 24 or 32 autocorrelation coefficients are generated and inputted to the XDS 930 computer through its Memory Interface Connector. Within less than 20 μs after the burst of samples has been taken, a new burst can be started. Sampling of the IF channel, computation of the correlation coefficients, and outputting of data to the computer may all take place simultaneously.

The Digital Autocorrelator, as implemented, performs several additional functions. It accepts sampled data from the ADCOM 8-bit unipolar ADC and controls the passing of these data to the computer's

Memory Interface Connector. The ADCOM ADC samples the receiver's detected video signal, which is used to generate electron density profiles. The sampling of the detected video channel is asynchronous with the sampling of the IF channel.

The correlator also receives several synchronizing signals from the radar system and generates appropriate interrupts for the computer to allow the computer's real-time program to stay in synchronization.

Data are entered into the computer through its Memory Interface Connector. This is essentially a direct path to memory and allows data to be stored in memory without program control. A single computer cycle is "stolen" from the running program for each data word placed in memory by the correlator. The correlator controls the inputting of both correlation coefficients and sampled video data to the computer by generating appropriate computer memory addresses and control signals.

For our application, the correlator is normally so set up that nine bursts (range gates) of autocorrelation channel samples are taken in each interpulse period. The first burst is centered at a nominal range of 200 km, and the next seven bursts are taken at 50-km intervals out to 550 km. The ninth burst is usually positioned at a range greater than 1000 km, where no incoherent scatter signal is present. This allows the autocorrelation function of the received noise to be determined so that the noise can be subtracted from the first eight gates where both signal and noise are present.

As an example of the time savings made possible through the use of the correlator, the off-line computer processing that took one hour prior to the implementation of the correlator now takes about 5 minutes. This represents an order of magnitude savings in the cost of both data reduction personnel and computer time. It also greatly reduces the time lag between the running of an experiment and the availability of results.

2. Description

The prime function of the Digital Autocorrelator is to perform certain computations on quantized signals representing radar returns. The nature of the computations is such that they can be done by a general purpose digital computer, but only very inefficiently with respect to the time required. The autocorrelator does these computations essentially in real time, releasing the computer for other calculations at which it is more efficient.

Consider a time-varying voltage, $v(t)$, which represents a known function of received signal amplitude and/or phase. At regular intervals this voltage is sampled and quantized by an ADC. The quantization is to an 8-bit, signed, 2's complement binary number, and is done in bursts of either 24 or 32 samples. Each burst results in a group or sequence of numbers, v_i, where i ranges from 1 to L, and L is either 24 or 32. Each group of v_i's is treated as a separate set of input data by the autocorrelator and it computes a set of output numbers, AC_ℓ, where

$$AC_\ell = \sum_{i=1}^{L-\ell} v_i v_{\ell+i} \qquad \begin{Bmatrix} 0 \le \ell \le L-1 \\ 1 \le i \le L \\ L = 24 \text{ or } 32 \end{Bmatrix} , \qquad (27)$$

Included in the unit are circuitry for establishing delays from an externally supplied synchronizing signal to the beginning of each group of samples and for selecting L and the sampling interval (which may be either 10 or 12.5 μs).

The computation is done continuously, while samples of a group are being accepted and is complete within 10 μs of receipt of the last sample. The transfer of the results to the computer takes slightly less

time than does the computation, and a new group may commence as soon as AC_0 of the preceding group has been transferred.

The unit is designed to communicate with an XDS 930 computer equipped with Multiple Access to Memory (MAM) and Memory Interface Connector (MIC) options. Certain control functions are accepted from the computer as well. A second data channel is built into the unit, so that raw output from a second ADC can also be transferred to the computer. Transfer is to specified blocks of memory, and the two types of data are stored in separate sets of locations.

A brief description of the operation of the autocorrelator follows, referencing the block diagram, Figure 17. Eight-bit parallel data from the ADC are fed to the Input Register, an 8-bit-wide-by-32-bit-long shift register. Initially, the register is cleared to all zeroes. The first End-of-Conversion (EOC) pulse shifts the 8-bit ADC word into the first rank of the register. The second EOC shifts the first word down to the second rank, at the same time that the current word is shifted into the first rank. Subsequent EOC pulses continue to shift previous words down the register and place the new word into the first rank. Each rank of the Input Register is also connected to a corresponding Arithmetic Unit, for which the register word serves as a multiplicand.

The output of the ADC is also fed to the Arithmetic Control Logic. The EOC pulse sets the ADC word into a multiplier register in this section. Other circuitry in this section, triggered by the EOC, provides a sequence of signals which cause the Arithmetic Units to form the product of the multiplier and the respective multiplicand and to add this to the accumulated sum of previous products.

Each of the 32 identical Arithmetic Units contains a 20-bit accumulator which is a register capable of being either shifted or loaded in parallel. The parallel inputs are provided by a 20-bit parallel adder

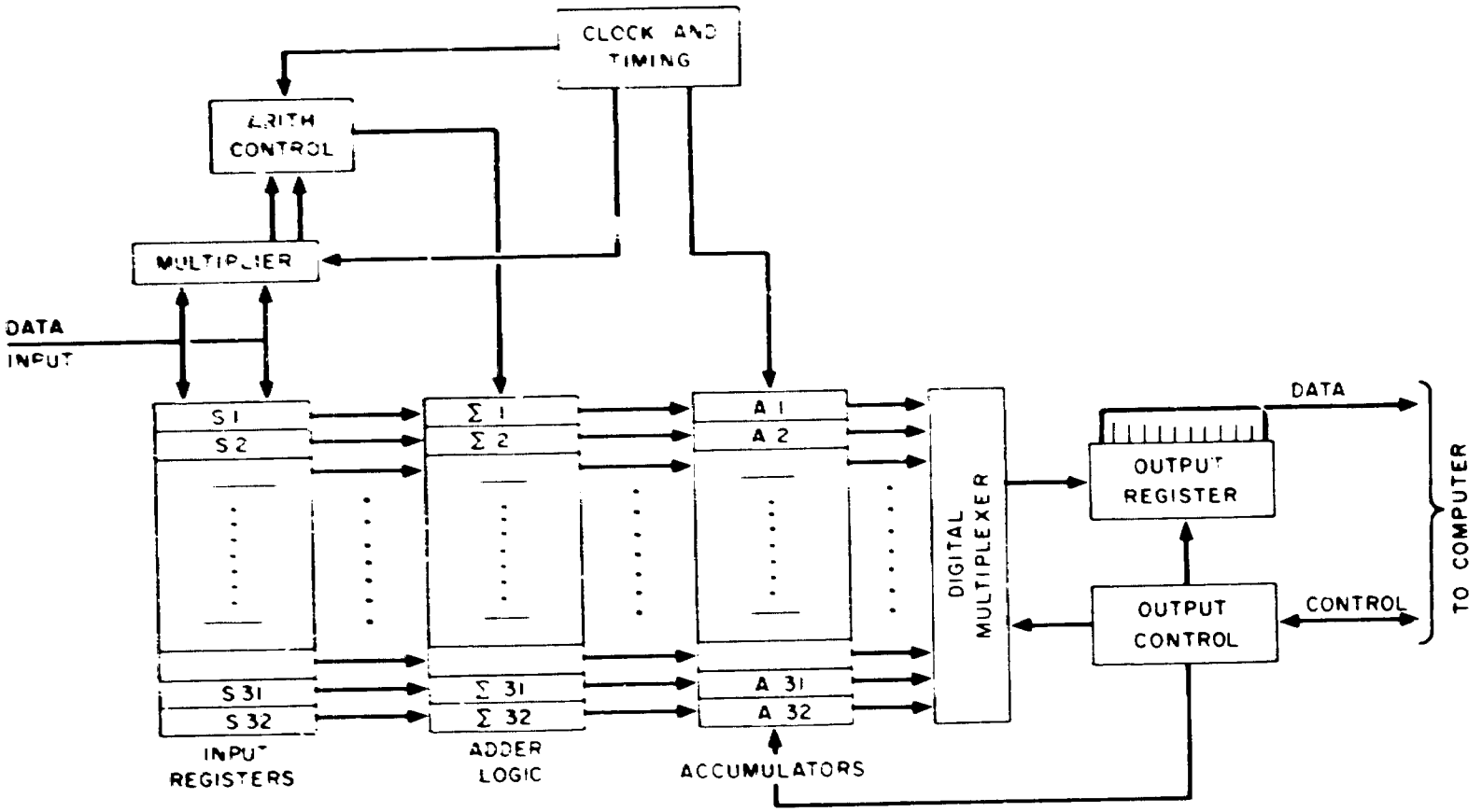

FIGURE 17 SIMPLIFIED AUTOCORRELATOR BLOCK DIAGRAM

network, which forms the sum of the accumulator contents and the multiplicand. Multiplication is done by an alternating sequence of adding into the accumulator followed by shifting the accumulator one bit. The adding is conditional on the state of low-order bits in the multiplier register. The result of such a multiply sequence is to form the product of the current multiplier and multiplicand and add it to the number previously held in the accumulator.

Before any computation starts, all accumulators contain zeroes. After the first multiply sequence, the first accumulator contains the product of the first ADC word multiplied by itself, of v_1^2. The remaining accumulators are still zero, since all multiplicands except the first are zero. After the second multiply sequence, the first accumulator contains $v_1^2 + v_2^2$, the second one contains $v_1 v_2$, and the rest are zero. After the third sequence, the accumulators contain $(v_1^2 + v_2^2 + v_3^2)$, $(v_1 v_2 + v_2 v_3)$, $(v_1 v_3)$, and the rest zeroes. In other words, arithmetic operations produce significant results at first in the first accumulator, next in the first two, then the first three, etc. After the 32nd, or last multiply sequence, the accumulators contain the 32 AC_ℓ which are now ready for transfer to the computer.

The End Compute signal is generated at this time to trigger the Output Control Logic. Here, control signals are generated that select each accumulator in order and do the following. First, the serial output of the accumulator is connected to the serial input of an output register. Next, a series of shift pulses is applied to the selected accumulator and to the output register, so as to transfer the accumulator contents to the output register. At the same time, the serial input to the accumulator is held at a logic zero level, so that zeroes are shifted into the accumulator. When the entire contents of the accumulator have been transferred to the output register, a Request signal is sent to the computer. The parallel outputs of the output register are permanently connected, through line

drivers, to the computer data inputs. When the computer recognizes the request, it starts a sequence of first reading the address and then the data word. When the computer has accepted the data word, it sends back an acknowledge signal, which triggers the sequence all over again for the next accumulator.

As has been pointed out, during an input-computation cycle, the accumulators are brought into significant use successively. Advantage is taken of this to permit subsequent computation cycles to begin before the contents of all the accumulators have been transferred to the computer. A signal is provided to each Arithmetic Unit (A_1 through A_{32}) by the Arithmetic Control Logic that positively inhibits arithmetic operation until such operation can produce nonzero results. As a result, some accumulators can retain their previously computed numbers, even while new numbers are being formed in lower-numbered units. The only limitations are: (1) that the subsequent computation cycle not start until accumulator number one has been output and cleared and (2) that the computer accept data at least as fast as the ADC is sampled. The ADC sampling rate is either 100 or 83 kHz (or one sample every 10 or 12 μs). The computer will accept words through the MIC at a rate of one word per memory cycle (570 kHz), but the Output Control will require time equivalent to three or four cycles to transfer each word to the output register. Thus, an output to the computer will take place at intervals of either 7.0 or 8.75 μs (4 or 5 memory cycles). In either case, this will be fast enough to stay ahead of the computation.

The autocorrelator is packaged in a 5-1/4-inch-high standard rack mounting unit. A separate external power supply provides power to the unit. Standard TTL integrated circuit logic is employed, mounted on 40 logic boards. Figure 18 is a photograph of the unit with the top cover removed. Figure 19 shows the front panel of the autocorrelator with the operator controls. The sample rate, number of sample bursts, and number of samples per burst are selectable by using the front panel toggle

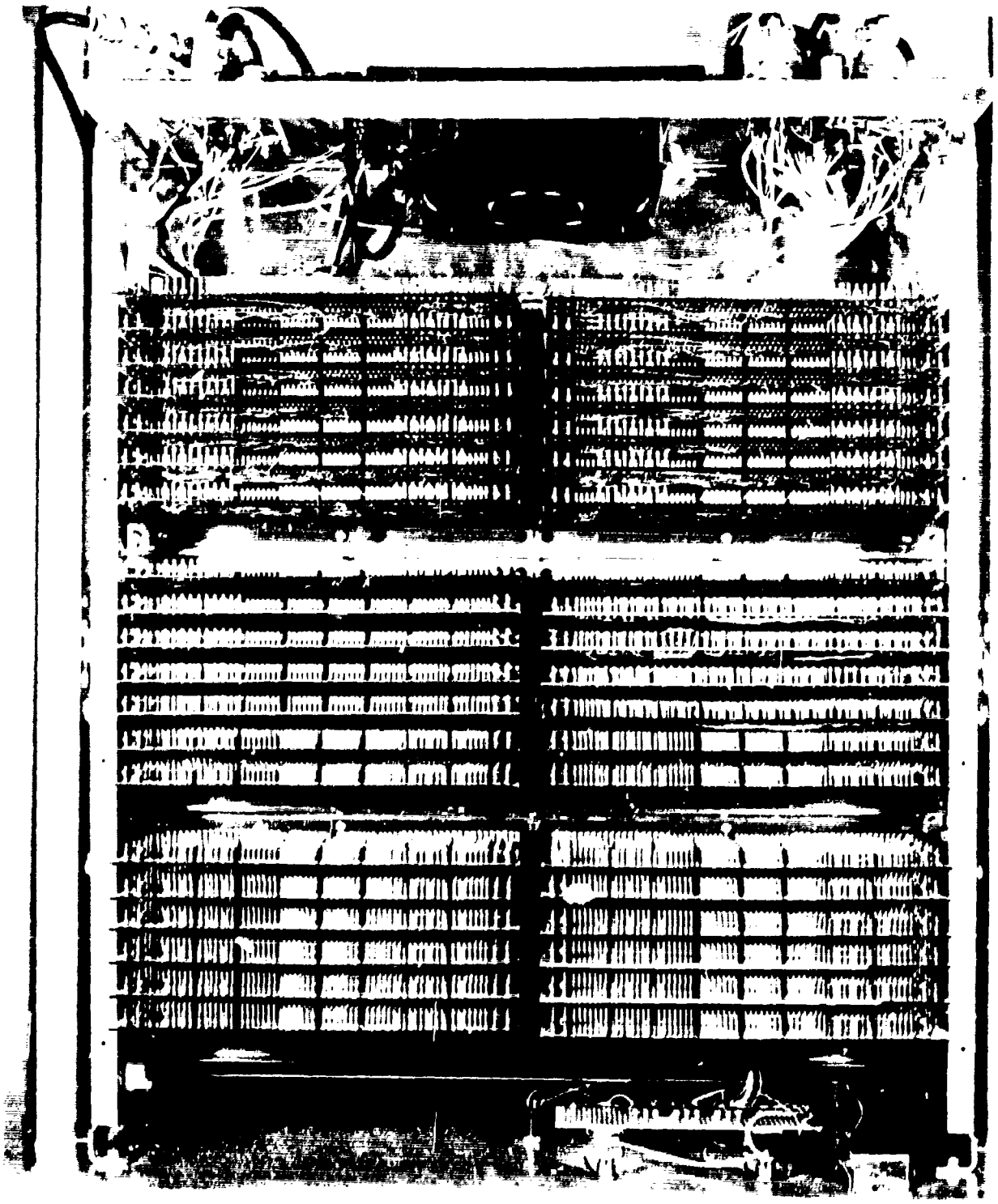

FIGURE 13 PHOTOGRAPH OF CORRELATOR TOP COVER REMOVED

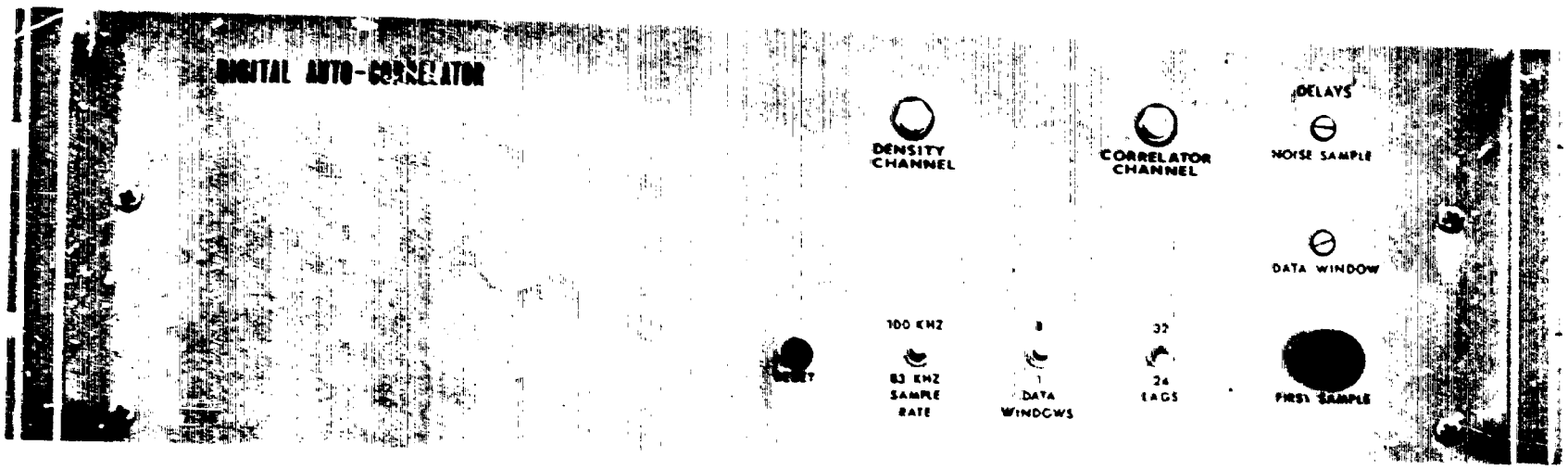

FIGURE 19 PHOTOGRAPH OF CORRELATOR — FRONT PANEL

switches. Potentiometers on the right-hand side of the unit are used for adjusting the delay to the first sample, delay between sample bursts, and delay to the noise burst. Also provided are a correlator reset button and indicator lights that show whether the correlator channel and/or the density channel have been turned on by the computer. An operating handbook for the Digital Autoco relator has been produced, which describes in detail the operation and maintenance of the unit.

3. Programming Information

Since the correlator works in conjunction with the XDS 930 computer, certain computer commands were implemented that enable interchange of information between correlator and computer.

Four System EOM commands are used to control operation of the correlator. These commands have the form

EOM 03400X (0 02 3400X) ,

where the significance of X is as follows:

X = 0		Disable both channels.
X = 1		Enable density channel, disable correlator.
X = 2		Disable density channel, enable correlator channel.
X = 3		Enable both channels.
X = 4 through 7		No effect.

The EOM is completely decoded so that any other EOM will have no effect. The computer Start button disables both channels.

Three sense outputs are provided so that the positions of the three toggle switches can be determined with SKS commands. Two of these

are presently connected. The command codes used are:

SKS 030001	Skip if 32 lags, no skip if 24.
SKS 030020	Skip if 100-kHz sample rate, no skip if 83.3 kHz.

The remaining sense signal would produce a skip if set for one data window, no skip for eight.

It is necessary for the on-line computer program to stay in synchronization with the radar. This is accomplished through the use of priority interrupts. The interrupts are listed in Table II below, by location and in order of priority (highest first).

Table II

PRIORITY INTERRUPT ALLOCATION

Interrupt Location	Time of Occurrence
200	Data Pulse Sync
201	Delay Time End (first density channel sample)
202	End Noise Group (correlator)
203	End each Data Group (correlator)
204	Track Pulse Sync
205	End ADCOM Data Transfer

Correlator output data are stored in Memory Locations 10000_8 through 10437_8. In the case of 24 lags, the final location is 10327_8. Density channel data are stored in Locations 10440_8 through 10737_8. The two most significant digits of these addresses may be changed by moving jumper wires on the MCTL cable plug module, which is installed in the

computer at Location 11B. The format of the data words as they appear in memory is shown below.

Correlator output word

S = sign bit (0 = positive, 1 = negative)

X = magnitude bits, 2's complement form

SSSSSXXXXXXXXXXXXXXXXX

bit 0 4 23

ADCOM output word

X = amplitude bits (unipolar)

0000XXXXXXXX000000000000

bit 0 4 11 23

D. Computer Interfacing Equipment

When the digital correlator was incorporated into the radar data processing system, a number of other changes were made in the routing of digital data and control signals amongst the various units of digital equipment. Figure 20 is an interconnection diagram for these equipments, and Table III lists the units and their functions.

As part of this year's contract, some additional pieces of computer equipment were procured and installed; they are operating satisfactorily. The items added to the XDS 930 computer system include the following:

(1) Memory Interface Connector option

(2) Multiple Access to Memory option

(3) Priority Interrupt control chassis

(4) Eight Priority Interrupts

(5) Arming feature for the Priority Interrupts.

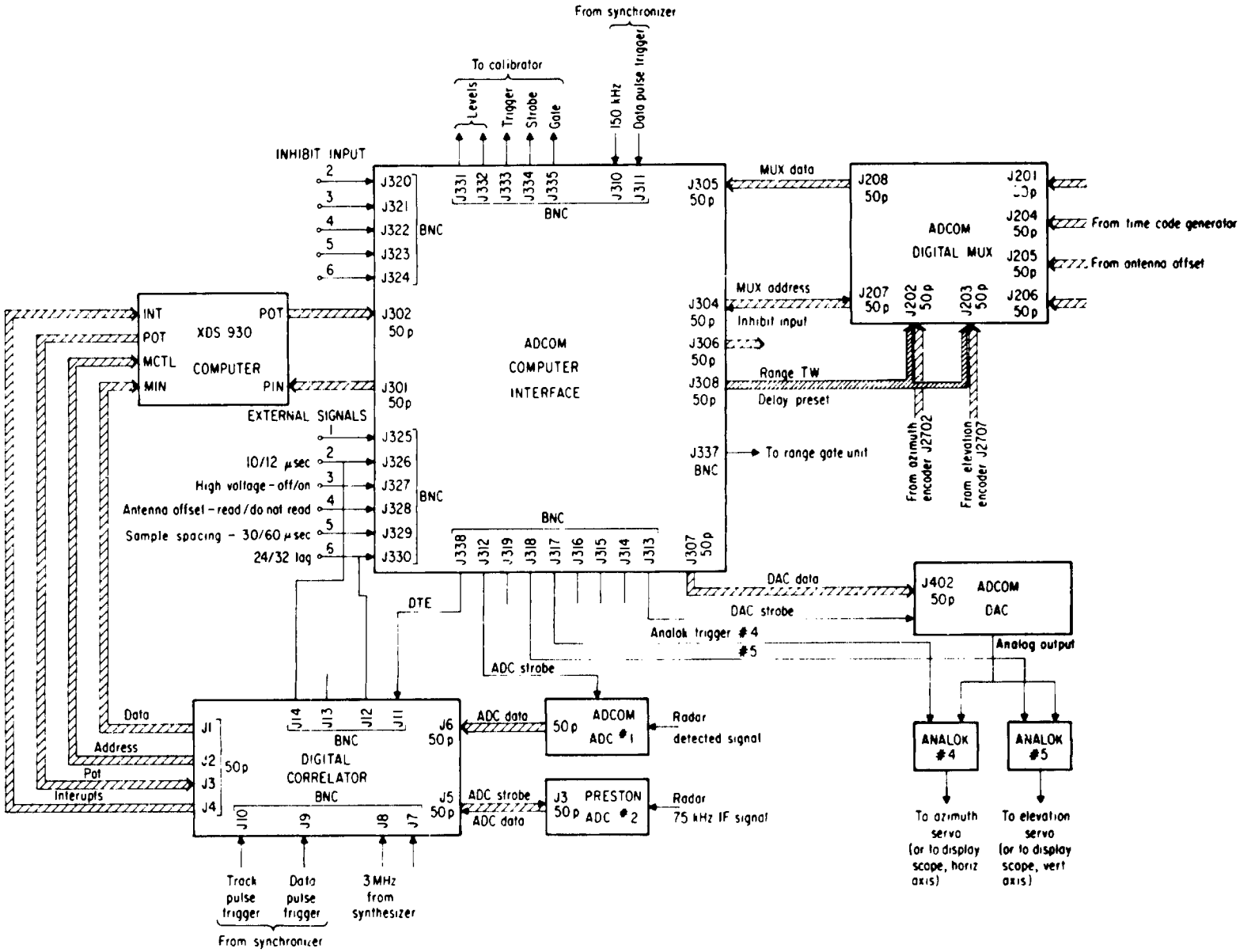

FIGURE 20 DIGITAL EQUIPMENT INTERCONNECTION DIAGRAM

Table III

DIGITAL EQUIPMENTS FUNCTION LIST

Unit	Functions
ADCOM Computer Interface	(1) Controls XDS 930 computer inputs and outputs through the PIN/POT channel (2) Controls pulsed noise source calibrator (3) Sets delay to first sample for density channel ADC (4) Generates sample triggers for density channel ADC (5) Controls digital-to-analog converter and Analok holding currents (6) Provides external sense line inputs to computer (7) Controls Digital Multiplexer
ADCOM Digital Multiplexer	Gates 24-bit parallel data from any of six selectable data sources to the computer interface
ADCOM Digital-to-Analog Converter	Converts digital numbers to an analog voltage
Analok Circuits	Holds the analog voltages supplied by the DAC
Analog-to-Digital Converters	(1) Digitizes detected radar signal (2) Digitizes IF radar signal
Digital Autocorrelator	(1) Computes autocorrelation coefficients (2) Controls transfer of data to the XDS 930 computer through its Memory Interface channel (3) Generates interrupt signals for the computer (4) Generates status levels for input to the computer interface
XDS 930 Computer	(1) Provides on-line data processing and recording capability (2) Controls various portions of the radar system (3) Is controlled by various portions of the radar system (4) Accepts data from various sources

A number of nonstandard computer commands have been implemented to enable the computer to communicate with the external digital equipments. These commands and their current functions are summarized in Table IV.

Table IV

COMPUTER COMMANDS

Input Channel Select Commands	(Follow with PIN command)
EOM 31001	Spare
EOM 31002	BCD Azimuth (lowest 18 bits)
	BCD units digit of Delay Thumbwheel Switch (Bits 2-5)
EOM 31003	BCD elevation (lowest 17 bits)
	BCD tens and hundreds digits of Delay Thumbwheel Switch (bits 2-6)
EOM 31004	BCD Time of Day
EOM 31005	Antenna Console Thumbwheel Switches--BCD
EOM 31006	Spare
Output Channel Select Commands	**(Follow with POT command)**
EOM 32001	Calibrate Code which controls noise source attenuator settings (0, 1, 2, 3 give 0-, 3-, 6-, 9-dB attenuation)
EOM 32002	Spare
EOM 32003	Spare
EOM 32004	Output to DAC and voltage held by Analok 4
EOM 32005	Output to DAC and voltage held by Analok 5
EOM 32006	Spare

Table IV (Concluded)

Device Enable Commands			
EOM 34001	Enable density channel ADC input through MIC, disable autocorrelator		
EOM 34002	Enable autocorrelator operation, disable density ADC input		
EOM 34003	Enable both above		
EOM 34000	Disable both above		
Sense Line Commands			
Op Code	Function	No Skip	Skip
SKS 30001	Number of lags in each autocorrelator window	24	32
SKS 30002	Sample spacing for density channel ADC	30 μs	60 μs
SKS 30004	Antenna Console Switch read/not read push-button	DO NOT READ	READ
SKS 30010	High-voltage status	OFF	ON
SKS 30020	Autocorrelator channel sample spacing	12 μs	10 μs
SKS 30040	Spare		

IV SOFTWARE

A large amount of new software was developed during the past year in order to make use of the new hardware, provide more operator feedback during operation, implement the processing and analysis procedures described in Section II, and speed up the entire data recording and processing procedures. These objectives have been met. Two major computer programs are used: one that runs on line in a real-time environment and controls the data taking and recording and one that is used off line to analyze the recorded data and to plot and print out the experimentally determined electron densities and electron and ion temperatures. This section describes these two programs.

A. On-Line Program

1. Description

This program is intended for use in conjunction with the data-taking facilities of the XDS 930 computer used by the Project 617 radar. The computer is presented with an externally clocked stream of input data (independent of the computer CPU functioning) consisting of 192 amplitude samples (power profile data) and 24 (or 32) lagged correlation coefficients from each of nine autocorrelation gates (spectral data). These data are input repetitively, once per radar interpulse period. The computer is required to perform a running summation (squared sums for the amplitude data) over successive radar interpulse periods for each input number and write the summations in formatted blocks on magnetic tape.

a. Amplitude Samples (Power Profile Data)

The amplitude data are presented to the computer as a sequence of 192 8-bit unipolar ADC voltages (one sample per computer word, Bits 4-11, in 192 sequential 24-bit computer words, from Address 10440_8 to 10737_8). Each of these samples s squared and added to an accumulating bin at the corresponding range. After summation over some predetermined number of these pulses has been completed, the data are formatted and output onto digital tape (if desired), all the accumulating bins are reset to zero, and the summation is repeated.

b. Autocorrelation Coefficients (Spectral Data)

The autocorrelation coefficients are presented to the computer as nine groups of either 24 or 32 points each, read into sequential computer words (Bits 4-23) for a total of 9 × 24 (9 × 32) 24-bit computer words per radar sync pulse (Locations 10000_8 to 10437_8). Each of these groups of 24 (32) points represents a precomputed (by interface hardware) autocorrelation function. These points are summed in 9 × 24 (9 × 32) accumulating bins, and after a predetermined number of pulses the data are output onto tape (if desired), along with the amplitude data that have been computed in a parallel fashion. After each tape write, the autocorrelation accumulating bins are reset to zero, and the summation is restarted.

c. Control of the Input Data Flow

Six priority interrupts are employed to notify the program of the completion of data transfers to the computer memory. Various sense lines are used to inform the computer of input modes--24 or 32 spectral samples per gate, 30- or 60-μs sample interval for amplitude data, etc. (see Table IV).

d. Control of the Output Data

The output from the program is in the form of digital tape records, one record per summation interval. Each record contains header information and double precision summations of all gates. Tape writing on Magnetic Tape Unit 1 is controlled by Break Point 1 on the computer console (set: write tape; reset: do not write). The writing of file marks on tape is controlled by Break Point 4 (set: write file mark; reset: omit file mark). The use of these switches is described in detail below. A secondary output from the program is in the form of typewritten error messages and visual displays of the summation bins; these are also described in detail below.

e. Operating Modes

Two modes of operation can be initially selected. Upon initiation of the program at Location 01000, the typeout--RUN(0), PLOT (1)--is made. If a zero is entered (terminated by a carriage return as with all typed input messages), the program branches to the "run" mode of operation (described below). If a one is typed in, the program enters a special "check" mode of operation designed to check individual records or magnetic tape which has already been written, by plotting these records on the CalComp plotter. This mode is simply a convenience for on-the-spot checking of tapes without loading the analysis program. Either mode asks the operator for the number of files he wishes spaced forward on MT1 with the message "FILES FWD---."

1) Plot Mode. After positioning the tape to the desired file, the program types the message "PEN TO LH MARGIN, HIT RETURN." The operator then positions the plotter pen and types a carriage return. The program next outputs the message "SAMP(0), AC(1), BOTH(2)---," asking the operator whether he wishes a plot of the 192-point amplitude data,

of the nine autocorrelation functions, or of both. After accepting a number (0, 1, or 2), the program reads one record from tape, draws the desired plots, and repeats the message. This loop occurs repetitively until the program is restarted, at which time the "RUN(0), PLOT(1)---" message is typed.

2) Run Mode. Figure 21 is a simplified flow chart of the run mode loop. The run mode initially executes a check loop, which ensures that MT1 is ready and positioned as required. Input parameters are entered through the typewriter in response to typed messages. The program then enables the interface logic and interrupts and goes into a wait loop sequence while processing in errupts. The wait loop consists of a visual display driver and a typewriter error message driver. Errors are flagged by the interrupt routines and typed out when required. If no error flags are set, the visual display is driven repetitively. Details of this operation are described below.

f. Console Breakpoint Switches

At the end of each sequence of pulses over which a summation is performed, the computer formats the data for output onto tape and interrogates BP1 to see whether tape output is desired. If BP1 is set, the data are output onto tape. If BP1 is reset, no tape write occurs, unless BP1 was reset during the current summation sequence. If that is the case, the buffer is dumped onto tape, and no further buffers are output until BP1 is again set. If BP4 is set, a file mark is written following the last data record, and the block counter (record numbers within a file) is reset for the start of the next file, when and if it occurs. An EOF message is typed, containing a file number, time, and date. If BP4 is reset, no file mark is written, the block counter is left set, and no message is typed. This enables the operator to maintain block

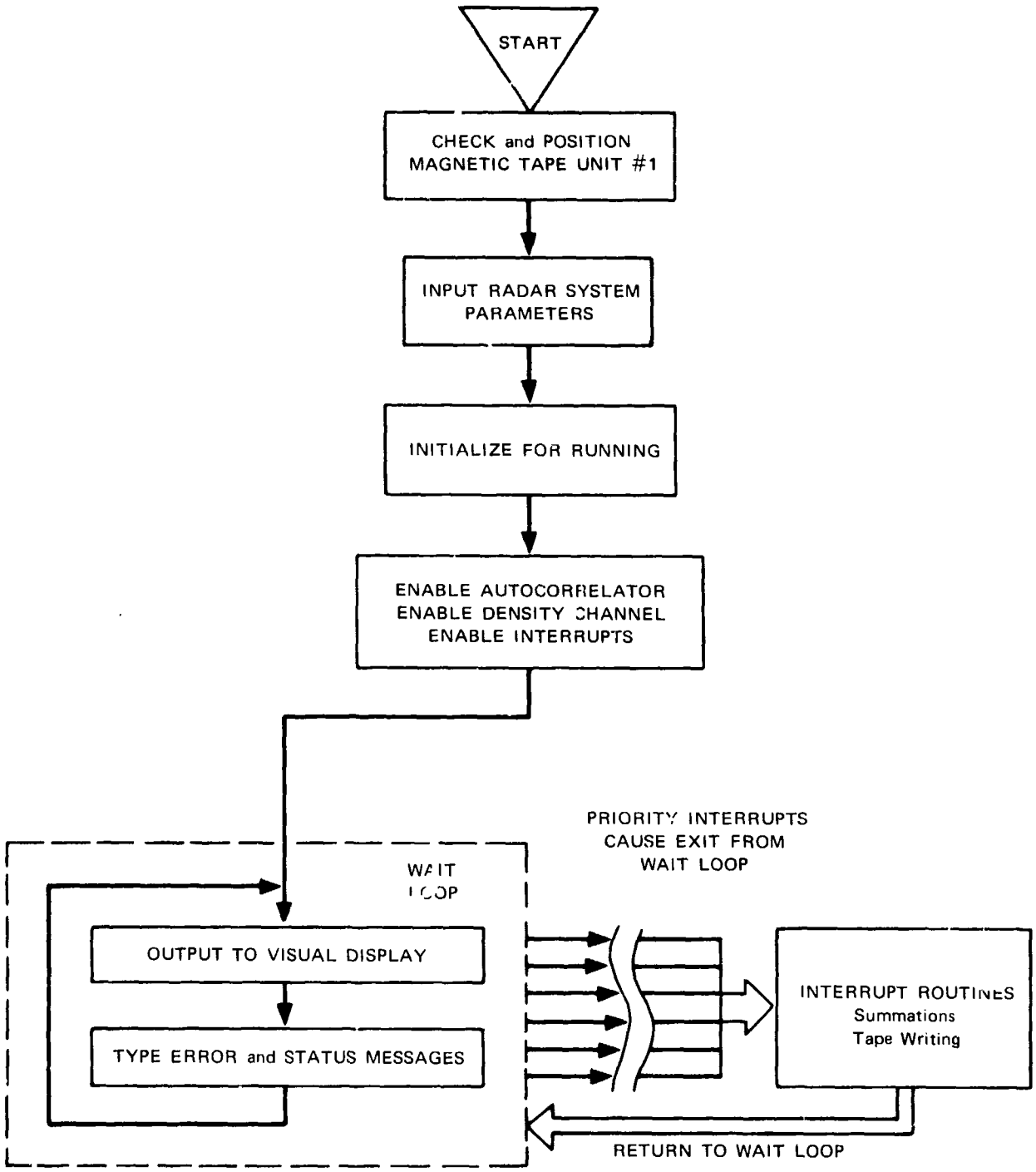

FIGURE 21 RUN MODE FLOW CHART

continuity within files, even when it is not desired to have the blocks contiguous in time. Unless a change of input parameters is desired, it should never by necessary to restart the program between records or between files. Even when magnetic tape is not being written, the program remains in synchronization with the external interrupts; summations continue to take place; and program functioning remains the same as though tape were being written. When the first record in a new file has been written, a message is typed giving the file number, time, and date, thereby generating a series of messages defining file events by a sequence number, time, and date. If the program is restarted, the file number counters are not reset unless MT1 is at the load point, thereby maintaining file sequence continuity when input parameters are to be changed. An EOF should be written before restarting the program, since the program initially expects to begin a new file upon startup. If this is not done, a loss of file continuity in the typewritten messages will result, since block numbers will be reset within a file.

g. Program Monitoring

The operation of the program is monitored in two different ways:

(1) Foreground and background typewriter messages that allow the operator to determine the time and sequence of events recorded on tape, as well as recording the occurrence of possible timing errors. Foreground messages also allow for the input of program parameters during the setup phase.

(2) On-line visual monitoring of the data-taking/computation process by means of ten selectable oscilloscope displays (the 192-point power profile data and the nine autocorrelation gates).

h. Typewriter Messages

Several types of messages are typed out during the running of the program. Only the first type requires an operator response. The various message types are listed below.

(1) Messages controlling the initial setup of the run mode. Certain of these messages inform the operator of error conditions in the initial setup for running:

MT1 556 (set MT1 to 556 bpi)

MT1 FPT (no file ring on MT1)

MT1 NOT RDY (MT1 not ready)

WRONG AC SAMPLE SIZE (program size does not match sample size of autocorrelation gates (24 or 32) as controlled by autocorrelator switch setting).

All these messages may be cleared by hitting a carriage return when the condition has been corrected. The program repeats the typeouts until it senses a completely correct condition.

Another set of messages controlling the initial setup requests the operator to input system parameters, some of which are used to control program operation and others of which are simply output onto tape for use by the analysis program. These messages are:

FILES FWD---

SYSTEM PRF(150)-

POWER (KW)--

PULSE WIDTH(MICROSECS)--

CALIB CODE--

BANDWIDTH(KCS)--

AC START RANGE(KMS)---

AC NOISE RANGE(KMS)-

DATE(MO/DY/YR)--

NO PULSES(PRF=75)--.

Responses to these messages (with the exception of the date) should consist of numeric input only (0-9) or a minus sign; they require termination by a carriage return. Any other character input results in a repetition of the message. The date type-in is a straight BCD input of eight characters terminated by a carriage return. If more than eight characters are input, the message repeats. The FILES FWD--- message accepts either plus or minus numbers. A minus one (-1) typed in, for example, backs the tape up to the nearest file mark and then spaces forward over the file mark. A plus one advances the tape past the next file mark. If the tape is backed up to the load point, the message

LOAD POINT,FILE CNTRS RESET

is typed, and control is returned to the FILES FWD--- message. The PRF(150)- message accepts only even numbers as answers to the total PRF, including both data and blank pulses. If a PRF greater than 150 is typed in, a warning message is typed out:

CAUTION: PRF NE 150; IF 60-MICROSEC SAMPLE GATE IS USED, AT LEAST 80 SAMPS MUST BE READ IN BEFORE INT204 OCCURS--.

See SYNC2 interrupt description under Program Timing for more detail on this message.

(2) Messages specifying the beginning and end of files written on digital tape:

hh:mm:ss mo/da/yr BOF xxx

hh:mm:ss mo/da/yr EOF xxx

These messages contain a BCD time of day as read from the time-code generator, the BCD date as input during setup (and possibly updated during running when the date changes at 0000 hours Greenwich), and a

three-digit number indicating the file sequence number within a time (initially set by the FILES FWD--- message).

(3) A message typed out during running whenever BP2 is set, which gives the system noise temperature, TN, as computed from the last complete record over which summation occurred:

hh:mm:ss mo/da/yr TN=xxx K

This message again contains the date, time of day, and a three-digit temperature in degrees Kelvin.

(4) Messages flagging the occurrence of run-time timing errors or of various fail conditions:

hh:mm:ss	mo/da/yr	WRONG AC SAMPLE SIZE
hh:mm:ss	mo/da/yr	REC xxxx,PULSExxxxx,xx AC18 INTS
hh:mm:ss	mo/da/yr	REC xxxx,PULSExxxxx,PREV SAMP GATE UNFIN
hh:mm:ss	mo/da/yr	HVFAIL
hh:mm:ss	mo/da/yr	REC xxxx-MT1 NOT RDY

The first message can occur only when the ac-sample-size switch on the interface box is inadvertently changed during running. Since the memory layout is different for the two possible sample sizes (24 or 32), two separate program tapes are provided. This condition is therefore treated as an irrecoverable one and results in a complete program restart. The file sequence counters are maintained, however, and the digital tape may be repositioned to the nearest file mark by typing in a minus one to the FILES FWD--- message. The second message flags the occurrence of more than eight interrupts on INT203, the autocorrelation interrupt for the first eight (signal) range gates. If this occurs, certain of the autocorrelation gates may be processed before the values are actually updated in the MIC data input area. The third message flags the occurrence of an overlap in sample gate computations. This is a recoverable error, provided

it is not flagged on successive pulses. Tape record numbers within the digital tape file are given for each of these errors, along with the pulse number (of the total number of pulses summed in any given tape record) in which the error occurred. The fourth message flags the occurrence of a high-voltage fail in the transmitter. The computer types out the fail and writes the partially completed record on tape (if tape is being written). No file mark is written, regardless of the state of BP4. For this error it is assumed that when the error is cleared the current file continues to be written; hence, block-count continuity is maintained. A flag is set in the partially summed record, and a true count of the number of pulses summed over is recorded on tape. The HV fail condition (tape-write inhibited) continues until BP1 is toggled reset-set (or simply set if tape write was not in process when the HV fail occurred). If the computer still senses an HV fail condition when BP1 is toggled, the HV fail message is repeated and the wait loop reentered. All background functions and data processing remain active during the HV fail period. The fifth message flags the occurrence of an MT1 busy condition during an attempted tape write. This condition is fully recoverable, provided the tape has been set ready before the next summation period ends. The background error messages and visual display are suppressed, since the computer hangs up in a tape-ready wait loop while processing input interrupts. The message is not actually typed out until after the condition has been corrected, since the background loop is replaced by the tape-ready loop. The error is detectable by the lack of background displays.

The messages are sequenced in such a way as to provide for an orderly record of events typed in the sequence in which they occur (typewriter speed being an obstacle to this if multiple flags are set). All error messages are stacked to allow for the flagging of multiple errors having the same message typeout (up to five per message). The time of day typed out with each message is the time at which the typewriter message is typed out and not the exact time of occurrence of the error.

i. Visual Monitoring

Visual monitoring of the data-taking process is executed as a background function and is part of the wait loop (along with the typewriter error messages) continually being executed while the program awaits interrupts. Ten displays are possible in this loop: the 192-point power profile or any of the nine autocorrelation gates. If the antenna-console read-do-not-read switch is off, the computer outputs only the 192-point amplitude data in the form of the current summation. If the read-do-not-read switch is on, the computer interrogates the antenna-console thumbwheel switch. If the switch is set to C001,C002,C003..., C009, the computer displays the corresponding autocorrelation gate. At any other setting of the thumbwheel switch, the computer displays the 192 points of amplitude data.

Figures 22 and 23 are photographs of the visual displays. Figure 22 shows the averaged received power as a function of range after about 40 seconds of integration. The F-layer return is quite visible, peaking at about 300 km, as is ground clutter between 140 and 160 km. The 70°K noise pulse, which is injected for calibration purposes, can be seen between 950 and 1000 km. This display enables the operator to continuously monitor the performance of the radar system while taking data. The other display (Figure 23) that can be selected by the operator is a presentation of the autocorrelator output for each of the nine range gates where the autocorrelation function is computed. This enables operation of the digital autocorrelator to be monitored in real time without interruption of the data taking. The visual display is always active regardless of the error state (HV fail) of the data-taking, unless the computer is hung up in a tape-not-ready loop. Thus, by resetting BP1 before starting a run, all the data processing functions can be visually monitored, and data taking can be initiated by simply setting BP1. Tape block numbers are incremented only when tape is actually

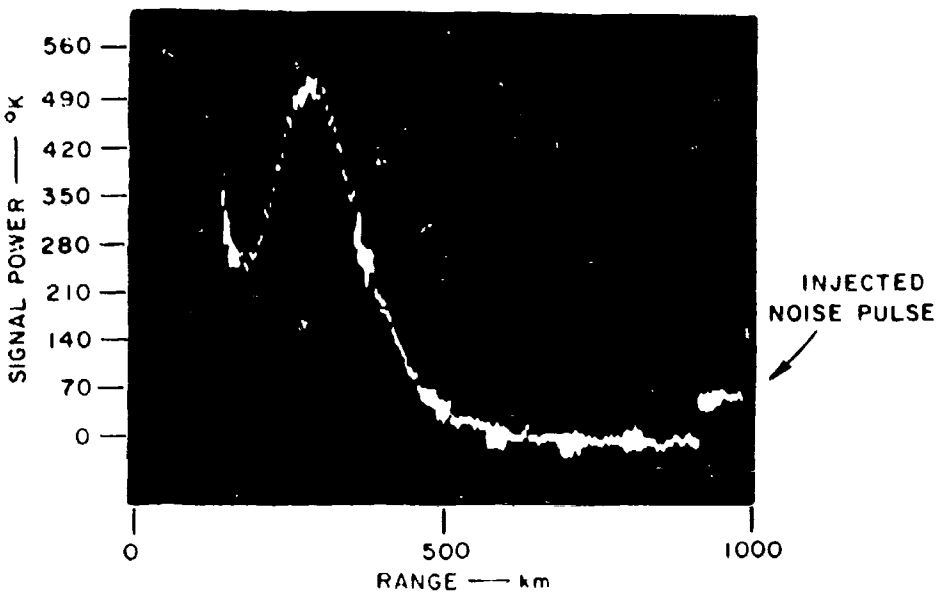

FIGURE 22 ON-LINE DISPLAY — INTEGRATED POWER AS A FUNCTION OF RANGE — 20 FEBRUARY 1970, 2304 GMT

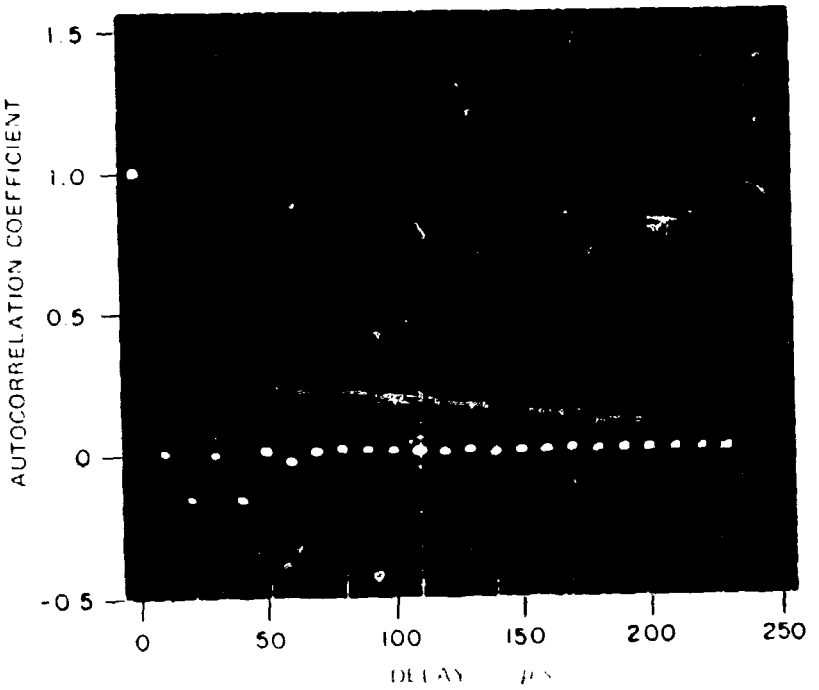

FIGURE 23 ON LINE DISPLAY — AUTOCORRELATION FUNCTION

written, thereby maintaining block-count continuity within files. The displays are all representations of the current state of the summation buffers and are reset along with these buffers at the end of each summation period. Although tape writing at low summation numbers is not normally desirable, the displays may be run at summations of anywhere from 2 on up. It should be kept in mind, however, that the display loop is subject to interrupt and that buffers may be updated in the middle of the display sweep. This effect is not noticeable for larger summations but is definitely noticeable over sums of only a few pulses. The visual display is output in the form of an XY plot on the digital-to-analog converter and Analok holding circuits. One Analok contains the signal to be displayed and the other a sweep voltage to drive the X-axis of the XY display.

2. Interrupt Processing

This section describes in detail the timing sequence in which interrupts are processed in the run mode of operation. Names enclosed between dashes (-SAMPGATE-) refer to labels in the program listing.

Six interrupts are processed, occurring as follows:

INT200 Data pulse sync (start of interpulse period)

INT201 Start of 192-point sampling gate

INT202 End of Autocorrelation Gate 9

INT203 End(s) of Autocorrelation Gates 1 through 8

INT204 Track pulse sync (middle of interpulse period)

INT205 End of 192-point sampling gate.

The basic time frame is taken to be the 13.33-ms (PRF of 75) interval between any two consecutive data pulse syncs. For 30-μs sample spacing, Interrupts INT201 and INT205 are used to control processing of the

192-point sample gate, and INT204 is ignored. For 60-μs sample spacing, Interrupts INT204 and INT205 are used, and INT201 is ignored.

Interrupt processing is such that, at any given time, one of three basic interrupt states exists, with a "catch-up" timing transition between the second and third states (formatting for tape write). These states are as follows:

a. State I--Initialization

Let zero or more time frames p ,s as defined by the count number in -SYNCSKIP- [five frames skipped at start of processing to get into sync, then two frames skipped for every tape write (end of summation)]:

```
INT200  BRM     -LOADBLK2-
INT201  BRM     -NOP201-
INT202  BRM     -NOP202-
INT203  BRM     -NOP203-
INT204  BRM     -NOP204-
INT205  BRM     -NOP205-
```

-LOADBLK2- counts down -SYNCSKIP-, then loads State II.

NOP201,NOP202,NOP203,NOP204,NOP205 clear their respective interrupts and take no other action.

b. State II--Processing

Perform the required summations of the autocorrelation gates and squaring-and-summing of the 192-point sample gate:

```
INT200  BRM     -SYNC-
INT201  BRM     -SAMPSTRT-
INT202  BRM     -ACGATE9-
INT203  BRM     -ACGATE18-
```

INT204 BRM -SYNC2-

INT205 BRM -SAMPGATE-

-SYNC- checks current value of -SYNCCNT- for -SYNCCT- = -NXPRF- [(no. of sync pulses passed) = (no. of sync pulses typed in)] and bumps -SYNCCT- if not equal. If equal, -SYNC- reads the current time, azimuth, and elevation codes and loads State III.

-SAMPSTRT- checks the 30- to 60-μs interval sense line. If 60 μs, no action is taken. If 30 μs, -SAMPSTRT- checks for completion of the previous sample-gate computation (-SAMPFLAG- = 0). If -SAMPFLAG- = -1, -SAMPGATE- (INT205) has not finished processing the previous 192 samples, and an error is flagged.

-ACGATE9- checks for more than eight interrupts on INT203 (-ACGATE18-) and flags an error if -ACCOUNT- > 8; if -ACCOUNT- ≤ 8, computation of all remaining autocorrelation gates is completed. It also checks for -SYNCCNT- = -NXPRF- and formats for output.

-ACGATE18- computes one autocorrelation gate (24 or 32 values) corresponding to current value of -ACCOUNT- and bumps -ACCOUNT- by 1.

-SYNC2- checks 30- to 60-μs interval sense line. If 30 μs, no action is taken. If 60 μs, -SYNC2- checks -SAMPFLAG- for completion of the previous sample gate and initiates background (to the autocorrelation interrupts) computation of the first 80 samples [minimum number of samples if sample gate ends at next autocorrelation sync pulse = $(192 \times 60 - 13333/2)/60 \approx 80$].

-SAMPGATE- completes (or begins) computation of the 192-point sample gate. If the sample interval is 30 μs, all 192 samples must be computed before the next -SAMPSTRT- interrupt. If the sample interval is 60 μs, the last 192 - 80 = 112 samples must be computed before the next -SYNC2- interrupt. Since -SAMPGATE- is of lower priority than -SYNC2-, computation of the last 112 samples cannot begin until the first 80 have been completed. Also, -SYNC2- and -SAMPSTRT- can interrupt -SAMPGATE- and thereby detect if processing of the previous frame has not been

completed in time. Upon completion, -SAMPGATE- checks for -SYNCCNT- = -NXPRF- and initiates formatting for tape output if yes. -SAMPGATE- remains active into State III if tape formatting is taking place.

c. State III--End Processing, Start Output

Complete processing in current time frame; format for tape output while skipping two time frames (13.33 ms):

```
INT200  BRM    -LOADBLK1-
INT201  BRM    -NOP201-
INT202  BRM    -NOP202-
INT203  BRM    -NOP203-
INT204  BRM    -NOP204-
INT205  BRM    -SAMPGATE-
```

-LOADBLK1- (same as State I) counts down -SYNCSKIP- (lets two time frames pass) and loads State II.

-NOP201,NOP202,NOP203,NOP204- clear their respective interrupts without taking any other action.

-SAMPGATE- is still active from State II and waits for all computation to be complete prior to formatting for tape output. An error is flagged if MT1 is not ready. Tape write is initiated, range summing bins are zeroed out for the next summation, and -SYNCSKIP- is set to one so that -LOADBLK2- skips two frames before reloading State II. This routine checks BP1 and BP4 and sets any flags necessary for file start-stop messages. At completion, -SAMPGATE- loads BRM -NOP205- into -INT205-.

3. Miscellaneous

The on-line program was written in METASYMBOL, the assembly language for the XDS 930 computer. It uses approximately 6700 24-bit words of core storage, including both program and data storage. Magnetic tapes written by this program are used as input to the off-line analysis

program described in Section IV-B. The format of the output tape is shown in Table V. Each computer word shown in the table requires four consecutive 6-bit characters on the output tape. The length of the tape records depends on whether the 24-lag or the 32-lag autocorrelator option has been selected, as indicated by parentheses for the last four entries in Table V. Recording is done in binary (odd parity) at a packing density of 556 bpi, resulting in record lengths of 6 inches (3344 characters) or 7 inches (3920 characters). Standard 3/4-inch gaps separate records on the output tape. For an on-line integration period of 1 minute, a 2400-ft roll of computer tape lasts about 70 hr.

B. Off-Line Analysis Program

We have seen in the preceding section (IV-A) that during an electron backscatter radar run, two sets of data are preintegrated and recorded on tape: the power samples, also called density samples, and the autocorrelation coefficients. This section describes how the data are manipulated in order to give, as a function of time and altitude, the electron density and the ion and electron temperatures.

The input data to this program, data which were integrated over relatively short time periods by the on-line program, are integrated over a longer period of time. For each of these second integration periods, the program computes the Fourier transform of the autocorrelation coefficients, thus giving the spectra at each altitude. It next computes a raw electron density curve at the altitudes of the 192 power samples ("raw density" because it assumes that the Debye length is small compared to the operating wavelength). The program also computes the ion and electron temperatures, which are then used to recalculate the density, to greater accuracy, this time taking into account the nonzero value of α.

Table V

MAGNETIC TAPE FORMAT

Word Number	Contents
1	Record Sequence Number
2	Radar Pulse Repetition Frequency (75)
3	On-Line Summation Interval (number of pulses)
4	Time of Day--BCD codes from Clock
5	Antenna Azimuth--hundredths of degrees
6	Antenna Elevation--hundredths of degrees
7	Peak Transmitted Power--kilowatts
8	Pulse Width--microseconds
9	Calibration Pulse Attenuation--0,3,6,9 dB
10	Receiver Bandwidth--kilohertz
11-12	Date--BCD codes
13	Delay Number--from interface thumbwheel switch
14	Density Channel Sample Interval--30 or 60 μs
15	Range to First Autocorrelator Gate--kilometers
16	Range Interval Between Gates--kilometers
17	Number of Lags in Each Gate--24 or 32
18	Correlator Channel Sample Interval--10 or 12 μs
19	High-Voltage Fail Flag: 0, No Fail; 1, Fail
20	Range to Ninth Autocorrelator Gate--kilometers
21-236 (21-305)	Low-Order Words of 9 × 24 (9 × 32) Autocorrelation Coefficients
237-452 (309-596)	High-Order Words of 9 × 24 (9 × 32) Autocorrelation Coefficients
453-644 (597-788)	Low-Order Words of 192 Density Channel Summations
645-836 (789-980)	High-Order Words of 192 Density Channel Summations

Figure 24 shows the main tasks of this off-line software. The physical assumption and most of the mathematical formulas have been described in Section II of this report. Details of the programming procedures follow, including descriptions and explanations of each of the subroutines.

The computer used is an XDS 930, with a core memory of 16K 24-bit words. Approximately 13,000 words of storage are required by the program. The graphs are plotted during the computer run on a CalComp plotter.

Most of the routines are coded in FORTRAN. Because of timing considerations for the on-line program, the input tape is not in a FORTRAN format. Therefore, the input subroutines are written in Machine Language.

The time required to analyze each integration period is roughly 5-1/2 minutes. About 4 minutes of this time are used to draw and label the final plot, where the true densities and the temperatures are presented.

1. Description of the Input Data

The data are inputted by three means.

a. Magnetic Input Tape

The on-line data-taking program, described previously, generates the digital tape that is the input of this program (the tape format has been given in Table V). Included on the tape are:

(1) A header of 20 words

(2) Twenty-four or 32 autocorrelation coefficients in each of nine range gates (eight gates where signal is present and one containing noise only; the eight signal gates are usually $\Delta r \sim 50$ km apart, as shown in Figure 14).

(3) The 192 power samples.

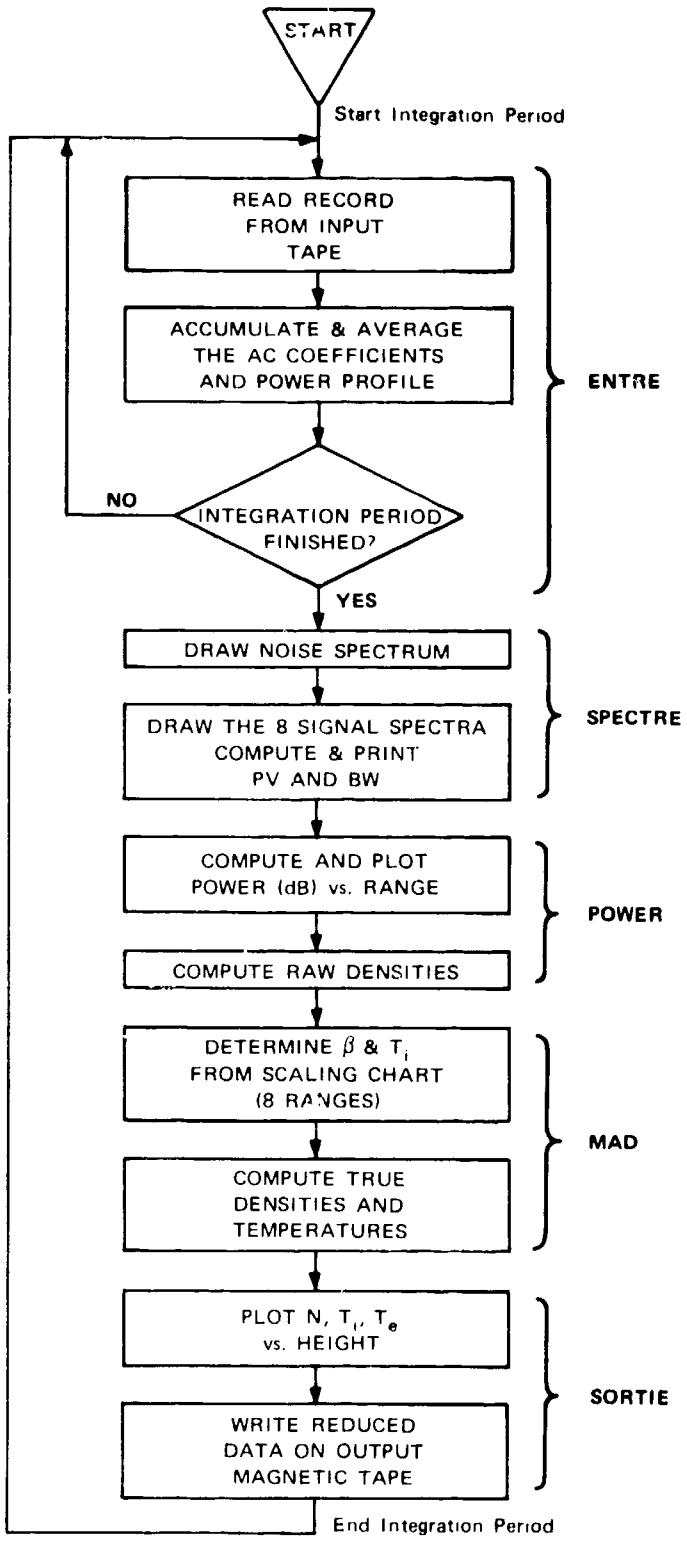

FIGURE 24 OFF-LINE ANALYSIS PROGRAM GENERAL FLOW CHART

Table VI

THE VARIABLES IN COMMON

Name	Number of Words	Definition
D	192	Density samples
NUH	20	Header on output tape
		(1) Last block number read in
		(2) PRF (Hz)
		(3), (4) Start time, BCD characters
		(5) Azimuth (degrees * 100)
		(6) Declination (degrees * 100)
		(7) Power (kW)
		(8) Pulsewidth (μs)
		(9) Calib code
		(10) Bandwidth (kHz)
		(11), (12) Date in BCD
		(13) Delay code
		(14) Interval between density samples (μs)
		(15) First range--R_0 (km)
		(16) Δr-interval between AC gates (km)

Table VI (Concluded)

Name	Number of Words	Definition
		(17) Number of AC samples (μs)
		(18) Interval between AC samples (μs)
		(19) f_oF2 (MHz * 100)
		(20) Number of pulses integrated
PV	8	Peak-to-valley ratios
BW	8	Half-power widths of spectra (kHz)
SN	8	Signal-to-noise ratios of spectra
PC		Calibrate level power
PN		Noise level power
IB		First index of density plot
IE		Last index of density plot
MORE	6	Additional parameters, written on output tape
		(1) Record number on output tape
		(2), (3) Last time, BCD characters
		(4) C_f * 1000, where $C_f = [N(f_oF2)]/N_{max}$
		(5), (6) Blanks

b. Typewriter Input

For each integration time, the number of pulses, NP, on which the integration is to be performed is typed in, and also the value of the F-layer critical frequency, f_oF2, as measured by a nearby ionosonde.

Optional input: The number of sample points to be included in the calibration pulse and in the noise pulse and the value of SNMAX. SNMAX is the lowest signal-to-noise ratio that a spectrum can have if it is to be used to infer temperatures. These numbers are asked for only if Sense Switch 4 is set.

c. Spectrum Scaling Chart

This chart (Figures 7 through 10) is on paper tape and is read in just once during a computer run. The ion temperature and the temperature ratio are derived from this chart, as has been seen in Section II-B.

For more detail on these various inputs, refer to the descriptions of each subroutine which follow. The routines are described in their calling order (see the general flow chart, Figure 24). Most of the variables are in common, and are listed with their definitions in Table VI.

2. MAIN Program

Subroutines called: ENTRE
POWER
MAD

Description. To make the program more versatile, the MAIN program calls the major routines, instead of having them linked one to the other. Its flow is a simple loop:

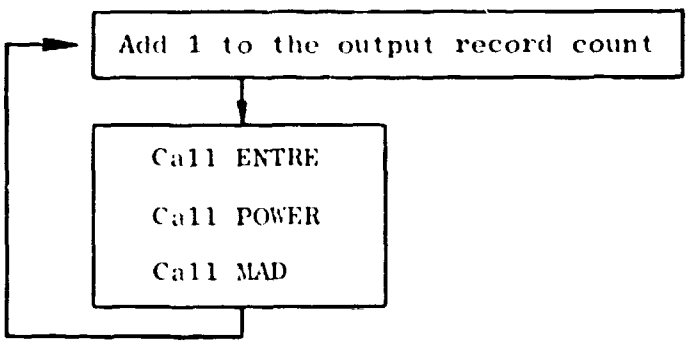

When the computer run has ended, the operator branches to an instruction which writes an end of file on the output tape. Then the program comes to a halt, which, once cleared, is followed by a REWIND of the output tape.

3. Input Routine ENTRE

Arguments: None

Called by: MAIN

Routines called: STARTR
CONTR
UNPACK
INTEGRE
INTOF
SATOFF
SPECTRE

Description. ENTRE is the routine that performs the input of the recorded data to be analyzed. It reads an appropriate number of records from the input tape, tests each of them for the presence of a satellite (in which case it drops the record), and integrates these data.

Let us now follow step by step the flow chart of the subroutine (see Figure 25).

a. Tape Ready Test

This is performed by a call to STARTR, a machine language subroutine; the input tape has to be on Unit 3 and Density 556.

b. Input Tape Positioning

The first time in the program, one might want to start the integration on a record somewhere in the middle of the input tape. If Sense Switch 3 is set, the time to position the tape is asked for by the message: WANTED TIME. After the wanted time, WT, has been typed in, the input tape is read in until the tape time, which is decoded by the Machine Language Routine UNPACK, is equal to or greater than WT. The following message is then typed: READ TIME hh mm sss.

c. First Record Read

After the message, NUMBER OF PULSES, the operator types in NP, the number of pulses on which he wishes to perform the integration. For a 15-minute integration period and a PRF of 75 per second, NP = 67500. One minute is usually the integration period used during the on-line radar run. ENTRE reads the first input record into the buffer IB and prints all the header information (Words 1 through 20 of the input buffer). The reading routine, called CONTR, is an entry of STARTR. Then, the value

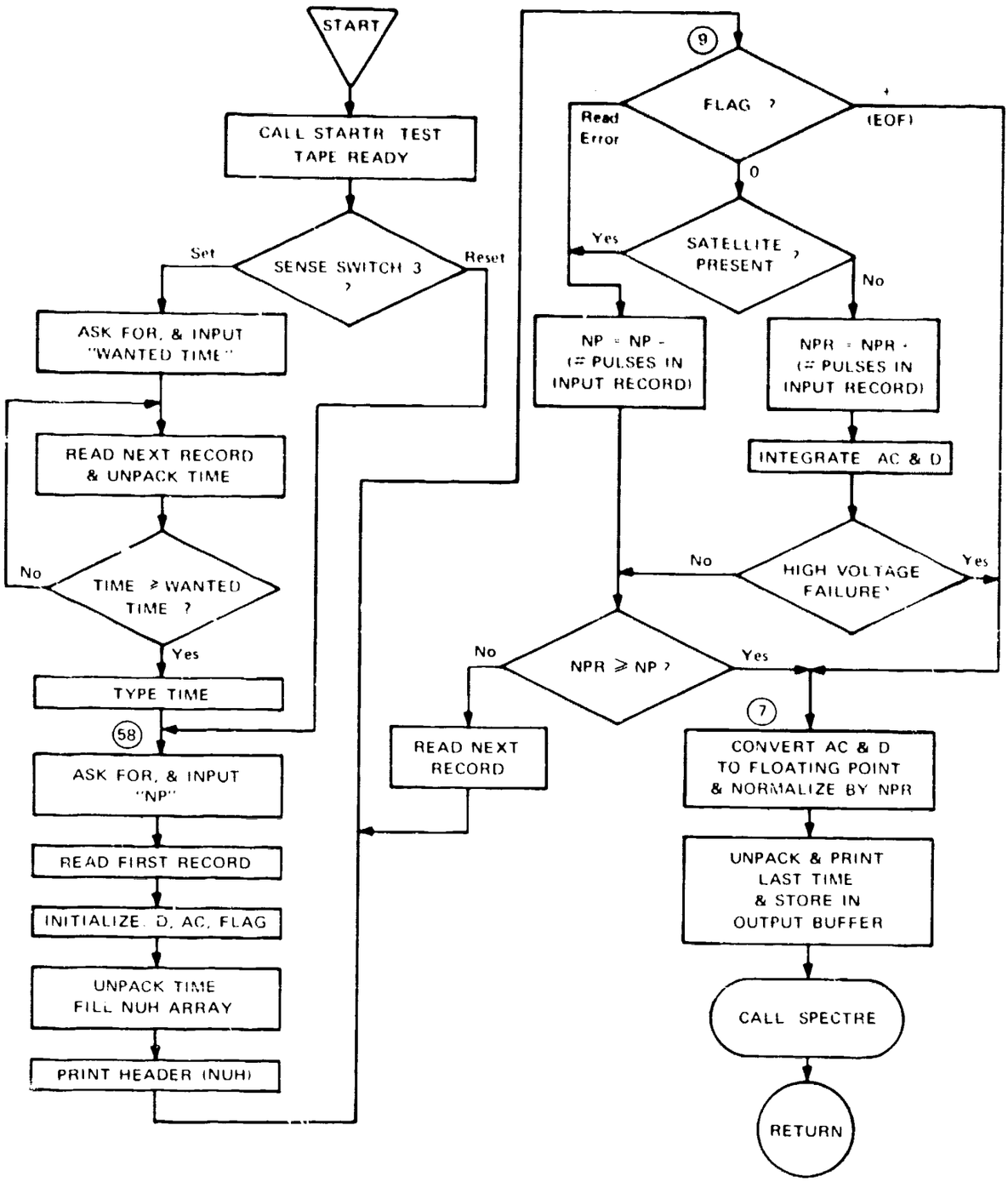

FIGURE 25 ENTRE FLOW CHART

of the ionosonde frequency f_oF2 is asked for (see MAD, for the use of this parameter).

d. Input Record Test

A flag [IB(981)] is set by CONTR, to a negative number if there was a read error, is set to a positive number if the record read was an END OF FILE mark, or remains zero if the input record was properly read.

The other test performed here is the search for satellites. It was noticed that frequently the data for an entire 15-minute integration period were spoiled by a satellite passing through one of the radar side lobes for a few seconds. This is why, before being integrated, the power profile is screened by SATOFF. If there was a satellite, the argument IBUMP returned by SATOFF is equal to the power sample index of the beginning of the "bump" caused by the reflection on the satellite. If IBUMP is not zero, the data are not added to the accumulating buffer, and a message giving the time and IBUMP is printed.

e. Integration

The autocorrelation coefficients and power samples have been recorded as double precision integers, with the lower-order words grouped together first, followed by the higher-order words (Table V). After each record has been read, the autocorrelation coefficients and power profile sample are accumulated in Arrays AC and D, by Machine Language Subroutine INTEGRE.

At the end of the integration period the accumulated values, $AC(\ell,g)$ and $D(j)$ are converted into floating point variables by Routine INTOF. However, the integration is terminated if an end of

file has been encountered in the input tape, or a high-voltage failure in the transmitter occurred during the data collection period.

In brief, when ENTRE has finished, Arrays D and AC contain

$$D(j) = \frac{1}{NP} \sum_{i=1}^{NP} P_i(j) \tag{28}$$

$$AC(\ell,g) = \frac{1}{NP} \sum_{i=1}^{NP} AC_i(\ell,g) \quad , \tag{29}$$

where

j = range index

i = pulse index

ℓ = lag number

g = gate number.

The autocorrelation coefficients array is the argument of Routine SPECTRE which is called at this point to compute and plot the spectra.

4. Satellite Detection Routine SATOFF

Arguments: IB, IBUMP. IB is the read buffer array; IBUMP is the index of the power sample where the satellite, if any, was detected.

Called by: ENTRE

Routines called: FOS1 and FOS2

Description. Since the analyzed data had often been spoiled by an interface of a satellite passing in one of the sidelobes during the radar run, this subroutine was written to screen out the bad records.

As an example, Figure 26 shows the power, in decibels, plotted as a function of the range. Two satellites were detected during the integration period. The low-altitude satellite spoiled the spectral data, and the high-altitude one gave a wrong noise level. The importance of not integrating data containing satellite echoes is apparent.

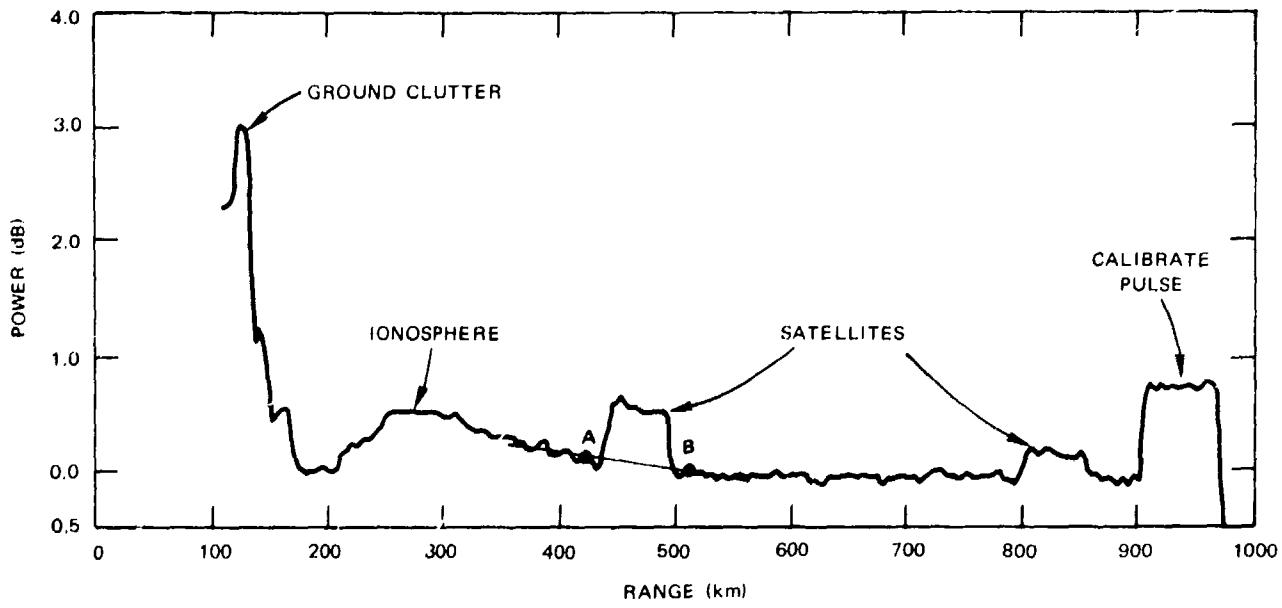

FIGURE 26 POWER PLOT SHOWING SATELLITE ECHOES

A satellite echo is a square pulse, equal in length to the transmitted pulse. With a typical pulse length of 360 μs and a sample interval, Δd, of 30 μs, the number of samples in the echo is $\tau/d = 12$.

To screen out the satellite echoes, we first test whether a detected bump in the power profile encompasses eleven or twelve samples. Since the satellite echo can be anywhere in the power profile, we cannot compare the value of twelve samples to the ground level but must draw a line joining two power samples without satellite influence (Line A-B in Figure 26).

Starting at an altitude of 375 km, each sample D(j) is compared with the preceding one; the difference,

$$DIF = D(j - 1) - D(j), \tag{30}$$

is compared to SIG4

$$SIG4 = 5 \cdot \sigma = \frac{5}{\sqrt{N}} \cdot \frac{D(j - 1) + D(j)}{2} \tag{31}$$

(N is the number of pulses per input record, typically 4500).

If DIF is bigger than 5σ, the point is deemed aberrant. In the case of a satellite, we can anticipate two of these aberrant points, the first with a positive DIF, the second with a negative DIF, the difference in their indexes being 11 or 12. This is what is done in the first part of the program (see Figure 27 for the flow chart).

This test was found not to be sufficiently refined, since received signals from interfering radars frequently caused DIF to exceed 5σ when no satellite was present. Consequently, a further test was introduced: The equation of the line AB is computed:

$$y = aj + b \quad , \tag{32}$$

and all the satellite echo samples must have an amplitude greater than $aj + b + 5\sigma$. The last sixteen samples are treated differently, because they represent the calibration pulse. When $j \geq 177$ (177 is the index of the first calibration sample), the power D(j) is divided by the ratio PC/PN. Then the sample is submitted to the above test procedure.

If the data do not satisfy this last condition, IBUMP is set to zero again, and the remaining samples are screened. The samples in

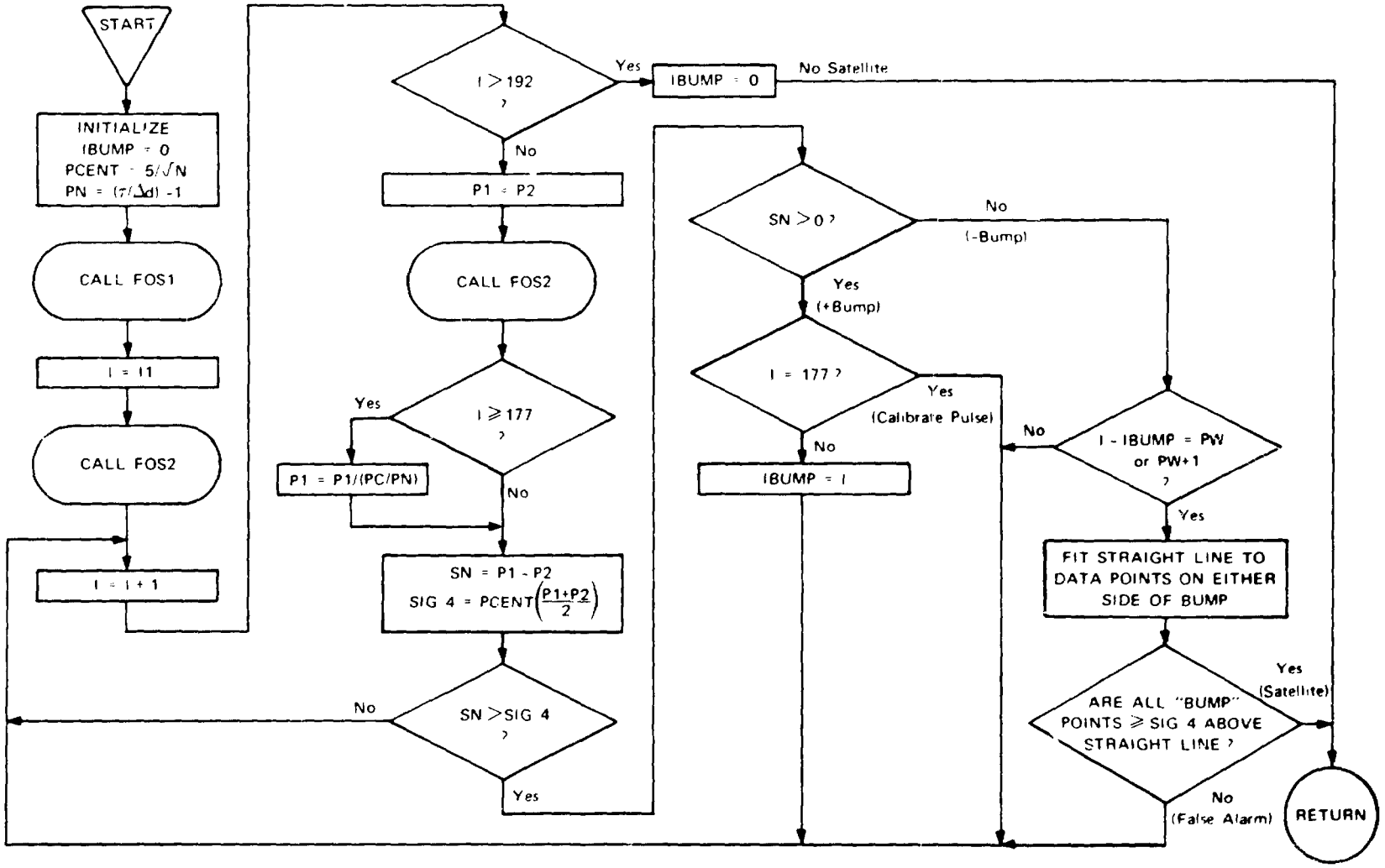

FIGURE 27 SATOFF FLOW CHART

the read-buffer array IB are not in a format suitable to FORTRAN. Therefore, a Machine Language subroutine was written to convert a particular power sample from the IB array into a floating point number. This conversion is performed by Subroutines FOS1 and FOS2.

5. Spectrum Routine SPECTRE

Argument: AC(ℓ,g)

Called by: ENTRE

Routines called: PTRANS
PLOT

Description. It has already been said (Section III-B) that the Fourier transform of the autocorrelation coefficients is the backscattered spectrum in which we are now interested and that from two parameters of this spectrum--the peak-to-valley ratio and the bandwidth--one can compute the electron and ion temperatures. Hence, the three tasks of SPECTRE are:

(1) To compute the Fourier transforms of the nine autocorrelation functions

(2) To draw the noise spectrum and the eight signal spectra. These plots, in fact, are here only for diagnostic purposes.

(3) To compute the PV and BW of the eight signal spectra.

The AC array is double-indexed: ℓ is the lag index (ℓ = 0 to 23 or 31), and g is the gate index (g = 1 to 9), with g = 9 corresponding to the noise gate. The Fourier cosine transform is used:

$$S(f) = \Delta t \sum_{\ell=0}^{L} AC(\ell,g) \cdot \cos(2\pi \ell f \Delta t) \quad , \qquad (33)$$

where

S is the energy at the frequency f,

Δt is the interval between two samples.

Δt limits our spectral definition: FF = $1/(2\Delta t)$ is the maximum frequency we can resolve. Numerically, for Δt = 10 μs, we have FF = 50 kHz.

The subroutine performing this Fourier transform is PTRANS. It computes, for each frequency f,

$$S'(f) = AC(0,g) + 2 \sum_{\ell=1}^{L-1} AC(\ell,g) \cdot \cos(2\pi f \ell \Delta t) + AC(L,g) \cdot \cos(2\pi f L \Delta t) \quad . \tag{34}$$

Figure 28 is a simplified flow chart of this subroutine.

a. Noise Subtraction and Normalization

Each of these $AC(\ell,g)$ contains both signal and noise. The noise is subtracted and the coefficients are normalized to the zero-lag coefficient. The normalization factor, AC(0,g) - AC(0,9), is the total signal energy received in the g gate:

$$AC(\ell,g) \longrightarrow \frac{AC(\ell,g) - AC(\ell,9)}{AC(0,g) - AC(0,9)} \qquad \text{for } g \neq 9 \tag{35}$$

$$AC(\ell,g) \longrightarrow \frac{AC(\ell,9)}{AC(0,9)} \qquad \text{for } g = 9 \quad . \tag{36}$$

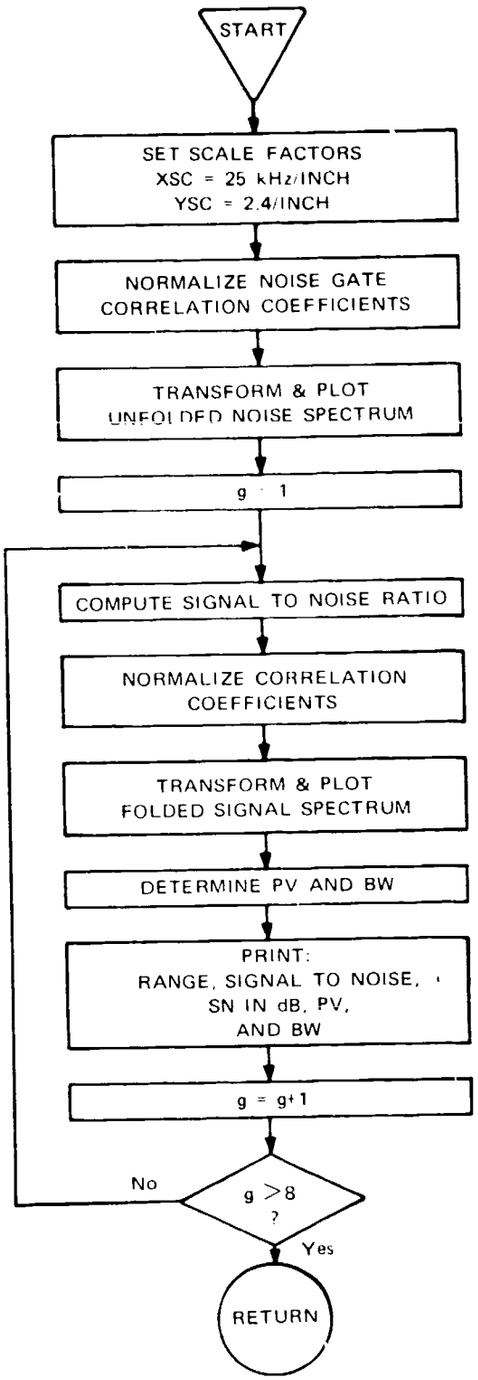

FIGURE 28 SPECTRE FLOW CHART

b. Bandpass Filter Correction

Since the filter shape is not a clear-cut battlement, the spectrum $S'(f)$ is corrected for the shape of the noise spectrum:

$$S(f) = S'(f) \cdot \frac{S_{noise}(CF)}{S_{noise}(f)} \quad .$$

This correction is done in Subroutine PTRANS.

c. Plots

Figure 29 is an example of the spectra. The scale is 25 kHz/inch in the abscissa, and the ordinate is relative power. The noise plot is drawn first, with f varying from 0 to FF. As stated previously (Section II-B), the scattered spectra are symmetric around zero Doppler shifts, assuming the effects of ionospheric drifts or currents to be negligible. Thus, the signal is assumed to be symmetric and folded around the center frequency, CF, which is related to the intermediate frequency, IF, and to the maximum frequency, FF, by

$$CF = 2FF - IF \quad . \tag{38}$$

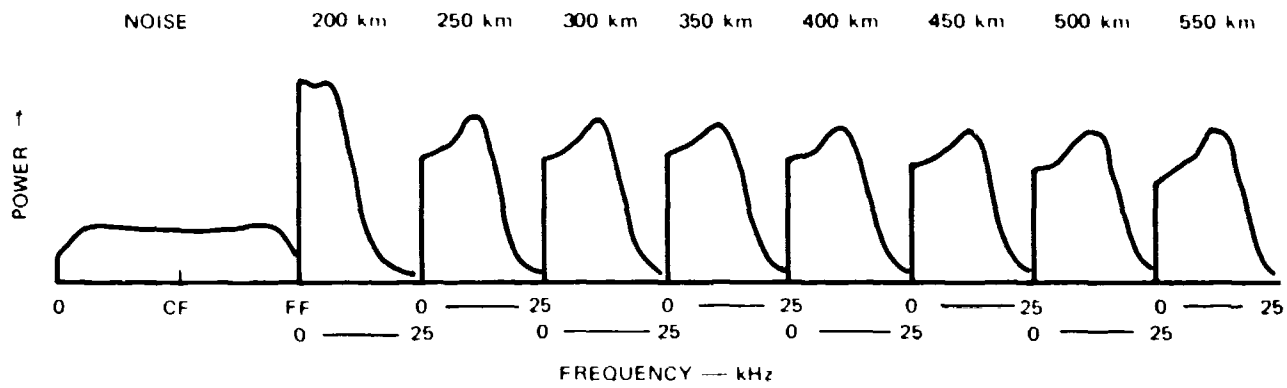

FIGURE 29 SAMPLE OUTPUT PLOTS OF SPECTRA

Typically, CF = 25 kHz. The plots at the eight different ranges are the "folded" spectra; that is, y = S(f) + S(2CF - f) is plotted against an abscissa f between the center frequency and the maximum frequency.

d. Peak-to-Valley Ratio, Bandwidth, and Signal-to-Noise Ratio

During the computation of the spectrum S(f) the program derives the peak-to-valley ratio,

$$PV = \frac{S_{max}}{S(CF)} \quad , \tag{39}$$

and the bandwidth BW, the frequency at which the spectral power has fallen to $S_{max}/2$. These two parameters enable us to derive the ion temperature T_i, and the temperature ratio ξ.

To determine whether our incoherent scatter spectrum is "good" enough to give a value for T_i and T_r, the signal-to-noise ratio (SNR) is used:

$$SNR = \frac{\text{Signal + Noise}}{\text{Noise}} - 1 = \frac{AC(0,g)}{AC(0,9)} - 1 \quad .$$

If the SNR exceeds SNMAX (described previously), the spectrum is considered "good" and is used to infer temperatures by Subroutine INTERP.

6. Power Profile and Raw Density Routine POWER

Argument: None

Called by: MAIN

Subroutine called: PLOT

Output: Power plot

Description. POWER does two different things: It plots the received power (in decibels) as a function of the range (in kilometers), and it calculates a raw electron density using Eq. (3).

Figure 26 is an example of the output. The plot scale is 2 dB/inch in the y axis and, in the x axis, 200 or 400 km/inch, depending on whether the interval Δd between the samples is 30 or 60 μs.

Figure 30 is a simplified flow chart of this program. One sense switch is used. If SS4 is set, the number of calibrate pulse samples, NC, and of noise samples, NN, is asked for. If it is reset, NC and NN are left unchanged.

a. Calibration

To measure the received power, a calibrated noise level is injected in the last sixteen density samples. This calibration pulse temperature is

$$T_K = 70 \cdot 2^{-CC/3} \text{ (degrees Kelvin)} \quad , \tag{41}$$

where CC is the calibration code, NUH(9). The exponent CC/3 is the number of 3-dB attenuators inserted prior to injection of the noise pulse (see Section III-A). For CC = 0, which is a typical value, $T_K = 70^\circ$. The only other values CC can have are 3, 6, or 9. We thus have

$$P_K = KT_K B_D \quad , \tag{42}$$

where P_K is the power injected in the calibration pulse, K is Boltzmann's constant, and B_D is the receiver bandwidth.

To determine the value of the noise level, the program averages the NN samples that are just before the NC calibration samples.

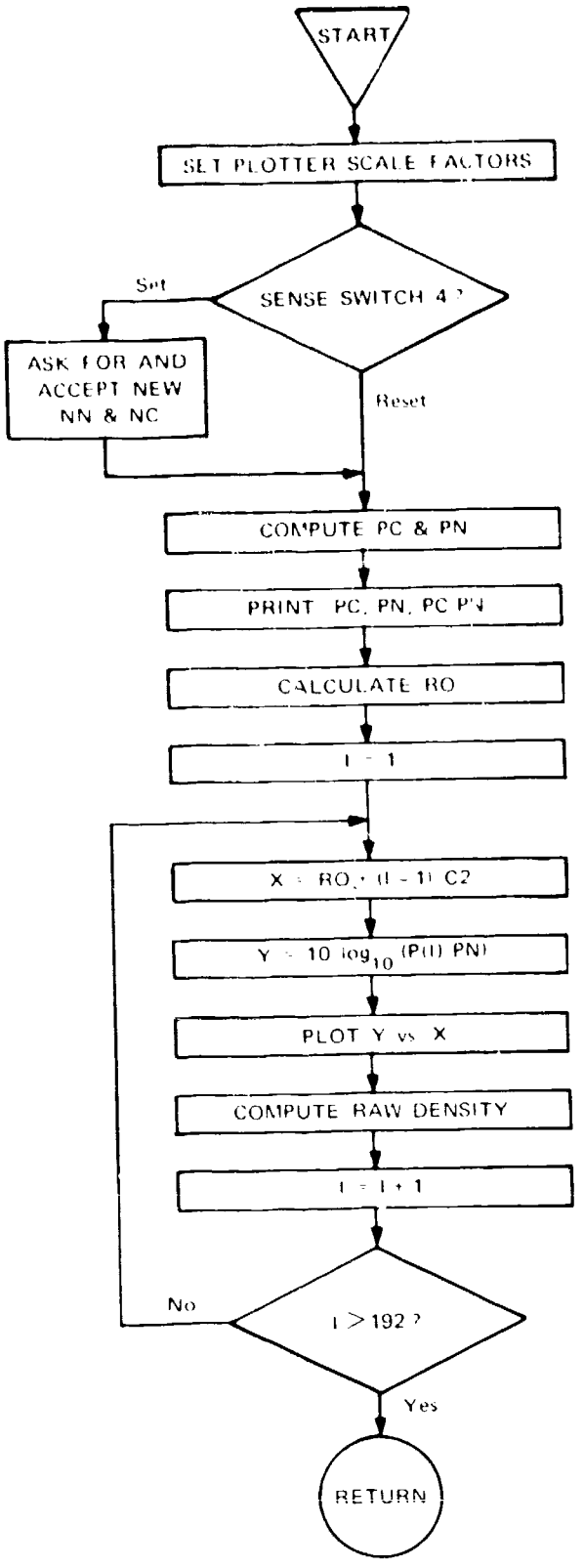

FIGURE 30 POWER FLOW CHART

Typically, NN is sixteen samples, but during the night periods, when the electron density is very low, this number can be greater for more precision--32 or 40. During daytime, the electron density is sometimes so high that, even at the range of these last pulses, some signal is still present, resulting in a computed noise level that is too high.

In brief, the values of PC and PN are given by

$$PC = \frac{1}{NC} \sum_{j=192-NC+1}^{192} P(j) \qquad (43)$$

$$PN = \frac{1}{NN} \sum_{j=192-NC-NN}^{192-NC-1} P(j) \quad . \qquad (44)$$

b. Power Plot

Along the Y coordinate, the quantity plotted is

$$Y(j) = 10 \log_{10} [P(j)/PN] \quad (dB) \quad . \qquad (45)$$

The axis is drawn at Y = -1 dB. The range along the X coordinate is

$$X(j) = R_0 + C2(j - 1) \quad (km) \quad , \qquad (46)$$

where C2 is the range interval between samples, and R_0 is the range of the first sample. Here R_0 is given by

$$R_0 = 20 * (D - 1) + 3.3 - \frac{\tau c}{4} \quad (km) \quad , \qquad (47)$$

where D is the delay code, τ is the pulsewidth, and c is the velocity of light.

c. Electron Density

In this routine (POWER) the raw electron density is next computed. By combining Eqs. (3), (4), (41), and (42) we arrive at the following equation for raw electron density:

$$D(J) = \frac{C_S K\ 70(2^{-CC/3})B_D[P(J) - PN]X(J)^2}{P_T \tau (PC - PN)} \ (el/m^3) \quad , \qquad (48)$$

where all the terms have previously been defined. For simplicity in the program, all the unchanging terms over an integration period are collected together into CON, where

$$CON = \frac{C_S K\ 70(2^{-CC/3})B_D}{P_T \tau (PC - PN)} \quad , \qquad (49)$$

and thus the raw density is

$$D(J) = CON \cdot X(J)^2 \cdot [P(J) - PN](el/m^3) \quad . \qquad (50)$$

The next thing to do is to compute the true electron density, which is the purpose of the program called MAD.

7. True Density Routine MAD

Argument: None

Called by: MAIN

Routines called: INTERP
SORTIE
PLOT
ANNOT

Function called: CLI (performs a linear interpolation)

Description. After going through Subroutine POWER, the array D contains the raw density. The values of PV and BW have previously been obtained from the spectra in Subroutine SPECTRE; thus we can now compute a More Accurate Density (MAD).

After first initiating the values of the parameters, MAD computes at each spectrum range T_i, δ, and α^2. Then, following the procedure described in Sections II-B-4 and II-C, it computes the true densities at each power sample range and the true temperatures corrected for nonzero α^2. Let us now see in more detail how these operations are performed. Figure 31 is the flow chart of MAD.

a. Initialization of Program

Two switches are used in this first part of the program:

(1) If SS1 is set, the value of SNMAX is asked for; if it is reset, the value 0.10 is assumed (if no other value has been given previously).

(2) If SS2 is set, the program pauses, then reads from paper tape the spectrum scaling chart. This has to be inputted only once, the first time the program is executed.

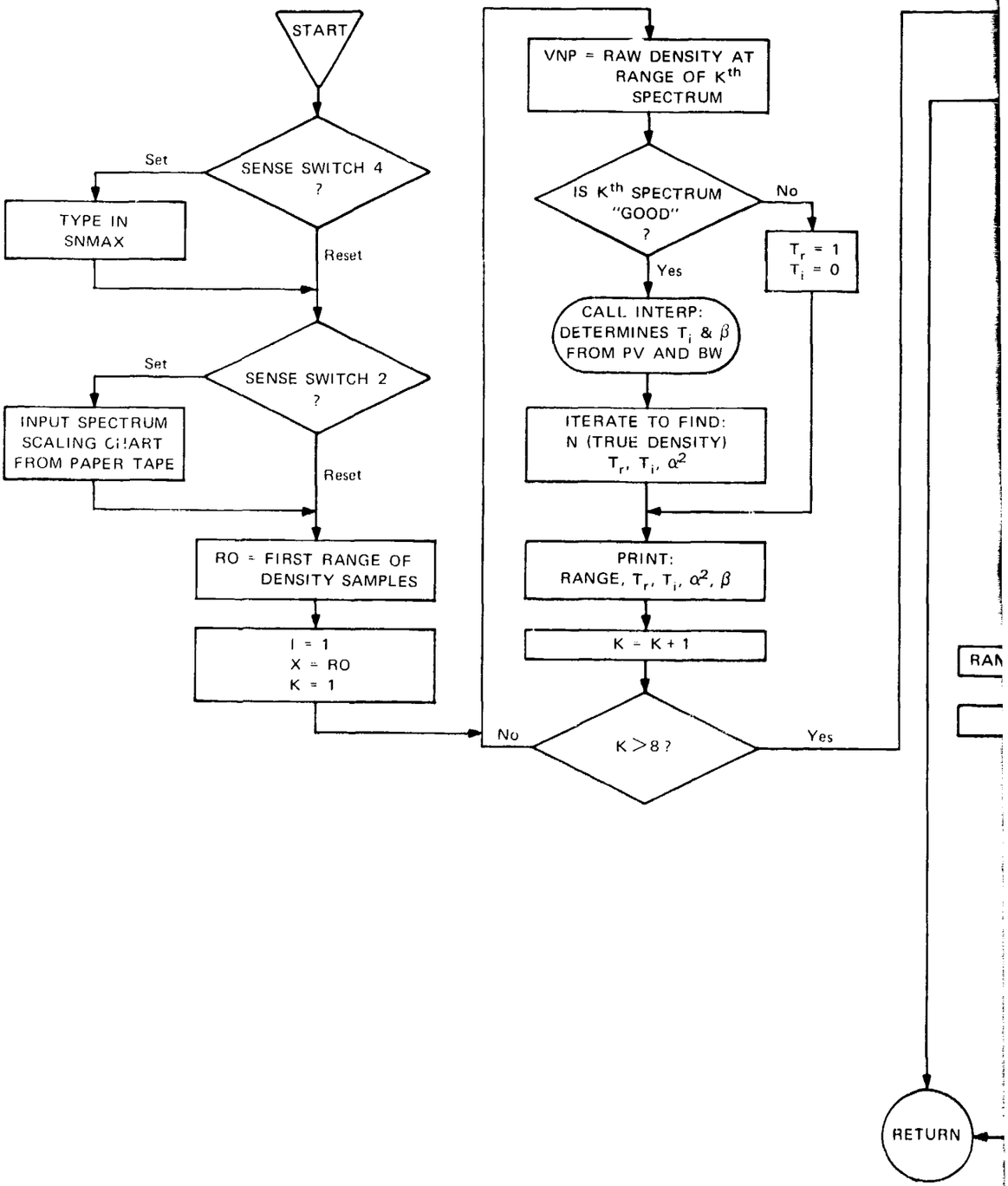
START
SENSE SWITCH 4 ?
Set
TYPE IN SNMAX
Reset
SENSE SWITCH 2 ?
Set
INPUT SPECTRUM SCALING CHART FROM PAPER TAPE
Reset
RO = FIRST RANGE OF DENSITY SAMPLES
I = 1
X = RO
K = 1
VNP = RAW DENSITY AT RANGE OF K^th SPECTRUM
IS K^th SPECTRUM "GOOD" ?
No
Yes
T_r = 1
T_i = 0
CALL INTERP: DETERMINES T_i & β FROM PV AND BW
ITERATE TO FIND: N (TRUE DENSITY) T_r, T_i, α^2
PRINT: RANGE, T_r, T_i, α^2, β
K = K + 1
K > 8 ?
No
Yes
RETURN

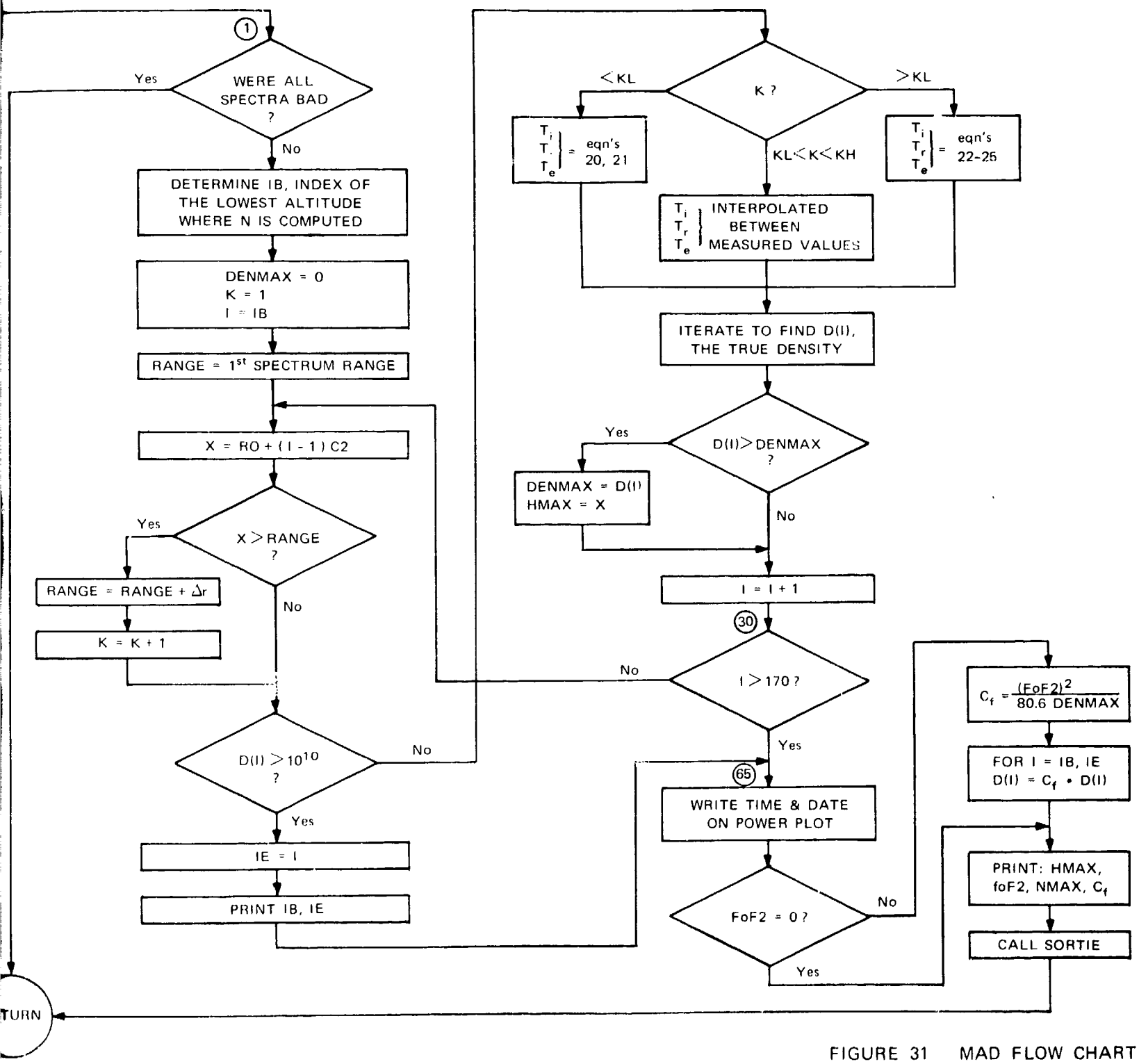

FIGURE 31 MAD FLOW CHART

b. Computation of T_i and β at Each "Good Spectrum" Altitude

The two parameters of a backscatter spectrum, the peak-to-valley ratio and the bandwidth, are functions of the temperatures T_i and T_e, and also of the α^2. The data are first processed by assuming $\alpha^2 = 0$, which gives a first value of T_i and of the temperature ratio, T_r. The value of the raw density is then used to correct these T_i and T_r, which, in turn, are used to correct N. After the raw density has been replaced by this new N, the T_i and T_r are recalculated, and the process loops until consistent values are found for N, T_i, and T_r. This iteration is done for each altitude at which a spectrum has been computed.

Before being used to infer T_i and β, a spectrum must satisfy these four criteria:

(1) $9 \leq BW \leq 26$

(2) $1 < PV \leq 2.6$

(3) $N' \neq 0$ (raw density at the altitude of the considered spectrum)

(4) $SN > SNMAX$.

The index of the lowest good spectrum is called KL, and he index of the highest one is KH. For each K spectrum, $KL \leq K \leq KH$, Subroutine INTERP is called in, which uses the spectrum scaling chart (paper tape input of this program) to interpret PV and BW in terms of T_i and β. The program then iterates around the equations

$$T_r = \beta(1 + \alpha^2) \tag{51}$$

$$T_e = T_i * T_r \tag{52}$$

$$VN = \frac{N'}{2}(1 + \alpha^2)(1 + \alpha^2 + T_r) \tag{53}$$

$$\alpha^2 = 14.22 \times 10^6 \, T_e/VN \tag{54}$$

until the temperature T_c and the density converge. At this point, the temperature and the density are printed out.

When this loop over K has been terminated, KL is tested; if it equals zero, this means that all the spectra were bad and the densities cannot be accurately measured; control is returned to the MAIN program, and a new integration is started. There will be no density plot and no output on tape.

c. Computation of True Density

It is meaningless to compute the density at an altitude where ground clutter is present or where the density is smaller than the accuracy of the measurement.

Therefore we next determine the altitude extent over which to compute true densities. The index IB of the first density is determined in the following way. Starting at the altitude of the first good spectrum, one follows down the D(j) curve until D(j) is less than 10^{10} el/m^3. IB is then set equal to the index, j, at this point. If D(j) is never less than 10^{10}, IB is set to the index of the minimum of the density curve.

Similarly, the index, IE, of the highest altitude at which the density is plotted is determined by the altitude at which D(j) exceeds 10^{10} el/m^3. If the density never gets smaller than 10^{10} el/m^3, then IE is set to 170, equivalent to a range just before the calibrate pulse.

To compute true densities, T_r and T_i are computed at each range between IB and IE where a power profile sample exists. The temperatures are computed differently, depending on whether the range is (1) under the lowest good spectrum; (2) between two good spectra; or

(3) above the highest good spectrum. Section II-C describes the procedures used for each of these three cases.

The iteration that gives the true density from the raw density uses the two equations

$$\alpha^2 = 14.22 \times 10^6 * T_e/VNP \qquad (55)$$

$$N = \frac{N'}{2} * (1 + \alpha^2)(1 + \alpha^2 + T_r) \quad , \qquad (56)$$

where VNP is the previous N.

To converge faster, a first α^2 is computed from Eq. (55) and then an N1 from Eq. (56), and the first VNP is taken to be the geometrical mean between N′ and N1,

$$VNP = \sqrt{N' \cdot N1} \quad . \qquad (57)$$

When the density profile has been computed, the D array is multiplied by C_f,

$$C_f = N(f_oF2)/N_{max} \quad , \qquad (58)$$

where

$$N(f_oF2) = (f_oF2)^2/80.6 \qquad (59)$$

N_{max} = maximum density computed from incoherent measurement alone,

so that the value of DENMAX is equal to the one deduced from f_oF2.

After the data have been processed by MAD, all the computations for this integration period are finished. All that needs to

be done is to plot these values and to write them on the output tape; this is the task of SORTIE, which is called at this point.

8. Output Routine SORTIE

Arguments: TI,TR

Called by: MAD

Routines called: PLOT
ANNOT
LABEL

Description. This output routine plots the values of the electron densities, the electron temperatures, and the ion temperatures as a function of altitude. Figure 32 is an example of this plot. SORTIE also writes the computed true densities and temperatures on a magnetic tape. Figure 33 is the flow chart for this routine.

a. Plotting of the Densities

To eliminate some noise fluctuation, and since the transmitted pulse length is not zero, the density profile is smoothed before being plotted.

Typically, the pulse width is τ = 360 μs, and Δd = 30 μs, so the smoothing should be over

$$\frac{\tau}{2} \times \frac{1}{\Delta d} = 6 \text{ samples} \quad .$$

In the program we average over five samples and plot the averaged density at the altitude of the middle sample. The density is plotted on a linear scale of 2×10^{11} el/m^3 per inch of graph. If the

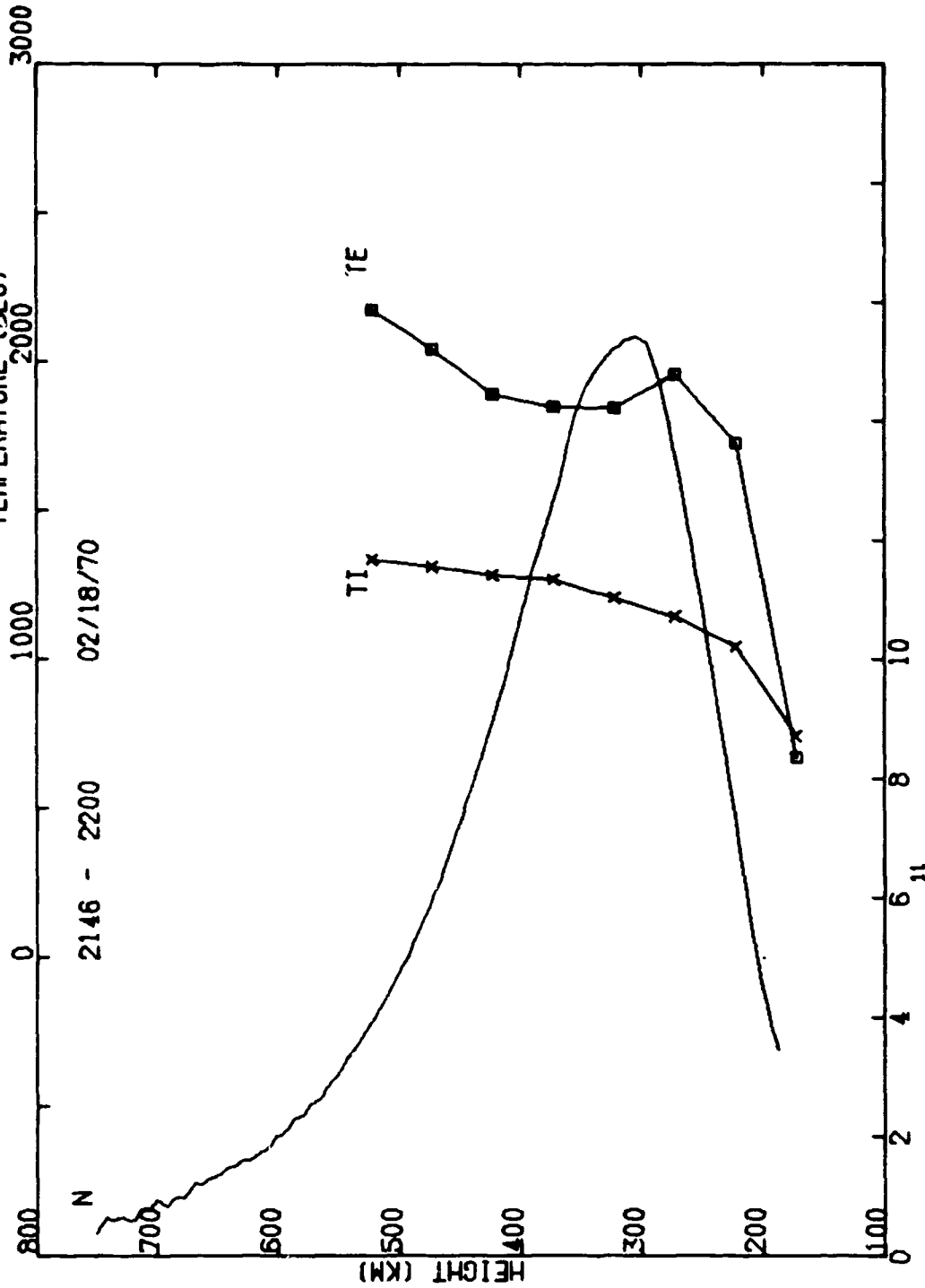

FIGURE 32 EXAMPLE OF DENSITY AND TEMPERATURE PROFILES

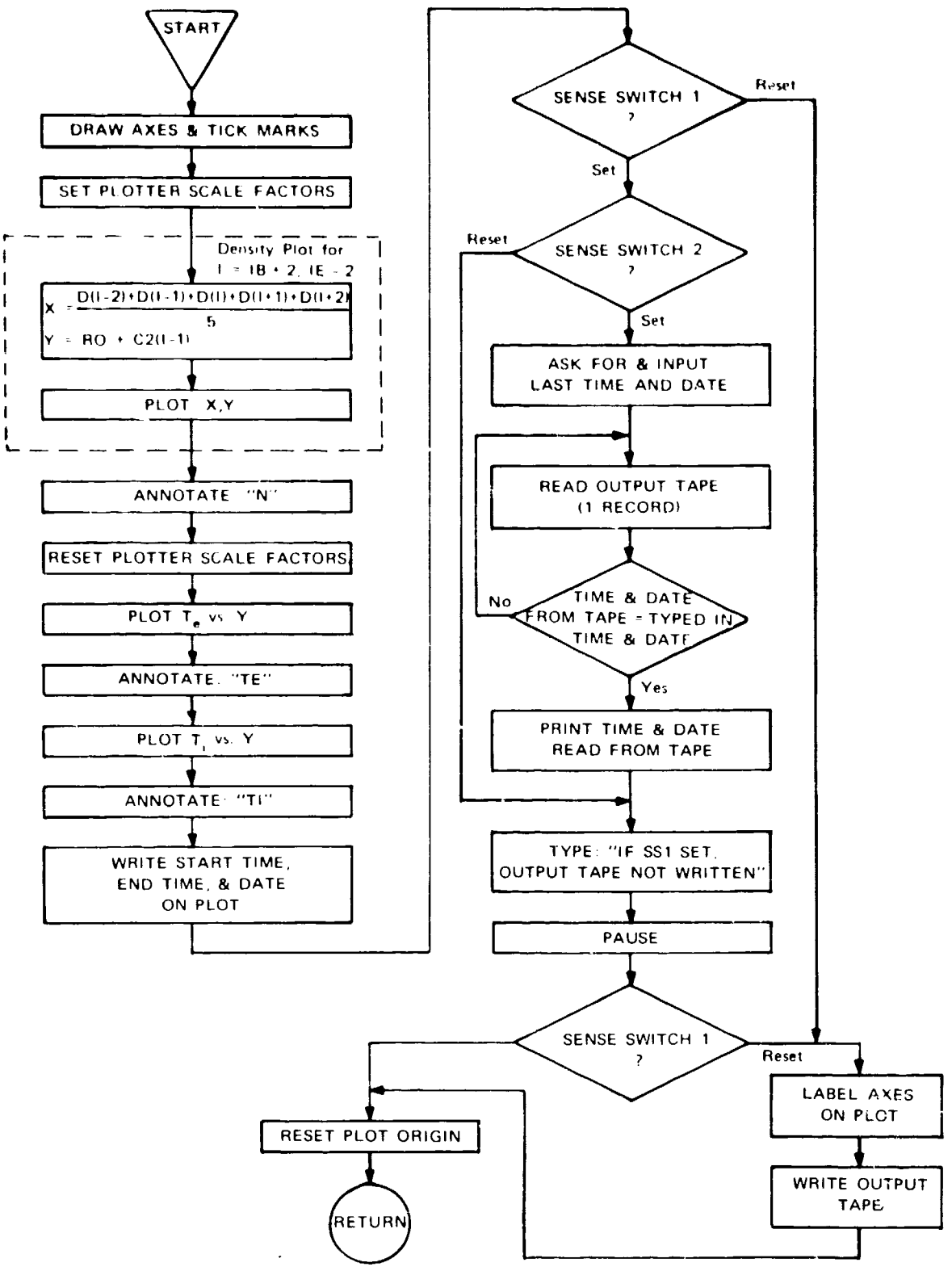

FIGURE 33 SORTIE FLOW CHART

calculated density is bigger than 20×10^{11} el/m^3, the values are plotted with a new origin shifted 10 inches to the left.

b. Plotting of the Temperatures

The electron and ion temperatures are plotted only at the altitudes at which the spectra were good. They are plotted on a linear scale of 400°K per inch of graph. The measured T_i's are identified by an "X" and the T_e's by a small square. Straight lines connect the measured temperatures. If one of the values is out of the scale ($T > 3000°$), the pen is lifted, and the point is shown at the 3000° edge of the graph.

c. Labeling of the Graph

The graph is labeled in the upper center with the start and end times of the integration period and the date. All times and dates are GMT. When these values have been written, Sense Switch 1 is tested. If it is set, the message

IF SS1 SET, OUTPUT TAPE NOT WRITTEN

is typed out, and the program halts. If, when the halt has been cleared, SS1 is still set, the labeling is not finished, and, more important, the output tape is not written with the data corresponding to this integration period.

d. Output Tape

The tape has to be mounted on Unit 2, the density is 556 bpi, and the tape is written in BCD format. This format has been adopted so that the BCD output tapes can be reread by any other computer (XDS, CDC, or IBM alike), hopefully!

1) Positioning of the Tape. One might need to position the output tape after a specific record in order to stack additional data on a previously written output tape. To do this, set both Sense Switches 1 and 2. Program SORTIE, after plotting the temperatures and writing the time and date, tests SS1 and SS2. If both are set, it types the message

GIVE LAST TIME (A4), AND DATE (2A4) .

The operator types in the last integration time of the record on which he wishes to position the tape. The tape is read, record by record, until:

(1) The date read is the same as the one asked for

(2) The last time read is equal to or bigger than the typed-in time. The message OUTPUT TAPE ON hhmm sss is then typed.

The next data will be written following this last read record.

2) Tape Format. A BCD written tape has a physical record length of up to 132 characters. One logical record contains one or more physical records. In our case, in one logical record, the data corresponding to one integration period are written, with the following coding:

```
      WRITE OUTPUT TAPE 2 , 101, NREC, NUH, D, TI, TR, PC, PN, IB, IE
     1,[MORE[J],J=2,6]
101   FORMAT [16, 216,2A4, 616, 2A4 ,816, /,
     1 19[10E12.6,/],2E12.6,/, 2[8E12,6,/]
     1 ,2E12.6,16,16,A4,A3, /,316,15X]   .
```

Table VII shows the output tape format.

Table VII

OUTPUT TAPE FORMAT

Symbol	Definition	Format	Number of Physical Records
NRE	Sequential output record number	I6	1
NUH	Header (see COMMON)	I6 or A4	
D	Densities in el/m^3 (192 values)	E12,6	20
TI	Ion temperatures (8 values)	E12,6	1
TR	Temperature ratios (8 values)	E12,6	
PC,PN	Calibration and noise level	E12,6	1
IB,IE	Start and end index of true density	I6	
MORE(2),MORE(3)	Last time	A4,A3	
MORE(4)	C_f * 1000	I6	1
MORE(5),MORE(6)	Blanks	--	

PRECEDING PAGE BLANK-NOT FILMED

V SUMMARY AND RECOMMENDATIONS

In this report we have explained in detail the use of the Project 617 radar for making incoherent scatter measurements of the ionosphere. The data processing and analysis methods have been fully described, including all the assumptions, interpolations, and extrapolations. Those portions of the radar hardware that are especially important to the incoherent scatter measurements and those portions that have been developed, modified, or improved during the past year have also been described. The new computer software, in combination with the digital autocorrelator, has resulted in an order-of-magnitude improvement in data processing time, as well as an improvement in measurement accuracy.

The major improvements incorporated in the radar system during the past year have not only eliminated many inaccuracies and uncertainties that previously existed but also enabled us to detect small (5- to 10-percent) semi-systematic errors that were previously unnoticed. The larger quantities of data that we have been able to process with the new system have also made us aware of the need for additional computer programs to aid in the interpretation of the data. These two areas should be the object of system improvement work in the future. Listed below are several recommendations for future work that would further improve measurement accuracy and increase the convenience and flexibility of the data interpretation.

In comparing the incoherent scatter measurement of the F-layer maximum electron density, N_{max}, with the maximum density, N_{foF2}, as determined by an ionosonde, we have found small (±0.25-dB) systematic discrepancies on top of a roughly equal random discrepancy. Since all

the incoherent scatter profiles are normalized to f_oF2, the final accuracy of the density measurement is determined by the accuracy to which f_oF2 can be scaled, and this accuracy ($\approx$0.25 dB) is the main cause of the random discrepancies between N_{max} and N_{f_oF2}. We believe the systematic discrepancy which varies slowly with time is due to a poor choice of filter in the detected output channel of the receiver. A single-pole filter is used which causes relatively less energy to pass under conditions of high electron temperature (more energy in the spectrum wings) than low. Consequently, when the electron temperature is high, the electron density is underestimated. A redesigned filter would eliminate this problem and would tend to make the accuracy of the incoherent scatter measurement better than the accuracy to which f_oF2 can be scaled from the ionosonde.

In the area of computer software, the following items would be useful:

(1) A facility for having different--instead of the same--integration times for the power profile data and spectral data. To obtain equivalent accuracies, longer integration times are needed for the spectral data than for the power profile data.

(2) A program that would produce a motion picture of the density and temperature profiles. Presently, these profiles are drawn on the graph plotter (e.g., Figure 33). This consumes most of the processing time and results in many graphs--typically about 200 for a 48-hour run. A movie condensing 24 hours of data into 5 to 10 minutes of viewing would be useful and informative.

(3) A flexible parameter plotting package. All the reduced data are now available on one output tape, but no programs exist to make use of this tape to study ionospheric parameters. A desirable program would be one capable of reading back the tape and plotting any parameter versus any other parameter, e.g., N_{max} versus

time, N at altitude h versus T_e at the same altitude, scale height versus height, and T_r versus N_{max}/N_{f_oF2}. This program would eliminate most of the hand plotting now required to study these ionospheric parameters.

(4) Segmentation of the present off-line analysis program to allow it to be run on the on-site computer. Currently, the program requires almost twice the core storage available in the on-site computer. If the program were split into segments, probably it could be made to run on the project-owned computer. Alternatively, the computer's memory size could be increased.

In summary, the objectives of this year's program have been met. Significant improvements have been made to the Project 617 radar hardware and software, resulting in increased usefulness of the radar for studying both the natural and the disturbed ionosphere.

PRECEDING PAGE BLANK-NOT FILMED

GLOSSARY OF TERMS

A	Effective antenna aperture (m^2)
AC(ℓ,g)	Autocorrelation coefficient for lag, ℓ, and Gate g
AZ	Azimuth angle of antenna measured clockwise from north (degrees)
α	kD = 4π × Debye length/wavelength
α^2	$1.22 \times 10^6 T_e/N$ at λ = 0.23 m
B	Bandwidth (Hz)
B_C	Receiver bandwidth of correlation channel
B_D	Receiver bandwidth of density channel
BW	Measured bandwidth of incoherent scatter spectra from the center frequency to the frequency at which the power is half of its peak value (Hz)
β	Measured electron-to-ion temperature ratio with kD assumed to be equal to zero
c	Velocity of light = 3×10^8 (m/s)
C_j	Calibration factor = N_p/N_m
C_s	System constant = $\dfrac{128\sqrt{2}\,\pi^2}{eG_o^2\theta_{1/2}^2\lambda^2 B(\sigma_e/2)}$
$D_{e,i}$	Debye length = $\left(KT_{e,i}\epsilon_o/Ne^2\right)^{1/2} = 69\left(T_{e,i}/N\right)^{1/2}$ (m)
DN	Thumbwheel switch delay number to first density channel sample
DR	Apparent range (on scope) to first density channel sample = 3.3 + 20(DN - 1)km

Δd	Time interval between samples for density channel (either 30 or 60 μs)
Δr	Range interval between autocorrelation range gates (km)
Δt	Time interval between samples for autocorrelation channel (either 10 or 12,5 μs)
e	Electronic charge = $1,6 \times 10^{-19}$ coulomb
EL	Elevation angle of antenna measured upward from horizon (degrees)
ε_o	Permittivity of free space = $8,854 \times 10^{-12}$ (farads/m)
η	Product of transmit and receive system losses
$f_o F2$	Ordinary wave penetration frequency of the F2 layer as measured by the ionosonde
$\theta_{1/2}$	Antenna half beamwidth measured from center to angle at which gain is decreased by 3 dB (radians)
g	Range gate number ($1 \leq g \leq 9$) for autocorrelation channel
G_o	Antenna gain along main axis
h	Height above earth's surface (m)
h_m	Height of maximum electron density (m)
k	Boltzmann's constant (joule/deg K) = $1,38 \times 10^{-23}$
L	Radar wave number = $4\pi/\lambda$
L	Maximum number of lags (24 or 32)
ℓ	Lag number in autocorrelation computation ≤ 32
λ	Radar wavelength (m)
m_e	Electron mass (kg)
m_i	Ion mass (kg)
N	Electron density (el/m^3)

n — Number of pulses over which integration is performed

N' — A row measured electron density calculated by assuming $T_r = 1$, $\alpha^2 = 0$

N_m — F2-layer maximum density as measured by the incoherent scatter radar

N_p — F2-layer maximum density calculated from $f_o F2 = \left(f_o F2\right)^2 / 80.6$

P_c — Average measured density channel power at last sixteen sample points ($177 \leq j \leq 192$), where injected noise pulse is positioned =

$$\frac{1}{16} \sum_{j=177}^{192} P_j$$

P_j — Average measured density channel power = $\overline{v_j^2}$;
includes both signal power and noise power at most values of j

P_k — Injected calibrate noise pulse power = $KT_k B_D$ (watts)

P_n — Average measured density channel power at sixteen sample ranges immediately preceding calibrate pulse, where received noise alone (no incoherent scatter signal) is present =

$$\frac{1}{16} \sum_{j\ 161}^{176} P_j$$

P_r — Received power (watts)

P_t — Peak transmitted power (watts)

Prf — Pulse repetition frequency (Hz)

PV — Measured peak-to-valley ratio of incoherent scatter spectra

R — Radar range (m)

R_L — Lowest altitude at which measured temperatures are obtained

R_M	Range to maximum electron density
R_U	Uppermost altitude at which measured temperatures are obtained
R1	Apparent range (on scope) to center of first autocorrelation range gate (km)
RN	Apparent range (on scope) to center of autocorrelation range gate in which noise alone is sampled
SNR	Signal-to-noise ratio
SPNR	Signal-plus-noise-to-noise ratio
σ	Effective backscatter cross section of single electron for incoherent scatter = $\sigma_e / \left[1 + \alpha^2 + T_r\right]\left[1 + \alpha^2\right] (m^2)$
σ_e	Backscatter cross section of single electron = $10^{-28} (m^2)$
T_e	Electron temperature (degrees K)
T_i	Ion temperature (degrees K)
T_k	Injected calibrate noise pulse temperature (degrees K)
T_r	T_e / T_i = electron-to-ion temperature ratio
τ	Transmitted pulse length (seconds)
v_j	Measured density channel voltage at j^{th} sample point ($1 \leq j \leq 192$)
w	Range gate width (km)

REFERENCES

1. J. Fejer, "Scattering of Radio Waves by an Ionized Gas in Thermal Equilibrium," Can. J. Phys., Vol. 38, pp. 1114-1133 (1960).

2. J. P. Dougherty and D. T. Farley, "A Theory of Incoherent Scattering of Radio Waves by a Plasma," Proc. Roy. Soc. (London), Vol. A259, pp. 79-99 (1960).

3. T. Hagfors, "Density Fluctuations in a Plasma in a Magnetic Field with Applications to the Ionosphere," J. Geophys. Res., Vol. 66, pp. 1699-1712 (1961).

4. J. V. Evans, "Theory and Practice of Ionospheric Study by Thomson Scatter Radar," Proc. IEEE, Vol. 57, pp. 496-530 (1969).

5. R. I. Presnell, ed., "Electron Backscatter Radar," Final Report, Contract DA-49-146-XZ-259, DASA Report 1823, SRI Project 4740, Stanford Research Institute, Menlo Park, California (1966).

6. M. J. Baron, H. F. Bates, E. J. Fremouw, and J. Petricoks, "Electron Backscatter Research (U)," Final Report, Contract 01-67-C-0019, DASA Report 2088, SRI Project 6291, Stanford Research Institute, Menlo Park, California (1968).

7. D. R. Moorcroft, "On the Determination of Temperature and Ionic Composition by Electron Backscatterings from the Ionosphere and Magnetosphere," J. Geophys. Res., Vol. 69, pp. 955-970 (1964).

8. M. J. Baron, ed., "Electron Scatter Research Using the Project 617 Radar," Final Report, Contract 01-67-C-0019, DASA 2088-II, SRI Project 6291, Stanford Research Institute, Menlo Park, California (1969).

9. W. B. Hanson, "Electron Temperatures in the Upper Atmosphere," in Space Research, Vol. 3, W. Priester, ed., pp. 282-302, North Holland Publishing Co., Amsterdam (1963).

10. P. M. Banks, "Ion Temperature in the Upper Atmosphere," J. Geophys. Res., Vol. 72, pp. 3365-3385 (1967).

11. H. Carru, M. Petit, and P. Waldteufel, "Mesures de températures électroniques et ioniques par diffusion incohérente," J. Atmos. Terrest. Phys., Vol. 29, pp. 351-366 (1967).

DISTRIBUTION LIST

DEPARTMENT OF DEFENSE

Director
Advanced Research Projects Agency
Washington, D.C. 20301

Attn: J. P. Wade

Director
Defense Atomic Support Agency
Washington, D.C. 20305

Attn: RAAE

Director,
Defense Atomic Support Agency
Washington, D.C. 20305

Attn: Technical Library (APTL) 2

Commander
Field Command
Defense Atomic Support Agency
Sandia Base
Albuquerque, New Mexico 87115

Attn: Technical Library FCTG5

Commander Test Command
Defense Atomic Support Agency
Sandia Base
Albuquerque, New Mexico 87115

Attn: Document Control

Commander
Joint Task Force Eight
Sandia Base
Albuquerque, New Mexico 87115

Attn: Technical Operations

Administrator
Defense Documentation Center
Cameron Station - Bldg. 5
Alexandria, Virginia 22314

Attn: Document Control 20

Commander in Chief
North American Air Defense Command
Ent AFB, Colorado 80912

Attn: Chief Scientist

DEPARTMENT OF THE ARMY

Chief of Research & Development
Department of the Army
Washington, D.C. 20310

Attn: AREDA-00

Chief of Research & Development
Department of the Army
Washington, D.C. 20310

Attn: Air Defense Division

Director
Advanced Ballistic Missile Defense Agency
Commonwealth Bldg.
1320 Wilson Blvd.
Arlington, Virginia 22209

Attn: Mr. Archie Gold, CRDABM-DD

Commanding General
Army Missile Command
Redstone Arsenal, Alabama 35809

Attn: AMSI, Chief Scientist

Commanding General
Army Safeguard System Command
P.O. Box 1500
Huntsville, Alabama 35807

Attn: SAFSC-DB, Mr. Solomonson

DEPARTMENT OF THE NAVY

Chief of Naval Research (Code 418)
Department of the Navy
Arlington, Virginia 22217

Attn: Dr. T. P. Quinn

Chief of Naval Research
Navy Department
Washington, D.C. 20360

Attn: Code 402

Commander
Naval Electronics Laboratory Center
San Diego, California 92152

Attn: Technical Library

DISTRIBUTION LIST (continued)

Director
Naval Research Laboratory
Washington, D.C. 20390

Attn: Equipment Research Branch
Code 5360

DEPARTMENT OF THE AIR FORCE

Headquarters
USAF (AFTAC)
Washington, D.C. 20333

Attn: AFTAC TD-3

AF Cambridge Research Laboratories, OAR
L. G. Hanscom Field
Bedford, Massachusetts 01730

Attn: Dr. W. Priester, CRP

AF Cambridge Research Laboratories, OAR
L. G. Hanscom Field
Bedford, Massachusetts 01730

Attn: Dr. G. J. Gassmann, CRPR

Commander
Rome Air Development Center, AFSC
Griffiss Air Force Base, New York 13440

Attn: EMTLD, Documents Library

ATOMIC ENERGY COMMISSION

University of California
Lawrence Radiation Laboratory
Technical Information Division
P.O. Box 808
Livermore, California 94550

Attn: Asst. Dir. for Tests -
Dr. Harry Reynolds

Los Alamos Scientific Laboratory
P.O. Box 1663
Los Alamos, New Mexico 87544

Attn: John S. Malik

Sandia Laboratories
Livermore Laboratory
P.O. Box 969
Livermore, California 94550

Attn: Technical Library

OTHER GOVERNMENT

Environmental Laboratories
Environmental Science Services Admin.
Boulder, Colorado 80302

Attn: W. F. Utlaut

U.S. Arms Control & Disarmament Agency
21st & Virginia Avenue
Washington, D.C. 20451

Attn: Reference Information Center,
Room 5720

DEPARTMENT OF DEFENSE CONTRACTORS

Cornell Aeronautical Laboratory, Inc.
4455 Genessee Street
Buffalo, New York 14221

Attn: Mr. R. Tsunoda

Cornell University
Ithaca, New York 14850

Attn: Dr. D. T. Farley

General Electric Company
P.O. Box 1122
Syracuse, New York 13201

Attn: George H. Millman

General Electric Company
TEMPO - Center for Advanced Studies
816 State Street
Santa Barbara, California 93102

Attn: DASIAC

Geophysical Institute
University of Alaska
College, Alaska 99735

Attn: Technical Library

Massachusetts Institute of Technology
Lincoln Laboratory
P.O. Box 73
Lexington, Massachusetts 02173

Attn: J. V. Evans

MITRE Corporation
Route 62 & Middlesex Turnpike
Bedford, Massachusetts 01730

Attn: Dr. Gerald Meltz

DISTRIBUTION LIST (concluded)

MITRE Corporation
Route 62 & Middlesex Turnpike
Bedford, Massachusetts 01730

Attn: J. Morganstern

Radio Corporation of America
David Sarnoff Research Center
201 Washington Road
West Windsor Township
Princeton, New Jersey 08540

Attn: David Dewolf

Radio Corporation of America
Defense Electronics Products
Missile & Surface Radar Div.
Marne Highway and Borton Landing Road
Moorestown, New Jersey 08057

Attn: Engineering Library, 101-222

Stanford Research Institute
333 Ravenswood Avenue
Menlo Park, California 94025

Attn: Dr. W. Chesnut

Stanford Research Institute
333 Ravenswood Avenue
Menlo Park, California 94025

Attn: Dr. David A. Johnson

Stanford Research Institute
333 Ravenswood Avenue
Menlo Park, California 94025

Attn: Mr. Ray Leadabrand

Stanford Research Institute
333 Ravenswood Avenue
Menlo Park, California 94025

Attn: Dr. Allen M. Peterson

Westinghouse Electric Corporation
Research and Development Center
1310 Beulah Road, Churchill Borough
Pittsburgh, Pennsylvania 15235

Attn: Dr. A. V. Phelps

University of Illinois
Urbana Campus
112 English Bldg.
Urbana, Illinois 61801

Attn: S. Bowhill

UNCLASSIFIED

Security Classification

DOCUMENT CONTROL DATA - R & D

Security classification of title, body of abstract and indexing annotation must be entered when the overall report is classified)

1 ORIGINATING ACTIVITY (Corporate author)
Stanford Research Institute
333 Ravenswood
Menlo Park, California 94025

2a. REPORT SECURITY CLASSIFICATION
UNCLASSIFIED

2b. GROUP
N/A

3 REPORT TITLE
PROJECT 617 RADAR--READINESS ACHIEVEMENT PROGRAM--PART A - DATA PROCESSING AND ANALYSIS

4 DESCRIPTIVE NOTES (Type of report and inclusive dates)
Final Report - Part A

5 AUTHOR(S) (First name, middle initial, last name)
Murray Baron, Odile de la Beaujardiere, Bruce Craig

6 REPORT DATE	7a. TOTAL NO OF PAGES	7b. NO OF REFS
May 1970	138	11

8a. CONTRACT OR GRANT NO	9a. ORIGINATOR'S REPORT NUMBER(S)
DASA01-67-C-0019	SRI Project 6291
b. PROJECT NO. NWER XAXH	
c. Task and Subtask A048	9b. OTHER REPORT NO(S) (Any other numbers that may be assigned this report)
d. Work Unit 01	DASA 2519-1

10. DISTRIBUTION STATEMENT
This Document May Be Further Distributed By Any Holder Only With Specific Prior Approval of Director, Defense Atomic Support Agency, Washington, D.C. 20305

11 SUPPLEMENTARY NOTES	12. SPONSORING MILITARY ACTIVITY
	Director Defense Atomic Support Agency Washington, D.C. 20305

13 ABSTRACT

This report describes in detail the use of the Project 617 radar for making incoherent scatter measurements of the ionosphere. The data processing and analysis methods are fully explained, including all the assumptions, interpolations, and extrapolations. Two new major computer programs were implemented. Portions of the radar hardware that are especially important to the incoherent scatter measurements and portions that have been developed, modified, or improved during the past year are also described. The development and implementation of a digital autocorrelator, in combination with new computer software, has resulted in an order-of-magnitude improvement in data processing time, as well as a significant improvement in measurement accuracy.

DD FORM 1 NOV 1473 (PAGE 1)
S/N 0101-807-6801

UNCLASSIFIED
Security Classif cation

14 KEY WORDS	LINK A		LINK B		LINK C	
	ROLE	WT	ROLE	WT	ROLE	WT
Incoherent Scatter Mighty Sky Proj. 617 Ionospheric Measuremonts Data Processing and Analysis						

Defense Threat Reduction Agency
45045 Aviation Drive
Dulles, VA 20166-7517

CPWC/TRC November 3, 1999

MEMORANDUM FOR DEFENSE TECHNICAL INFORMATION CENTER
ATTN: OCQ/MR WILLIAM BUSH

SUBJECT: DOCUMENT CHANGES

The Defense Threat Reduction Agency Security Office has performed a classification/distribution statement review for the following documents:

DASA-2519-1, AD-873313, STATEMENT A
DASA-2536, AD-876697, STATEMENT A
DASA-2519-2, AD-874891, STATEMENT A
DASA-2156, AD-844800, STATEMENT A
DASA-2083, AD-834874, STATEMENT A
DASA-1801, AD-487455, STATEMENT A
POR-4067, AD-488079, STATEMENT C, ADMINISTRATIVE/OPERATIONAL USE
DASA-2228-1, AD-851256, ~~STATEMENT C~~, ADMINISTRATIVE/OPERATIONAL USE
No Target only changed from SH to admin/oper.
RAND-RM-2076, AD-150693, STATEMENT D, ADMINISTRATIVE/OPERATIONAL USE
* AD-089546, STATEMENT A, ADMINISTRATIVE/OPERATIONAL USE
* ST-A JUN'65
DASA-1847, AD-379061, UNCLASSIFIED, STATEMENT C, ADMINISTRATIVE/OPERATIONAL USE
~~NOFORN DEC~~
~~RAND-RM-4812-PR~~, ELEMENTS OF A FUTURE BALLISTIC MISSILE TEST PROGRAM, UNCLASSIFIED, STATEMENT C, ADMINISTRATIVE/OPERATIONAL USE
370168 Conf
Authority to Declassify

If you have any questions, please call me at 703-325-1034.

Ardith Jarrett
ARDITH JARRETT
Chief, Technical Resource Center

Leave ST-A
Per A. Jarrett 23 Nov 99